

Overview: Recent advances on the understanding of the Northern Eurasian environments and of the urban air quality in China - Pan Eurasian Experiment (PEEX) program perspective

Hanna K. Lappalainen^{1,2}, Tuukka Petäjä^{1,2}, Timo Vihma³, Jouni Räisänen¹, Alexander Baklanov⁴, Sergey Chalov⁵, Igor Esau⁶, Ekaterina Ezhova¹, Matti Leppäranta¹, Dmitry Pozdnyakov^{7,46}, Jukka Pumpanen⁸, Meinrat O. Andreae^{9,42,43}, Mikhail Arshinov¹⁰, Eija Asmi³, Jianhui Bai^{11,44}, Igor Bashmachnikov⁷, Boris Belan¹⁰, Federico Bianchi¹, Boris Biskaborn¹², Michael Boy¹, Jaana Bäck¹³, Bin Cheng³, Natalia Ye Chubarova⁵, Jonathan Duplissy^{1,45}, Egor Dyukarev¹⁴, Konstantinos Eleftheriadis¹⁵, Martin Forsius¹⁶, Martin Heimann¹⁷, Sirkku Juhola²⁰, Vladimir Konovalov¹⁸, Igor Konovalov¹⁹, Pavel Konstantinov^{5,33}, Kajar Koster¹³, Elena Lapsina²¹, Anna Lintunen^{1,13}, Alexander Mahura¹, Risto Makkonen³, Svetlana Malkhazova⁵, Ivan Mammarella¹, Stefano Mammola^{22,23}, Stephany Mazon¹, Outi Meinander³, Eugene Mikhailov^{24, 25}, Victoria Miles⁶, Stanislav Myslenko⁵, Dmitry Orlov⁵, Jean-Daniel Paris²⁶, Roberta Pirazzini³, Olga Popovicheva²⁷, Jouni Pulliainen³, Kimmo Rautiainen³, Torsten Sachs²⁸, Vladimir Shevchenko²⁹, Andrey Skorokhod³⁰, Andreas Stohl³¹, Elli Suhonen¹, Erik S. Thomson³², Marina Tsidilina³⁹, Veli-Pekka Tynkkynen³⁴, Petteri Uotila¹, Aki Virkkula³, Nadezhda Voropay³⁵, Tobias Wolf⁶, Sayaka Yasunaka³⁶, Jiahua Zhang³⁷, Yubao Qiu³⁷, Aijun Ding³⁸, Huadong Guo³⁷, Valery Bondur³⁹, Nikolay Kasimov⁵, Sergej Zilitinkevich (✉)^{1,2,3}, Veli-Matti Kerminen¹ and Markku Kulmala^{1,2,39,40,41}

Formatted: Font color: Auto

¹ Institute for Atmospheric and Earth System Research / Physics, Faculty of Science, University of Helsinki, Finland

² Tyumen State University, Department of Cryosphere, 625003 Tyumen, Russia

³ Finnish Meteorological Institute, 00101 Helsinki, Finland

⁴ World Meteorological Organization, WMO, Geneva, Switzerland

⁵ Faculty of Geography, Lomonosov Moscow State University, Lenin Hills, 119991, Moscow, Russia

⁶ Nansen Environmental and Remote Sensing Center/Bjerknes Centre for Climate Research, Bergen, Norway

⁷ Nansen International Environmental and Remote Sensing Centre”, Nansen Centre, NIERSC, St. Petersburg, Russia

⁸ Department of Environmental and Biological Sciences, PO Box 1627 (Address: Yliopistonranta 1 E), FI-70211 Kuopio, Finland

⁹ Max Planck Institute for Chemistry, Mainz, Germany

¹⁰ V.E. Zuev Institute of Atmospheric Optics (IAO) SB RAS, Tomsk, 634055, Russia

¹¹ LAGEO, Institute of Atmospheric Physics, Chinese Academy of Sciences (IAP-CAS), Beijing, 100029, PR, China

¹² Alfred Wegener Institute, Helmholtz Centre for Polar and Marine Research, Potsdam, Germany

¹³ Institute for Atmospheric and Earth System Research /Forest Sciences, University of Helsinki, Helsinki, Finland

- 38 ¹⁴ Institute of Monitoring of Climatic and Ecological Systems SB RAS, Tomsk, 634055, Russia; Yugra
 39 State University, Khanty-Mansiysk, 628012, Russia
- 40 ¹⁵ ERL, Institute of Nuclear and Radiological Science & Technology, Energy & Safety, NCSR
 41 Demokritos, Attiki, Greece
- 42 ¹⁶ Finnish Environment Institute SYKE, Latokartanonkaari 11, 00790 Helsinki, Finland
- 43 ¹⁷ Max-Planck-Institute for Biogeochemistry, Jena, Germany
- 44 ¹⁸ Institute of Geography RAS, Moscow, Russia
- 45 ¹⁹ Institute of Applied Physics, Nizhny Novgorod, Russia
- 46 ²⁰ Faculty of Biological and Environmental Sciences, University of Helsinki, Helsinki, Finland
- 47 ²¹ Yugra State University, Khanty-Mansiysk, 634012, Russia
- 48 ²² Finnish Museum of Natural History (LUOMUS), University of Helsinki, Helsinki, 00100, Finland
- 49 ²³ Molecular Ecology Group (MEG), Water Research Institute (IRSA), National Research Council of Italy
 50 (CNR), Verbania Pallanza, 28922, Italy
- 51 ²⁴ St. Petersburg State University, 7/9 Universitetskaya nab, St. Petersburg, 199034, Russia
- 52 ²⁵ Multiphase Chemistry and Biogeochemistry Departments, Max Planck Institute for Chemistry, 55020
 53 Mainz, Germany
- 54 ²⁶ Laboratoire des Sciences du Climat et de l'Environnement, IPSL CEA-CNRS-UVSQ, 91190 Gif-sur-
 55 Yvette, France
- 56 ²⁷ Institute of Nuclear Physics, Lomonosov Moscow State University, Moscow, Russia
- 57 ²⁸ GFZ German Research Centre for Geosciences, Telegrafenberg, Potsdam, Germany
- 58 ²⁹ Shirshov Institute of Oceanology, Russian Academy of Sciences, Moscow, Russia
- 59 ³⁰ A.M. Obukhov Institute of Atmospheric Physics, Moscow, Russia
- 60 ³¹ Department of Meteorology and Geophysics, University of Vienna, Vienna, Austria
- 61 ³² Department of Chemistry & Molecular Biology, University of Gothenburg, Göteborg, 41296, Sweden
- 62 ³³ Peoples' Friendship University of Russia (RUDN), Laboratory of sSart technologies for sustainable
 63 development of urban environment under global changes, Moscow, Russian Federation
- 64 ³⁴ Aleksanteri Institute, University of Helsinki, Helsinki, Finland
- 65 ³⁵ V B Sochava Institute of Geography SB RAS, Irkutsk, 664033, Russia; Institute of Monitoring of
 66 Climatic and Ecological Systems SB RAS, Tomsk, 634055, Russia
- 67 ³⁶ Japan Agency for Marine-Earth Science and Technology (JAMSTEC), Yokosuka, Japan
- 68 ³⁷ Aerospace Information Research Institute, Chinese Academy of Sciences, Beijing, 100094, China
- 69 ³⁸ Joint International Laboratory of Atmospheric and Earth System sciences (JirLATEST), Nanjing
 70 University, Nanjing, China
- 71 ³⁹ Institute for Scientific Research of Aerospace Monitoring "AEROCOSMOS", Moscow, 105064, Russia
- 72 ⁴⁰ Aerosol and Haze Laboratory, Beijing Advanced Innovation Center for Soft Matter Sciences and
 73 Engineering, Beijing University of Chemical Technology (BUCT), Beijing, China
- 74 ⁴¹ Guangzhou Institute of Geography, Guangzhou Academy of Sciences, Guangzhou, China
- 75 ⁴² Department of Geology and Geophysics, King Saud University, Riyadh, Saudi Arabia

Formatted: Font color: Auto

Formatted: Font color: Auto

⁴³ Scripps Institution of Oceanography, UCSD, La Jolla, CA, USA

⁴⁴ Interdisciplinary Scientific and Educational School of M.V.Lomonosov Moscow State

University «Future Planet and Global Environmental Change, Russia

⁴⁵ Helsinki Institute of Physics, University of Helsinki, 00014 Helsinki, Finland

⁴⁶ St. State Petersburg University (St. Petersburg State University, 7/9 Universitetskaya nab. St. Petersburg, 199034. Russia

Corresponding author(s): Hanna Lappalainen, hanna.k.lappalainen@helsinki.fi, Veli-Matti Kerminen, veli-matti.kerminen@helsinki.fi

Keywords

Grand Challenges, climate change, land-atmosphere interactions and feedbacks, biogeochemical cycles, Arctic Ocean, Northern Eurasia, China, Arctic marine ecosystem, atmospheric composition, air quality, Arctic greening, land use change, permafrost, Pan-Eurasian Experiment (PEEX), Global Earth Observatory, Digital Earth, Silk Road Economic Belt, Arctic societies, energy policy, boreal region, science diplomacy

ABSTRACT

The Pan-Eurasian Experiment (PEEX) Science Plan, released in 2015, addressed a need for a holistic system understanding and outlined the most urgent research needs for the rapidly changing Arctic-boreal region. Air quality in China together with the long-range transport of atmospheric pollutants was also indicated as one of the most crucial topics of the research agenda. These two geographical regions, the Northern Eurasian Arctic-boreal region and China, especially the megacities in China, were indentified as a “PEEX region”. It is also important to recognize that the PEEX geographical region is an area where science-based policy actions would have significant impacts on a global climate. This paper summarizes results obtained during the last five years in the Northern Eurasian region, together with recent observations on the air quality in the urban environments in China, in the context of the PEEX program. The main regions of interest are the Russian Arctic, Northern Eurasian boreal forests (Siberia) and peatlands, and the megacities in China. We frame our analysis against research themes introduced in the PEEX Sceince Plan in 2015. We summarize recent progress towards an enhanced holistic understanding of the land – atmosphere – ocean systems feedbacks. We conclude that although the scientific knowledge in these regions has increased, the new results are in many cases insufficient and there are still gaps in our understanding of large-scale climate-Earth surface interactions and feedbacks. This arises from limitations in research infrastructures, especially the lack of coordinated, continuous and comprehensive in situ observations of the study region as well as integrative data analyses, hindering a comprehensive system analysis. The fast-changing environment and ecosystem changes driven by climate change, socio-economic activities like the China Silk Road Initiative, and the global trends like urbanization further complicate such analyses. We recognize new topics with an increasing importance in the near future, especially “the enhancing biological sequestration capacity of greenhouse gases into forests and soils to mitigate the climate change” and the “socio-economic development to tackle air quality issues”.

Formatted: Font color: Auto

Formatted: Font color: Auto

Formatted: Font color: Auto

Formatted: Font color: Auto

Formatted: Font color: Auto

Formatted: Font color: Auto

Formatted: Font color: Auto

Formatted: Font color: Auto

Formatted: Font color: Auto

Formatted: Font color: Auto

Formatted: Font color: Auto

Formatted: Font color: Auto

115	
116	Contents
117	Table of contents
118	ABSTRACT
119	1. INTRODUCTION
120	2. RESULTS
121	2.1. LAND ECOSYSTEMS
122	2.1.1 Changing land ecosystem processes (Q1)
123	<i>High-latitude photosynthetic productivity</i>
124	<i>Vegetation changes</i>
125	<i>New methodologies determining Earth surface characteristics</i>
126	2.1.2 Thawing permafrost (Q2)
127	<i>Observations of ground temperature evolution</i>
128	<i>Changing GHG fluxes and VOCs due to permafrost thaw</i>
129	2.1.3 Ecosystem structural change (Q3)
130	<i>Changes in microbial activity</i>
131	<i>Effects of forest fires on soils</i>
132	2.2. ATMOSPHERIC SYSTEM
133	2.2.1 Atmospheric composition and chemistry (Q4)
134	<i>Boreal forests carbon balance</i>
135	<i>Arctic methane (CH₄) balance</i>
136	<i>Northern Eurasian carbon monoxide (CO)</i>
137	<i>Northern Eurasian Ozone (O₃)</i>
138	<i>Sources and properties of atmospheric aerosols in boreal and Arctic environments</i>
139	<i>Black carbon and dust in the atmosphere and snow</i>
140	<i>Methodological and model developments related to atmospheric chemistry and physics</i>
141	2.2.2 Urban air quality and megacities (Q5)
142	<i>Air quality in China – recent observations</i>
143	2.2.3 Weather and atmospheric circulation (Q6)
144	<i>Cold and warm episodes</i>
145	<i>Cyclone density dynamics and atmosphere-ocean interaction</i>
146	<i>Circulation effect on temperature</i>
147	<i>Cloudiness in Arctic</i>
148	<i>Boundary layer dynamics and urban heat islands</i>
149	2.3 ARCTIC-BOREAL AQUATIC SYSTEM
150	2.3.1 Changing water systems, snow, sea ice and ocean sediments (Q7)
151	<i>Sea ice and thermodynamics with atmospheric and ocean dynamics</i>
152	<i>Snow depth/mass and sea ice thickness</i>

Formatted: Font color: Auto

153	<i>Ocean floor and Sediments: composition and fluxes</i>
154	2.3.2 Marine ecology (Q8)
155	<i>Living marine organisms weaken or even subdue CO₂ accumulation</i>
156	<i>Organic carbon in lakes</i>
157	<i>Lake ice cover</i>
158	<i>Lake Baikal and Selenga River delta</i>
159	<i>Asian water lakes</i>
160	2.4 SOCIETY
161	2.4.1. Anthropogenic impact (Q10)
162	<i>Mitigation</i>
163	2.4.2 Environmental impact (Q11)
164	<i>Reindeer (Rangifer tarandus L.) grazing and ground vegetation structure and biomass</i>
165	2.4.3 Natural hazards (Q12)
166	<i>Naturally-determined diseases</i>
167	<i>UV variations</i>
168	3. SYNTHESIS AND FUTURE PROSPECTS
169	3.1 Future research needs from the system perspectives
170	3.2 Feedback mechanisms under changing climate, cryosphere conditions and urbanization
171	3.3 Climate scenarios for the Arctic-boreal region
172	ACKNOWLEDGEMENTS
173	REFERENCES
174	
175	

1. INTRODUCTION

Earth system is facing major challenges, including climate change, biodiversity loss, ocean acidification, epidemics and energy demand on a global scale (Ripple et al., 2017). These “Grand Challenges” are highly connected and interlinked. This creates a need for an approach of a multidisciplinary scientific program, which could deliver science-based messages to fast-tracked policy making (Kulmala et al., 2015). The recent estimates based on observed atmospheric concentrations of CO₂ (ftp://aftp.cmdl.noaa.gov/products/trends/co2/co2_mm_mlo.txt) and business-as-usual scenario show that humankind should find solutions to answer the Grand Challenges (IPCC, 2021). Deep understanding of the feedbacks and interactions between the land, atmosphere and ocean domains, and accounting for social aspects in the regions of substantial changes, are needed for effective technical solutions, mitigation and adaption policy actions. The northern regions (> 45°N), together with the arctic coastal zone and Siberian region in Russia, are among the most critical areas for the global climate (Smith 2011; Kulmala et al., 2015; Kasimov et al., 2015).

The idea of the Pan-Eurasian Experiment (PEEX) (www.atm.helsinki.fi/peex), originating from a group of Finnish and Russian scientists and research organizations in 2012, is a bottom-up research and capacity building program concentrating on the sustainable development of the Arctic-boreal regions of the Northern Eurasia under changing climate and socio-economic megatrends (Kulmala et al., 2015, Lappalainen et al., 2016). The program was laid on four interconnected parts, namely research agenda, research infrastructures, capacity building and societal impacts (Lappalainen et al., 2014; Kulmala et al., 2016a, Lappalainen et al., 2017, Kulmala 2018). In addition to a strong involvement of the Russian partners, the PEEX China collaboration was established in 2013. China has a strong economic interest on Arctic regions (Tillman et al. 2018). Furthermore, China is already facing extensive environmental and air pollution challenges and has a major interest to find technical solutions for environmental monitoring of the Silk Road Economic Belt Program (SREB) initiated by the President XI Jinping in 2013 (Kulmala 2018, Lappalainen et al., 2018, Dave and Kobayashi, 2018). In Russia the program is an umbrella for several bilateral scientific projects and activities (e.g. Chalov et al., 2015, 2018; Esau et al., 2016; Alekseychik et al., 2017; Bobylev et al., 2018; Malkhazova et al., 2018; Kukkonen et al., 2020; Ezhova et al., 2018b; Ziltinkevich et al., 2019; Petäjä et al., 2020 submitted; ; Bondur et al, 2019 a,b,c,d,e,f; Yuanhuizi He et al, 2020), while in China the primary focus is on the development of atmospheric in-situ stations and advanced air quality monitoring in megacity environments (e.g. Ding et al., 2016 b; Yao et al., 2018; Ying et al., 2020; Wang et al., 2020). Furthermore, PEEX is closely collaborating with the Digital Belt and Road (DBAR) Program coordinated by the Institute for Digital Earth and Remote Sensing (RADI). The PEEX collaboration with DBAR is driven by a need for a novel in-situ station network and ground-based data as a complementary information for the remote sensing in the Silk Road economic region. Long-term development on a “Station Measuring the Earth Surface and

Formatted: Font color: Auto

Formatted: Font color: Auto

Formatted: Font color: Auto

Atmosphere Relations” (SMEAR) concept could provide baselines for this (Hari et al. 2016; Kulmala 2015, Kulmala 2018; Lappalainen et al., 2018).

The PEEEX program is motivated by the need for obtaining scientific information that combines research in the Arctic and boreal environments, and for understanding large-scale feedbacks and interactions operating in land-atmosphere-ocean systems (Kulmala et al., 2004; Kulmala et al., 2016a; Vihma et al., 2019) and large-scale weather impacts related to the Arctic amplification (e.g. Coumou et al., 2014; Vihma et al., 2020). One of the scientific backbones of PEEEX is the previously coordinated research frameworks and their synthesis. For example, the latest comprehensive overview on the interactions between the atmosphere, cryosphere and ecosystems at northern high latitudes was performed by the Nordic Center of Excellence in “Cryosphere-atmosphere interactions in a changing Arctic climate“, CRAICC) community (Boy et al., 2019). The PEEEX program can upscale the CRAICC results into a wider geographical context.

Climate change, as a main driver for environmental changes in the Northern Eurasian Arctic-boreal region and China, sets environmental boundaries for the future socio-economic activities of these regions in general. The harsh climate of this region puts a pressure on the ecosystems and living conditions of the local people (e.g. IPCC, 2019). PEEEX introduced fifteen large-scale research questions, which would also help us to fill the key gaps in our holistic understanding of land-atmosphere interactions and their connections to societies living in the northern Eurasian region (Kulmala et al., 2015; Lappalainen et al., 2018). This approach also sets the framework of the current paper. Here we introduce the recent research progress in the large-scale scientific themes relevant to the PEEEX region. The PEEEX study region consists of the Northern Eurasian Arctic and boreal (taiga) environments, thus the major geographical part of the environments is located in the Russian territory. China was added to the study area in 2013 as it was seen as locally and globally consequential region for climate change, air quality and long-term transport of atmospheric pollutants (Kulmala et al., 2015 a,b; Lappalainen et al., 2016, 2018).

Here we introduce the scientific results from PEEEX scientific output, review the main results from PEEEX scientific papers and present an analysis of the key gaps in the current scientific understanding. We use the PEEEX research agenda structure (Kulmala et al. 2016, Lappalainen et al. 2018) as a reference and mirror new a rising themes and results against this plan. For the literature material, we used the following sources for demonstrating the results: (i) individual input sent by the PEEEX research community, (ii) content of the scientific papers published in Atmospheric Chemistry and Physics (ACP) PEEEX special issue in 2016-2019 (www.atmos-chem-phys.net/special_issue395.html) and (iii) scientific output from PEEEX-labeled projects (www.atm.helsinki.fi/peex/index.php/projects) and other relevant results reported by the PEEEX partners. For the individual input we asked the PEEEX research community to identify the main published papers in peer reviewed journals for each question out of their own work and connect the work to one of the 15 science questions introduced in the PEEEX science plan. Based on the abstracts we listed “addressed research themes” over last 5 years per PEEEX key topical areas (Table 1), which we review in more detail in section 2. The

Formatted: Font color: Auto

Formatted: Font color: Auto

Formatted: Font color: Auto

Formatted: Font color: Auto

Formatted: Font color: Auto

Field Code Changed

Formatted: Font color: Auto

Formatted: Font color: Auto

Formatted: Font color: Auto

Field Code Changed

results are first discussed with a holistic approach and then we categorize the advances through a set of identified feedbacks and interactions within the Arctic boreal environment. We follow up with a discussion on the need for a future research infrastructure to be able to provide relevant data and underline the future socio-economics development of the region setting the boundaries for proposed new science-based concepts and technical solutions.

2. RESULTS

In the PEEEX Science Plan we indicated four main thematic research domains: the land system, the atmospheric system, the water system and the society with 15 thematic research areas and related large-scale research questions (Q) presented in Table 1 (Lappalainen et al., 2015), also indicated in the structure of the “Table of Contents”. This is the framework we re-visited and utilized in the synthesis of new results of the PEEEX community brought together in this paper. Furthermore, we synthesized the results and discuss their contribution to the large - scale feedbacks and interactions in the Arctic context in the sections below.

2.1. LAND ECOSYSTEMS

2.1.1 Changing land ecosystem processes (Q1)

High-latitude photosynthetic productivity

High-latitude terrestrial ecosystems are crucial to the global climate system and its regulation by vegetation. These ecosystems are typically temperature limited, and thus also considered especially sensitive to climate warming. Better understanding of an inter-annual and seasonal dynamics and resilience of the photosynthetic activity of forest vegetation as a whole is needed for the quantification of photosynthesis, or gross primary production (GPP), and analyzing the carbon balance of boreal forest. The carbon sink and source dynamics of the boreal forests have been intensively studied during the last five years at the SMEAR (Stations Measuring Atmosphere Ecosystem Relations) II station in Finland (Hari and Kulmala 2005; Hari et al., 2009). Recent results show that the Norway spruce and Scots pine ecosystems are rather resilient to a short-term weather variability (Matkala et al., 2020). Overall, the analyses by Kulmala et al. (2019) and Matkala et al. (2020) on subarctic Scots pine and Norway spruce stands at the northern timberline in Finland serve as examples of the canopy scale dynamics, showing that these ecosystems are generally weak carbon sinks but have a clear annual variation. Kulmala et al. (2019) observed that there is a difference between tree canopy photosynthesis compared to forest floor photosynthesis which starts to increase after the snowmelt. Thus, the models for photosynthesis should also address the snow cover period in order to better capture the seasonal dynamics of photosynthesis of the Northern forests (Kulmala et al., 2019).

The abundance of tree species, stand biomass, increasing tree growth and coverage of broadleaf species may also affect biogenic volatile organic compound (BVOC) emissions from the forest floor and impact the total

Formatted: Font color: Auto

BVOC emissions from northern soils. At least the stand type has been shown to affect BVOCs fluxes from the forest floor in a hemi boreal-boreal region (Mäki et al., 2019). As a whole, BVOCs emitted by boreal evergreen trees are connected to the photosynthetic activity with a strong seasonality and have a crucial role in atmospheric aerosol formation processes over the boreal forest zone. BVOC emissions have low rates during photosynthetically inactive winter and increasing rates towards summer (Aalto et al., 2015). High emission peaks caused by enhanced monoterpene synthesis were found in spring periods simultaneously with the photosynthetic spring recovery (Aalto et al., 2015). This suggests that monoterpene emissions may have a protective functional role for the foliage during the spring recovery state, and that these emission peaks may contribute to atmospheric chemistry in the boreal forest in springtime. Vanhatalo et al. (2018) studied the interplay between needle monoterpene synthase activities, its endogenous storage pools and needle emissions in two consecutive years at a boreal forest in Finland. They found no direct correlation between monoterpene emissions and enzyme activity or the storage pool size. Monoterpene synthase activity of needles was different depending on seasonality and needle ontogenesis. However, the pool of stored monoterpenes did not change with the needle age (Vanhatalo et al., 2018). Also, clear annual patterns of primary biological aerosol particles have been measured from a boreal forest, with late spring and autumn being the seasons of a dominant occurrence. Increased levels of free amino acids and bacteria were observed during the pollen season in the SMEAR II station in Finland, whereas the highest levels for fungi were observed in autumn (Helin et al., 2017).

Extensive measurements of Scots pine photosynthesis and modelling resulted in optimized predictions of the daily behavior and annual patterns of photosynthesis in a subarctic forest (Hari et al., 2017). The study connected theoretically the fundamental concepts affecting photosynthesis with the main environmental drivers (air temperature and light), and the theory gained strong support through empirical testing. Understanding stomatal regulation is fundamental in predicting the impact of changing environmental conditions on photosynthetic productivity. Lintunen et al. (2020) showed that the canopy conductance and soil-to-leaf hydraulic conductance are strongly coupled, and that both soil temperature and soil water content influence the canopy conductance through changes in the belowground hydraulic conductance. In particular, the finding that the soil temperature strongly influences the belowground hydraulic conductance in mature, boreal trees may help to better understand tree behavior and photosynthetic productivity in cold environments. The plant photosynthetic rate is concurrently limited by stomatal and non-stomatal limitations, and recent modelling (Hölttä et al., 2017) and empirical (Salmon et al., 2020) studies suggest that stomatal and non-stomatal controls are coordinated to maximize leaf photosynthesis, i.e. non-stomatal limitations to photosynthesis increase with a decreasing leaf water potential and/or increasing leaf sugar concentration. This new approach allows including the effects of non-stomatal limitations in models of tree gas-exchange (Fig. 1).

Due to climate warming, it seems that trees in high-latitudes have been progressively decreasing their regional growth coherence in the last decades (Shestakova et al., 2019). Shestakova et al. (2019) showed

results that unequivocally linked a substantial decrease in the temporal coherence of forest productivity in boreal ecosystems to a less temperature-limited growth that is concurrent with regional warming trends. This emerging pattern points, for example, to an increasing dependence of the carbon balance on local drivers and the role of forests as carbon sinks in the northern Ural region.

Vegetation gross primary production (GPP) is the largest CO₂ flux of the carbon cycle in terrestrial ecosystems and impacts all of the carbon cycle variables (Beer et al., 2010). Ecosystem models usually overestimate GPP under drought and during spring, late fall and winter (Ma et al., 2015). Several new methodological improvements for a better quantification and scaling of GPP have been reported (Zhang et al., 2018; Pulliainen et al., 2017; Kooijmans et al., 2019). The GPP, measuring photosynthesis, is crucially important for the global carbon cycle and its accurate estimation is essential for ecosystem monitoring and simulation. Pulliainen et al. (2017) introduced a new proxy indicator for spring recovery from *in situ* flux data on CO₂ exchange. This made it possible to quantify the relation between spring recovery and carbon uptake, and to assess changes in the springtime carbon exchange, demonstrating a major increase in the CO₂ sink. Zhang et al. (2018) introduced a new water-stress factor that effectively mitigates the overestimation of GPP under drought conditions, while Bai et al. (2018 a,b) developed a method for quantifying the evapotranspiration of crops by using a remote sensing-based two-leaf canopy conductance model. These methods can provide novel insights into the quantification of GPP under different conditions and, in general, into the impacts of biosphere-atmosphere relations on a larger scale.

Methods for satellite-based remote sensing of photosynthesis have been developed recently based on solar-induced chlorophyll fluorescence signal, such as the OCO-2 product that has an improved spatial resolution, data acquisition and retrieval precision, as compared with earlier satellite missions with solar-induced chlorophyll fluorescence (SIF) capability, which allows for validation of the data directly against ground and airborne measurements (Sun et al., 2017). Interpretation of the solar-induced chlorophyll fluorescence signal has also been improved by many *in situ* studies. For example, Liu et al. (2019a, 2019b) simulated SIF in realistic 3D birch stand reconstructed from terrestrial laser scanning data and found a large contribution of the understory layer to the remote sensing signal.

Vegetation changes

The normalized difference vegetation index (NDVI) is used for detecting large-scale changes in vegetation productivity. In the past decades, these changes include an increasing NDVI, called “greening”, taking place in the tundra regions and a decreasing NDVI, called “browning”, in the Northern forest regions (Miles and Esau, 2016). A deeper analysis behind these changes are needed. For example, in Northern West Siberia only 18% of the total area had statistically significant changes in productivity either towards greening or browning, and having these opposite trends for different species within the same bioclimatic zone. The observed complexity of the patterns and trends in the vegetation productivity underlines the need for new

studies on how forest types and different species are responding to climate and environmental changes in the Northern environments (Miles and Esau, 2016). Also understanding the variations in small-scale plant communities, seasonality and biogeochemical properties are needed for modeling the functioning of the arctic tundra in global carbon cycling. Also the rapid development of the leaf area index (LAI, leaf area per ground area, $\text{m}^2 \text{m}^{-2}$) during the short growing season and the yearly climatic variation address the importance of optimal timing of the satellite data images when it is compared with the field verification data in the Arctic region (Juutinen et al., 2017).

Bondur and Vorobyev (2015) analyzed the vegetation indices and complex spectral transformations derived from processed long-term satellite data (1973-2013) for areas around the cities of Arkhangelsk and Zapolyarny (Murmansk oblast). They demonstrated that these areas are subject to a peak anthropogenic impact associated with specific industrial facilities, leading to changes in landscapes and depletion of natural ecosystems, consequently leading to the decline in the quality of life and health conditions (Bondur and Vorobyev, 2015). Region-wide changes in the vegetation cover and changes in and around several urbanized areas in Siberia reveal robust indications of an accelerated greening near the older urban areas. Many Siberian cities have turned greener while their surroundings have been dominated by wider browning. The observed urban greening could be associated not only with a special tending of within-city green areas but also with urban heat islands and succession of more productive shrub and tree species growing on warmer sandy soils (Koronatova and Milyaeva 2011, Sizov and Lobotrosova 2016). Tundra and forest-tundra biomes are sensitive to mean summer temperatures, which increases production and greening. Taiga biomes are sensitive to precipitation and soil moisture with increased production in wet summer (Miles et al., 2019).

New methodologies determining Earth surface characteristics

Earth surface characteristics are fundamental knowledge to the understanding and quantification land-atmosphere processes. The methods for determining Earth surface characteristics from satellites are improving. As an example, a method for recognition of the Earth surface types according to space images using an object-oriented classification was developed. The classification relies on Markov stochastic segmentation for object extraction and supervised classification of the objects (Gurchenkov et al., 2017). Furthermore, a prototype algorithm for hemispheric scale detection of autumn soil freezing using space-borne L-band passive microwave observations was developed (Rautiainen et al., 2016) and is currently an operative soil freeze and thaw product that delivers freely available data (<ftp://litdb.fmi.fi/outgoing/SMOS-FTService/>). The CryoGrid 3 land surface model provides improved descriptions of possible pathways of ice-wedge polygon evolution and describes better the complex processes affecting ice-rich permafrost landscapes (Nitzbon et al., 2019). In addition, there are new observations for validating satellite observations and permafrost models. Boike et al. (2016) introduced a new, 16-year permafrost and meteorology data set from the Samoylov Island Arctic research site, north-eastern Siberia. Terentieva et al. (2016) introduced

maps used as a baseline for validation of coarse-resolution land cover products and wetland data sets at high latitudes. Other examples of available data for the model validation are “BC emissions from agricultural burns and grass fires in Siberia” by Konovalov et al. (2018) and permafrost records at the Lena River delta” by Boike et al. (2016).

Tundra ecosystems are under pressure and intensifying permafrost thawing, plant growth and ecosystem carbon exchange under the changing climate. The heterogeneity of Arctic landscapes is an extra challenge for environmental monitoring. For example, remote sensing methods are not able to capture variations in moss biomass, which is dominating the plant biomass and controlling soil properties in the Arctic. The general accuracy of landscape level predictions in the land cover type (LCT) is good, but the spatial extrapolation of the vegetation and soil properties relevant for the regional ecosystem and global climate models still needs to be improved (Mikola et al., 2018). Furthermore, for the future, we need to have a land characterization, in order to perform quantification and assessment of the ecosystem services at different scales using integrative techniques and integrated field observations together with remote sensing and modelling at the landscape scale (Burkhard et al., 2009, Fu and Forsius, 2015). At smaller scales, the isotopic composition of carbon and oxygen in peat can be used for the climate reconstruction (Granath et al., 2018).

2.1.2 Thawing permafrost (Q2)

Observations of ground temperature evolution

Permafrost regions of the Northern Eurasia are warming along with the climate (IPCC, 2019). During the Global Terrestrial Network for Permafrost reference decade, 2007 - 2016, the temperature at the depth of zero annual amplitude increased by 0.39 ± 0.15 °C in the continuous permafrost zone and by 0.20 ± 0.10 °C in the discontinuous permafrost zone. At the same time, the mountain permafrost warmed by 0.19 ± 0.05 °C. The global average of the permafrost temperature increased by 0.29 ± 0.12 °C (Biskaborn et al., 2019). The observed trend in the continuous permafrost zone follows the air temperature trend in the Northern Hemisphere.

The changes in the permafrost region affect climate, hydrology and ecology from local to global scales (Arnell et al., 2010; Hinzman et al., 2005). Several local studies focused on differences introduced by vegetation, soil and hydrological characteristics at the same site (Göckede et al., 2017, 2019). Göckede et al. (2017, 2019) presented findings on shifts in energy fluxes from paired ecosystem observations in northeast Siberia comprising a drained and a corresponding control site. Drainage disturbance triggered a suite of secondary shifts in ecosystem properties, including alterations in vegetation community structure, which in turn influenced changes in snow cover dynamics and surface energy budget. First, the drainage reduced heat transfer into deeper soil layers, which may have led to shallower thaw depths. Second, the vegetation change due to the drainage led to an albedo increase, which decreased the total energy income, or net radiation, into

the system. Third, the drainage reduced water content available for evapotranspiration, which resulted in a reduced latent heat flux and increased sensible heat flux, transferring more energy back to the atmosphere. The reported affects led to surface and permafrost cooling (Göckede et al., 2019).

Kukkonen et al. (2020) compared temperature data from several shallow boreholes in the Nadym region, Siberia, and predicted permafrost evolution for different climate scenarios. The Nadym area represents a typical site located in the discontinuous permafrost zone. Kukkonen et al. (2020) found that the permafrost thawed most rapidly in low-porosity soils, whereas high-porosity soils in the top layer (e.g., peatland) retarded thawing considerably. Similarly, the depth of a seasonally frozen layer and the temperature regime of peat soils in the oligotrophic bog in the southern taiga zone of Western Siberia showed significant differences between the sites with high and low levels of bog waters (Kiselev et al., 2019). Both Kukkonen et al. (2020) and Kiselev et al. (2019) results are in line with previous conclusions on the importance of volumetric water content and unfrozen water content for soil thermal properties governing heat transfer and phase change processes (Romanovsky and Osterkamp, 2000). Locally, the sites with a thin snow cover (e.g., hill tops) demonstrated a higher resistance to the thawing (Williams and Smith, 1989; Kukkonen et al., 2020). To follow-up on the development of permafrost thaw in different soil types require continuous and comprehensive observations during the coming decades.

Changing GHG fluxes and VOCs due to permafrost thaw

Biogenic GHG emissions are strongly connected with permafrost conditions and changes in other related environmental conditions, such as soil temperature and moisture conditions. Here we discuss recent results on the observed emissions from these permafrost perspectives and, later in section 2.2.1, address the connections between GHG fluxes and the other environmental factors, like deforestation and forest fires.

During the permafrost thaw, even small changes in the soil carbon cycle can turn a terrestrial ecosystem from a sink into a source (Schuur et al., 2008). Based on regional *in situ* observations of CO₂ fluxes, Natali et al. (2019) estimated a winter-time carbon loss of 1 662 TgC per year, which is more than predicted by the process models estimates. Furthermore, Natalie et al. (2019) found that even if the soil CO₂ loss were enhanced due to winter warming, the growing season might start earlier and onset the carbon uptake under warming climate conditions. For a better understanding of these connections and both spatial and temporal dynamics of the Arctic carbon cycle, we need more observations from permafrost ecosystems. Additional flux measurements are urgently needed to understand the variation between the current measurements and, especially extended measurements on the CH₄ emissions to better quantify their role in the carbon balance. For example, a new data assimilation system estimates an Arctic carbon sink of -67 g C m⁻² yr⁻¹, but this value is associated with very high uncertainties. Furthermore, these estimates do not include methane, which is even more difficult to evaluate (López-Blanco et al., 2019). Based on the field flux measurements, the Carbon Cycle Report 2018 (Schuur et al., 2018) estimated that the Eurasian boreal wetland is a source of 14

Tg CH₄ per year. On the other hand, Kirschke et al. (2013) estimations, based on atmospheric measurements, ended up to the value of 9 Tg CH₄ per year. Locally, methane fluxes measured in 2005-2013 showed significant year-to-year variations. Interestingly, the observed variability in North America, specifically in the Hudson Bay lowlands, appears to have been driven partly by the soil temperature, while in the Western Siberian lowlands the variability was dependent on the soil moisture (Thompson et al., 2017). The comparison of high-resolution modelling of atmospheric CH₄ to CH₄ observations already in 2012 from the East Siberian Arctic Shelf (ESAS), a potentially large CH₄ source, confirms that methane releases are highly variable and inhomogeneous (Berchet et al., 2016).

Long-term flux measurements provide insight into the carbon sink - source dynamics. The flux measurements from the moist tussock tundra in the north-eastern Siberia indicated that drainage influences the carbon cycle and that the tundra is changing to a weaker CO₂ sink and CH₄ source. Another relevant observation was that the time outside the growing season influences the carbon balance of ecosystem processes, especially during the zero-curtain period (Kittler et al. 2017). This is in line with similar studies in Alaska (Commane et al., 2017; Euskirchen et al., 2017). Therefore, the autumn temperature was identified as a major driving factor describing the differences between the annual GHG fluxes. Notably, however, the seasonal amplitudes of CO₂ concentrations in Siberia were found to be significantly higher than those in the North American continent, likely due to the more intense biological activity here (Timokhina et al., 2015a). A recent study showed that the Siberian carbon cycle is a major contributor to the Northern Hemisphere amplitude of CO₂ variation (Lin et al., 2020).

Observations from non-permafrost sites may give us a clue on the future dynamics of fluxes, as the permafrost is thawing. The chamber measurements of CH₄ and CO₂ fluxes from a non-permafrost site in the Siberian peatland in August, 2015, showed that the highest values of methane fluxes were obtained in burnt wet birch forest and the lowest ones in seasonally waterlogged forests (Glagolev et al., 2018). The fluxes can vary even between different sites of a bog, as measured by Dyukarev et al. (2019). The net ecosystem exchange (NEE), ecosystem respiration (ER) and gross primary production (GPP), based on the measured CO₂ fluxes at a ridge-hollow complex bog and a model for ridge and hollow sites at oligotrophic bog in Middle Taiga Zone of West Siberia, showed that a two-year-average NEE at the hollow site was 1.7 times higher than at the ridge site (Dyukarev et al., 2019). The ecosystem processes are influenced by drying in tundra ecosystems. Kwon et al. (2019) reported from Alaska that drying in the tundra ecosystems increased contributions of modern soil carbon to the ecosystem respiration but, at the same time, decreased contributions of old soil carbon. These changes were attributed mainly to modified soil temperatures at different soil layers due to the altered thermal properties of organic soils following drainage. Furthermore, the drainage lowered CH₄ fluxes by a factor of 20 during the growing season, with post drainage changes in microbial communities, soil temperatures, and plant communities also affecting the flux reduction in an Arctic wetland ecosystem (Kwon et al., 2017).

Voigt et al. (2016) reported that, under warming conditions, the vegetated tundra in north-eastern European Russia shifted from a GHG sink to a source. The positive warming response was dominated by CO₂; however, N₂O emissions were also significant. N₂O was emitted not only from bare peat, already identified as a strong source, but also from vast vegetated peat areas not emitting N₂O under current climate conditions. These results can be explained by the dynamics between the temperature, nitrogen assimilation by plants and soil microbial activity, having a strong impact on the future GHG balance in Arctic (Voigt et al., 2016; Gil et al., 2017). Studying N₂O emissions from a typical permafrost peatland in Finnish Lapland, it was concluded that about 25% of the Arctic territory are areas that potentially emit nitrous oxide (Voigt et al., 2017). It seems that there is positive feedback mechanism between the permafrost thawing and moisture regime. Predicting the response of soils to climate change or land use is central to understanding and managing N₂O emissions. According to recent results, the N₂O flux can be predicted by models that incorporate soil nitrate concentration (NO₃⁻), water content and temperature (Pärn et al., 2018).

In addition to CO₂ and CH₄, thawing or collapsing of arctic permafrost can release volatile organic compounds (VOCs). Li et al. (2020a) examined the release of VOCs from thawing permafrost peatland soils sampled from Finnish Lapland in laboratory. The average VOC fluxes were four times as high as those from the active layer, and mainly attributed to direct release of old, trapped gases from the permafrost. These results demonstrate a potential for substantive VOC releases from thawing permafrost and suggests that future global warming could stimulate VOC emissions from the Arctic permafrost.

2.1.3 Ecosystem structural change (Q3)

Changes in microbial activity

Climate change is likely to cause an increased appearance of trees on open peatlands, but we do not know how this vegetation change will influence the below-ground microbiology and composition. Changes along bog ecotones at three Russian peatland complexes suggest that tree encroachment may reduce the trophic level of *Testate Amoeba* communities and reduce the contribution of mixotrophic *Testate Amoebae* to primary production. Thus, it seems that increased tree recruitment on open peatlands will have important consequences for both microbial biodiversity and microbial-mediated ecosystem processes (Payne et al., 2016). We also need to understand better the dynamics affecting the bacteria, fungi and other related species in the ground air layer. Recent studies by Korneykova and Evdokimova (2018) and Korneikova et al. (2018 a, 2018b) showed the influences of anthropogenic sources (Copper-Nickel Plant) and acidic soils in Russian northern taiga and tundra on the portion of the airborne fungi, and on the structure of algological and mycological complexes (Korneikova et al., 2018 a, 2018b). New methods were reported on how to improve soil conditions, developed on all kinds of materials made or exposed by human activity that otherwise would not occur at the Earth's surface, referred as "Techno sol engineering" (Slukovskaya et al., 2019), and how to

monitor climate change impacts on the functional state of bogs by using *Sphagnum* mosses (Preis et al., 2018).

Effects of forest fires on soils

Forest fires, a significant environmental factor in the Northern Eurasian region, change soil chemical and physical properties and may influence greenhouse gas fluxes and emissions of BVOCs. Recent results indicate that a slower post-fire litter decomposition has a clear impact on the recovery of soil organic matter following forest fires in northern boreal coniferous forests due to accumulated soil organic matter. The soil recovery is related to slow litter composition and reduced enzymatic and microbial activity (Köster et al., 2016).

Post-fire studies on the long-term evolution of the structure and functioning of bacterial communities are sparse. Sun et al. (2016) showed that the major drivers influencing bacterial community are the soil temperature, pH and moisture. Furthermore, Köster et al. (2015) analyzed long-term effects of fire on soil CO₂, CH₄ and N₂O fluxes in pine forest stands in the Finnish Lapland, and discussed the role of microbial biomass in this context. They did not detect significant effects of fires on CO₂ emissions or N₂O fluxes, but there were long-lasting strengthening of the CH₄ sink by the soil. Interestingly, Köster et al. (2018) did not find a similar kind of long-term effect on the CH₄ sink dynamics in studies carried out in Siberia.

Forest wildfires also regulate the BVOC emissions from boreal forest floors by changing the ground vegetation. Total BVOC emissions from a forest floor were found to decrease after a forest fire and then to increase again along with the succession of forests (Zhang-Turpeinen et al., 2020). For a comparison, Bai et al. (2017) showed that biomass burning resulted in increased BVOC emission fluxes and ozone concentration above canopy in a subtropical forest in China.

2.2. ATMOSPHERIC SYSTEM

Concerning critical atmospheric processes and large-scale climate implications, we concentrate here on greenhouse gases and aerosol particles over Northern Eurasia and Arctic, urban air quality, and issues related to the weather and atmospheric circulation. We summarize the recent measurements on the atmospheric composition relevant to sink and source dynamics in Siberia, on the sources and properties of atmospheric aerosols in Arctic-boreal environments, including black carbon and dust in the atmosphere and snow, and on the methodological and model developments related to atmospheric chemistry and physics (Q4, section 2.2.1). Furthermore, we introduce new results and observations on atmospheric pollution in rural, suburban and mega city environments in China and Russia (Q5, section 2.2.2). We briefly show some recent results related to synoptic-scale weather in Arctic-boreal regions, focusing on cold and warm episodes, cyclone

density and atmosphere-ocean interaction, effects of circulation on temperature and moisture, cloudiness in the Arctic, and boundary layer dynamics (Q6, section 2.2.3).

2.2.1 Atmospheric composition and chemistry (Q4)

Boreal forests carbon balance

As already discussed in section 2.1.1, boreal forests as a carbon sink and the related role of forestation have been under international debate. It seems that early snowmelt increases springtime carbon uptake of the boreal forests of Eurasia and North America and shows a major advance in the CO₂ sink (Pulliainen et al., 2017). A scenario of a complete global deforestation by Scott et al. (2018), combining radiative forcing to CO₂, surface albedo and short-lived climate forcers (SLCFs), suggests that global deforestation could cause a 0.8 K warming after 100 years, with SLCFs contributing 8% of the effect. However, deforestation as projected by the RCP8.5 scenario leads to zero net radiative forcing from SLCF, primarily due to nonlinearities in the aerosol indirect effect. Tuovinen et al. (2019) showed that methane fluxes vary strongly with a wind direction in a tundra ecosystem with heterogeneous vegetation. By combining very high-spatial-resolution satellite imagery and footprint modelling, they were able to estimate the relation between the main land cover types and ecosystem-level measurements. CH₄ emissions originated mainly from wet fen and graminoid tundra patches, whereas the areas of bare soil and lichen acted as strong CH₄ sinks (Tuovinen et al. 2019. Tsuruta et al. (2017) reported posterior mean global total emissions of 516±51 Tg CH₄ yr⁻¹ during 2000-2012, which indicates that these emissions had increased by 18 Tg CH₄ yr⁻¹ from the period 2001-2006 to the period 2007-2012. This increase can be explain by increased emissions from the temperate region in South America and from the temperate region and tropics in Asia.

Analysis of the trends and the diurnal, weekly and seasonal cycles of CO₂ and CH₄ mixing ratios derived from the long-term data of the “Japan–Russia Siberian Tall Tower Inland Observation Network” showed that the frequency of identified events of elevated concentration differs for CO₂ and CH₄ and may reach up to 20% of days in some months (Belikov et al., 2019). These observations made it possible to reduce uncertainties in the biosphere surface CO₂ uptake (Kim et al., 2017). Although the CO₂ uptake in boreal Eurasia estimated by Kim et al. (2017) was about 30% lower than that obtained without the assimilation of Siberian observation data, Siberia still remains a key contributor to the terrestrial CO₂ sink in the Northern Hemisphere.

There are tendencies of a significant growth or suppression of soil CO₂ fluxes across different types of human impacts, such as forest fires, trampling, settlements, reindeer grazing and clearcuts on cryogenic ecosystems in Russia (Karelin et al., 2017). For example Ivanhov et al. (2019) analyzed CO₂ measurements during 2010-2017 and reported CO₂ concentration increases of 20 ppm in Tiksi at a coast of Laptev Sea and of 15 ppm at the Cape Baranov station. They also detected that wildfires in Siberia can lead to a parallel

Formatted: Font color: Auto

Formatted: Font color: Auto

increase of the CO₂ concentration at the Russian Arctic. Furthermore, the measurements showed that the atmospheric CO₂ concentration increased on average by 2.0 ppm yr⁻¹ during 2006–2013 in central Siberia, with a large inter-annual variations. The highest increase were found in 2010 and 2012 (3.6 and 4.3 ppm yr⁻¹, respectively), when large wildfires released huge amounts of CO₂ in Siberia (Timokhina et al., 2015b). Repeated wildfires in boreal forests can combust a portion of the thick organic soil layer characteristic for this ecosystem, and change the forests from a carbon sink into a carbon source (Walker et al., 2019). A study on a fire chronosequence of the central Siberian permafrost soil showed that soils affected by fires over decades act as CO₂ sources, and that the CO₂ emissions from these soils increased with an increasing time since the last fire (Köster et al., 2018). However, there were no similar effects on CH₄ emissions, with soils acting as a CH₄ sink without any connection to forest fires. In addition to CO₂, wildfires also release large amounts of other trace gases and aerosols. Emission factors of several trace gases and aerosols from Siberian fires measured from the Trans-Siberian railway were reported by Vasileva et al. (2017). The impact of Siberian fires as elevated aerosol concentrations was at times observed to extend up on the Arctic coast (Asmi et al., 2016).

Arctic methane (CH₄) balance

Deep understanding on the dynamics of methane emissions in the Arctic is needed for identifying and quantifying GHG-related feedbacks and global methane cycle (Dean et al., 2018). The main source of methane in Arctic during winter is anthropogenic; on a smaller scale, emissions from oceans including the Eastern Siberian Arctic Shelf (ESAS) can play an important role. During the warm season, the balance is dominated by emissions from wetlands and freshwater bodies. Thonat et al. (2017) employed the CHIMERE model for an assessment of the methane cycle in Arctic. They reported that all methane sources, except biomass burning, contributed to measurements at six study sites. That study emphasizes the importance of a joint model-measurements approach for studies of complex phenomena at large spatial scales. Accounting for OH oxidation and soil uptake, two important sinks of methane, improved the agreement between observed and modelled methane concentrations (Thonat et al., 2017). Peltola et al. (2019) up-scaled CH₄ fluxes measured at 25 northern wetland sites and showed three different maps of wetland distribution with the annual methane emissions varying from 31 to 38 Tg(CH₄) yr⁻¹. (For the monthly up scaled CH₄ flux data products see doi.org/10.5281/zenodo.2560163). Multiple sources, together with different spatiotemporal dynamics and magnitudes, are influencing the total Arctic CH₄ budget and addresses the need for the further improved assessments (Peltola et al., 2019; Thonat et al., 2017).

Northern Eurasian carbon monoxide (CO)

Analysis of long-term trends in the atmospheric composition in remote Northern Eurasia (1998–2016) showed that the total column carbon monoxide (CO) amount has been stabilized or increased in summer and autumn months (Rakitin et al., 2018). The changes in the global photochemical system, especially changes in the ratio between the sources and sinks of minor atmospheric chemical species, could explain these trends (Skorokhod et al., 2017). A comparative study (1998–2014) on the atmospheric total column CO amount in

background and polluted regions of Eurasia indicated that this amount has decreased remarkably in the Moscow urban environments ($3.73\% \pm 0.39\%$ per year) compared to the background regions (0.9–1.7% per year) (Wang et al., 2018a).

Northern Eurasian Ozone (O_3)

Atmospheric measurements of ozone, its precursors and other pollutants over Siberia are important for the atmospheric chemistry modelling, satellite product validation and comparisons between Siberia and other regions of the Northern Hemisphere. Isoprene and monoterpenes together with nitrogen oxides impact tropospheric O_3 formation and lead to an increase in the daytime ozone-forming potential (OFP) in urban environments. Bai et al. (2021) showed that O_3 may respond either positively or negatively to isoprene and monoterpene emissions depending on the level of solar radiation and atmospheric loadings of trace gases and aerosol particles. It was demonstrated that monoterpenes have a major contribution to tropospheric O_3 formation, especially in cities in Siberia having high atmospheric NO_x concentration (10–20 ppb) and daytime temperatures ($>25^\circ C$) (Berezina et al., 2019). In contrast, isoprene is dominating the O_3 formation and the increasing OFP in the cities in Far East. The isoprene-derived OFP can originate from deciduous vegetation growing in city environments or nearby regions, or from an anthropogenic isoprene source. The monoterpene-derived OFP was found to be the lowest in medium-size cities and the highest in small cities (Berezina et al., 2019). The total contribution of benzene and toluene to photochemical O_3 production was found to be up to 60–70% in urbanized environments, indicating anthropogenic pollutant sources (Skorokhod et al., 2017). In addition to atmospheric chemistry, the connection between O_3 , UV radiation and health effects needs to be addressed in the populated urban environments of Siberia. Chubarova et al. (2019) estimated that winter O_3 depletion in northern regions of Siberia is not critical, but much weaker O_3 reduction in the early spring can lead to dangerous levels of erythema UV radiation (see also section 2.4.3 Natural Hazards and UV variation).

Sources and properties of atmospheric aerosols in boreal and Arctic environments

Atmospheric new particle formation (NPF) is the largest contributor to the number concentration of aerosol particles in the global troposphere. During the past couple of decades, NPF has been measured in more than 10 boreal forest sites (Kerminen et al., 2018). The annual frequency of NPF event days varies between about 10 and 30% in the boreal forest zone, being the highest in the western part of this region and lowest in the northern edge and Siberian part of it. Similar high nucleation frequencies were found at two very remote sites in boreal North America (Andreae et al., 2019). In contrast, annual NPF event frequencies below 2% were reported from central Siberia (Wiedensohler et al., 2019). Similarly, in the northern Siberia on the Arctic coast, NPF events were mainly connected with marine and coastal air masses and rarely observed in continental air masses (Asmi et al., 2016). Seasonally, NPF tend to be most frequent during spring, even though high NPF event frequencies can also be observed during summer or autumn. Winter-time NPF is rare throughout the boreal forest region. In the Arctic, NPF appears to be a major aerosol particle source from

Formatted: Font color: Auto

Formatted: Font color: Auto

Formatted: Font color: Auto

spring to summer, after which this source collapses during autumn and is practically absent over the whole winter (Freud et al., 2017). 20 years of NPF observations in a boreal forest at the SMEAR II station in Finland show higher frequency of NPF events under clear-sky conditions in comparison to cloudy conditions (Dada et al. 2017). Also oxidized organic vapors showed a higher concentration during the clear-sky NPF event days, whereas the condensation sinks and some trace gases had higher concentrations during the nonevent days.

The overall importance of atmospheric NPF in boreal and Arctic areas depends on the growth of freshly-formed particles to cloud condensation nuclei. In the boreal forest environment, both observations and model simulations indicate that the particle growth is tied strongly with the oxidation products of biogenic volatile organic compounds originating from forest ecosystems (Paasonen et al., 2018; Östrom et al., 2017). The important compound group in this respect are monoterpenes, even though also sesquiterpenes were found to have high secondary organic aerosol yields in boreal forest environments (Hellén et al., 2018). The observed particle growth rates were found to increase with an increasing particle size and to be highest in summer (Paasonen et al., 2018). The chemistry of new particle growth in the Arctic atmosphere is not well characterized, even though available observations suggest that this growth is associated mainly with biogenic emissions from high-latitude marine areas (Giamarelou et al., 2016; Heintzenberg et al., 2017; Kecorius et al., 2019).

Wildfires are an important source of particulate pollutants on a global scale and are affecting both air quality and climate (Andreae, 2019; Bondur et al., 2020). Satellite observations indicate that the annual burned area by wildfires in Russia decreased by a factor of 2.6 during 2005–2016 owing to early detection and suppression of fire sources, whereas in Ukraine the relative size of burned-out areas increased by a factor of 6–9 from 2010–2013 to 2014–2016 (Bondur et al., 2017; 2019d). For Siberia, Ponomarev et al. (2016) reported a strong increase both in number and burned areas based on satellite data, 1996–2015. Based on their data, the burned areas in Siberia doubled from 2005 to 2016. While biomass burning emissions have been measured widely over Russia (Bondur, 2016; Bondur and Ginzburg, 2016; Bondur et al., 2019d), there is still a need for further information on the atmospheric composition of wildfire emissions and related emission ratios from the Siberian region. Fire experiments provide important information on the emission and aging characteristics of smoke aerosols (e.g. Kalogridis et al., 2018).

Luoma et al. (2019) presented a detailed trend analysis for aerosol optical properties at the SMEAR II station in Finland. They found a statistically significantly decreasing trend for the scattering coefficient, and even a stronger decreasing trend for the absorption coefficient during 2006 – 2017. These trends are very likely indicative of decreasing influence of anthropogenic emissions, with the contribution from emissions containing black carbon decreasing even faster.

Measurements of carbonaceous aerosols over central Siberia during 2010-2012 showed that in fall and winter, high concentrations of such aerosols were caused by long-range transport from the cities located in southern and southwestern regions of Siberia (Mikhailov et al., 2015a). In spring and summer, pollution levels were high due to regional forest fires and agricultural burning in the Russian-Kazakh region. The variability of the background concentration of organic aerosols correlated with the air temperature in summer, implying that biogenic sources dominated the formation of organic particles at that time of the year (Mikhailov et al., 2015b). Based on a five-year study by Mikhailov et al. (2017), it seems that the atmospheric pollution originating from the biomass burning and anthropogenic emissions is significantly affecting the Siberian region. However, in summer precipitation is removing the pollutants from the air and leading to relatively clean atmospheric conditions in this region.

At circumpolar sites over the Arctic, aerosol optical properties were found to vary both seasonally and spatially (Schmeisser et al., 2018). Arctic haze aerosols in late winter and spring are characterized by increased concentrations of sulfate, whereas in summer rich organic chemistry seems to be associated with vegetation, local urban and shipping sources as well as secondary aerosol formation influenced by emissions from low latitude Siberia (Popovicheva et al., 2019a). In a longer perspective, Arctic observations show large decreases in both sulfate and black carbon concentrations since the early 1980s (Breider et al., 2017).

Observations on the elemental composition of surface aerosols on the coastal Kandalaksha Bay of the White Sea were indicative of the dominance of biogenic aerosol particles during summer time, with heavy metal concentrations in aerosols being at Arctic background levels (Starodymova et al., 2016). Increases in Ni and Cu concentrations were observed in air masses arriving from the western part of the Kola Peninsula indicative of emissions from the smelters in that region.

Black carbon and dust in the atmosphere and snow

Black carbon (BC) is a potentially large contributor to climate forcing in the Arctic region, however, the assessment of its pollution is hampered by the lack of aerosol studies in Northern Siberia (Popovicheva et al., 2019). Spatial variability of Arctic BC was studied using a harmonized dataset from 6 circumpolar Arctic observatories (Backman et al., 2017). These data suggested a significant spatial and seasonal variability (Schmeisser et al., 2018), addressing a need for more year-round data. BC observations (Sep 2014 – Sep 2016) at the Hydrometeorological Observatory Tiksi at a coast of the Laptev Sea showed a seasonal variation, with the highest concentrations (up to 450 ng/m³) from January to March and the lowest ones (about 20 ng/m³) in June and September. During winter, stagnant weather and stable atmospheric stratification resulted in the accumulation of pollution, depending also on the wind direction and air mass transport (Popovicheva et al., 2019a).

For Arctic, important sources of BC include industrial regions of Northern Europe, gas flares of the oil fields in the North Sea and Siberia, and Siberian biomass burning (Shevchenko et al., 2015; Kononov et al., 2018). For example in 2012 approximately a quarter of the biogenic BC emissions from Siberia after fire season were transported into the Arctic (Kononov et al., 2018). Popovicheva et al. (2017a) analyzed the BC origins over the Russian Arctic seas together with simulated BC concentrations. Concentrations were observed to be high ($100\text{--}400\text{ ng m}^{-3}$) in the Kara Strait, Kara Sea and Kola Peninsula, and extremely high (about 1000 ng m^{-3}) in the White Sea. It seems that the gas-flaring emissions from the Yamal-Khanty-Mansiysk and Nenets-Komi regions affected the measurements made in the Kara Strait (northerly 70°N) region, while the Near Arkhangelsk (White Sea) region was connected to the biomass burning in mid-latitudes. Combustion in Central and Eastern Europe were also identified as important BC sources.

Atmospheric aging promotes an internal mixing of BC with other aerosol constituents, leading to enhanced light absorption and radiative forcing. *In situ* observations at Arctic stations demonstrated an absorption enhancement due to the internal mixing of BC, which is a systematic effect and should be considered for quantifying the aerosol radiative forcing in this region (Zanatta et al., 2018).

Regional modelling of the Arctic aerosol pollution showed that long-range transported anthropogenic emissions and biomass burning are the main contributors to direct aerosol radiative effects in the region (Marelle et al., 2018). However, a scenario for 2050 indicates that shipping emissions in the Arctic Ocean could become the main source of surface aerosol and local flaring as a major source of BC, as the flaring already is a major source of BC in northwestern Russia. Kühn et al. (2020) assessed the effects of different BC mitigation measures on Arctic climate and showed that reducing BC emissions by the Arctic Council member states can reduce BC deposition by about 30 % compared to the current situation. A full execution of recommendation by the Arctic Council member and observer countries could reduce the annual global premature deaths due to PM by $\sim 9\%$ by 2030 (Kühn et al. 2020). Evangelidou et al. (2018) estimated the origin of elemental carbon (EC) in snow and showed that for western Siberia where gas flaring emissions is a major contributor, the model underestimation was significant. Furthermore, the model was evaluated by independent BC measurements in snow over the Arctic showed and, again, the model underestimated BC concentrations, especially in spring.

Climatically significant cryosphere effects of light-absorbing, high-latitude dust can be similar to the albedo and melt effects of BC (Peltoniemi et al., 2015; Svensson et al., 2016, 2018; Meinander et al. 2020a, 2020b). Iceland is the most significant source for European Arctic dust and plays a role in the cryosphere-atmosphere-biosphere interactions and feedbacks (Boy et al., 2019; Dragosics et al., 2016, Dagsson-Waldhauserova and Meinander, 2019). Dust storms from technogenic mining industry tailing dumps on the Kola Peninsula are also an important source of local atmospheric pollution for neighbor cities, e.g., Apatity and Kirovsk (Amosov et al., 2020). Besides regional-scale dust storms from deserts in Kazakhstan, also Mongolia and China are significant sources of aerosol pollution for these regions and for the Northern Asia.

Methodological and model developments related to atmospheric chemistry and physics

Several methods to characterize the atmospheric chemistry were introduced or improved. Motivated by the ability of atmospheric ion measurements to identify new particle formation (NPF) events in the atmosphere (Leino et al., 2016), a new classification method for atmospheric NPF was developed (Dada et al., 2018).

The new method uses both ion and aerosol particle number concentration measurements in the size ranges of 2-4 nm and 7-25 nm, respectively, is complementary to the traditional event analysis, and can also be used as an automatic way of determining new particle formation events from large data sets. Zaidan et al. (2018b) used a mutual information approach for a variety of simultaneously monitored ambient variables, including trace gas and aerosol particle concentrations and several meteorological variables, in order to identify key factors contributing to atmospheric NPF. This method can be used in the atmospheric studies also to discover other interesting phenomena and relevant variables. The NPF is directly observed by monitoring the time evolution of ambient aerosol particle size distributions. A new machine learning-based approach, a Bayesian neural network (BNN) classifier, points out the potential of these methods and suggest further exploration in this direction (Zaidan et al., 2018a).

The condensation sink, being proportional to the surface area of an aerosol population, is one of the major parameters controlling NPF. A simple model for the time evolution of the condensation sink in the atmosphere for intermediate Knudsen numbers was developed to describe the coupled dynamics of the condensing vapor and the condensation sink (Ezhova et al., 2018a). The model gives reasonable predictions of condensation sink dynamics during periods of particle growth by condensation in the atmosphere. A new empirical relation between the atmospheric cloud condensation nuclei (CCN) concentration and aerosol optical properties was derived (Shen et al., 2019), making it possible to estimate CCN concentrations at sites with continuous observations of aerosol optical properties.

Empirical models of solar radiation were developed and used for calibrations of solar radiometers (Bai, 2019). This method can be used to calibrate all kinds of solar radiometers. A solar radiation model combined with ceilometer and pyranometer measurements was used to classify clouds at SMEAR II (Ylivinkka et al., 2020) It opens new possibilities for studies of aerosol-cloud interactions.

Che et al. (2016) made an inter-comparison of three satellite (AATSR Level 2) aerosol optical depth (AOD) products (SU, ADV and ORAC) over China. The SU algorithm performs very well over sites with different surface conditions in mainland China from March to October, but slightly underestimates AOD over barren or sparsely vegetated surfaces in western China. The ADV product has the same precision and error distribution as the SU product. The main limits of the ADV algorithm are underestimation and applicability. The ORAC algorithm has the ability to retrieve AOD at different ranges, including high values of AOD, but

Formatted: Font color: Auto

its stability decreases significantly with an increasing AOD, especially when AOD > 1.0 (see also section 2.2.2 Urban air quality and megacities).

One of the major problems for both interpretation of satellite data and applications of empirical models of solar radiation is related to elevated aerosol layers in the atmosphere. It was demonstrated that their origin can be attributed at a higher confidence when back trajectories are combined with lidar and radiosonde profiles (Nikandrova et al., 2018).

Black carbon measurement methods have progressed. A representative value for the multiple scattering enhancement factor, a fundamental quantity correcting atmospheric black carbon measurement using an aethalometer, was derived for the first time in the Arctic environment (Backman et al., 2017). By analyzing BC measurements made with an Aethalometer in Nanjing, Virkkula et al. (2015) showed that the compensation parameter of a widely-used data processing method depends both on single-scattering albedo and backscatter fraction of the aerosol (see also section 2.2.2 Urban air quality and megacities). The multiple-scattering correction factor of quartz filters and the effect of filtering particles mixed in snow was estimated by Svensson et al. (2019) who applied the method for analyzing light absorption and BC in snow samples taken from the Finnish Lapland and the Indian Himalayas.

Measurement of atmospheric sub-10 nm particle number concentrations has been of substantial interest recently. A new high flow differential mobility particle sizer (HF-DMPS) was built, calibrated and operated in field conditions for one month (Kangasluoma et al. 2018). The counting uncertainties of the HFDMPs were reduced by about 50% as compared to the traditional DMPS. The HFDMPs detected about two times more particles than the DMPS in the size range of 3–10 nm. Below 3 nm, the HF-DMPS is currently limited by the inability of diethylene glycol to condense on biogenic particles. For collecting BVOC samples, a novel collection method offering portability and improved selectivity and capacity was developed. A solid-phase microextraction (SPME) Arrow sampling (Barreira et al. 2018) can be used for static and dynamic collection of BVOCs in the field conditions. A significant improvement on sampling capacity was observed with the new SPME Arrow system over SPME fibers. A fully automated online dynamic in-tube extraction (ITEX)–gas chromatography/mass spectrometry (GC/MS) method was introduced for continuous and quantitative monitoring of volatile organic compounds in air (Lan et al. 2019). The stability and suitability of the developed system was validated with a measurement campaign, and the ITEX method provided 2–3 magnitudes lower quantitation limits than established methods. Parshintsev et al. (2015) introduced a new, fast analysis method for the desorption atmospheric pressure photoionization high-resolution (Orbitrap) mass spectrometry (DAPPI-HRMS). The DAPPI results agreed with the aerosol particle number measured with an established method and was found to detect different compounds and giving complementary information about the aerosol samples.

Formatted: Font color: Auto

Formatted: Font color: Auto

Fragmentation of molecular clusters inside mass spectrometers is a significant uncertainty-source in many chemical applications. A novel model, capable of quantitatively predicting the extent of fragmentation of sulfuric acid clusters was developed (Passananti et al. 2019). The fragmentation cannot be described in terms of rate constants under equilibrium conditions, because clusters accelerate under electric fields (Zapadinsky et al. 2019). A model describing an energy transfer to the cluster internal modes caused by collisions with residual carrier gas molecules was developed. The model can be used to interpret experimental measurements done with atmospheric pressure interface mass spectrometers.

Recently, a new atmospheric observation site equipped with state-of-the-art atmospheric aerosol instrumentation was deployed in Beijing, China (Liu et al. 2020). At the Beijing University of Chemical and Technology (BUCT), the Aerosol and Haze Laboratory (AHL) was established in 2018 - 2019, providing novel insights into air pollution in a comprehensive manner. The station hosts comprehensive instrumentation to concentrations of atmospheric trace gases, aerosol particle size distributions and mass concentrations, particle chemical composition on the levels from molecules, clusters and nanometer to micrometer sized aerosol particles. For example, the first results showed increased cluster mode particle number concentrations during NPF events, whereas during haze days accumulation mode particle number concentrations were high (Zhou et al., 2020). The observations have enabled to quantify number emission factors and underlined the importance of traffic (Kontkanen et al. 2020). Daytime sulfuric acid concentrations in Beijing were typically around $4.9 \times 10^6 \text{ cm}^{-3}$ (Lu et al. 2019). During these measurements, an evidence was found on significant nighttime sulphuric acid production, yielding gaseous sulphuric acid concentrations of 1.0 to $3.0 \times 10^6 \text{ cm}^{-3}$ (Guo et al., 2021). For further results, see also section 2.2.2 Urban air quality and megacities.

Besides Beijing, measurements have been performed in several other locations inside the PEEX area. We used novel instrumentation to measure new particle formation and its precursors at the background Fonovaya station in the Tomsk region (Russia, Siberia), at the Värriö subarctic research station (Finland), in Ny-Ålesund (Svalbard, Norway) and on the German icebreaker, the Polarstern, during the MOSAIC project. As an example, the first results from Fonovaya station are shown in Fig. 2. Thanks to these deployments, in the next years we will be able to understand the identity of NPF precursors in those remote places. This will help us to elucidate the human impact on aerosol formation and thereby on aerosol-cloud interactions at high latitudes. In Siberia, we will finally understand why new particle formation occurs infrequently, and hopefully also identify the human role in this phenomenon. In the Arctic, we will understand the marine influence on NPF and will find out the detailed mechanism that leads to the formation of small clusters that which initiate NPF.

Model developments were made at several scales. Aerosol-radiation and aerosol-cloud interactions are among the main sources of uncertainties in climate models, and detailed information on anthropogenic aerosol number emissions is needed to improve this situation. Anthropogenic aerosol number emissions in

Formatted: Font: 11 pt, Font color: Auto

current large-scale models are usually converted from corresponding mass emissions in pre-compiled emission inventories using very simplistic methods. In the global aerosol-climate model ECHAM-HAM, the anthropogenic particle number emissions, converted originally from the AeroCom mass emissions, were replaced with recently-formulated number emissions from the Greenhouse Gas and Air Pollution Interactions and Synergies (GAINS) model (Xausa et al., 2018). However, revisions are still needed in the new particle formation and growth schemes currently applied in global modeling frameworks.

For regional and urban scales, a fully integrated /online coupled meteorology-chemistry-aerosol model Enviro-HIRLAM was developed (Baklanov et al., 2017) and tested for several applications in Europe, Russian Arctic and China (Shanghai) (Mahura et al., 2018, 2019). Key issues for seamless integrated chemistry–meteorology modeling for Earth System prediction were analyzed and formulated (Baklanov et al., 2018), highlighting the scientific issues and emerging challenges that require proper consideration to improve the reliability and usability of these models for three main application areas: air quality, meteorology, and climate modeling. Baklanov et al. (2018) also presents a synthesis of scientific progress in the form of answers to nine key questions, and provides recommendations for future research directions and priorities in the development, application, and evaluation of online coupled models.

2.2.2 Urban air quality and megacities (Q5)

The rapid urbanization and growing number of megacities and urban agglomerations requires new types of research and services that make the best use of science and available technology. There are urgent needs for examining what the rising number of megacities means for air pollution and local climate, and what effects these changes have on global climate (Baklanov et al., 2016). Such integrated studies and services should assist cities in facing hazards, such as storm surge, flooding, heat waves and air pollution episodes, especially in changing climates (WMO, 2019). We discuss here the recent observation on the atmospheric pollution in China and Russia.

Air quality in China – recent observations

China is one of the regions with highest concentrations of fine $PM_{2.5}$ in the world (Wang et al., 2017a). This has serious consequences on air pollution and the associated visibility reduction (haze) and adverse health effects (Zhao et al., 2017). The number of haze days in China has been growing during the recent decades, but detailed understanding of the factors governing the occurrence of haze is still not clear (Wang et al., 2019). Both NO_2 and SO_2 concentrations showed increasing trends during the 2004–2012 period, and these trends could be linked to increased power plant and traffic emissions (Wang et al., 2019). A key feature of haze formation seems to be an increased inorganic fraction of the aerosol, suggesting that the reduction of nitrate, sulfate and their precursor gases would improve air quality and visibility in China (Wang et al., 2019). In northern China, $PM_{2.5}$ concentrations declined over the period 2013–2017, and approximately half

Formatted: Font color: Auto

of the inter-annual variability in this region was attributed to atmospheric circulation changes (Li et al., 2020b). The maximum daily 8-h average O₃ concentrations increased over most of northern China during the same time period, with again large influences due to atmospheric circulation on daily basis (Liu et al., 2019b).

Compared with most other urban environments investigated so far, measurements in urban China demonstrated a relatively frequent occurrence of atmospheric new particle formation (NPF), and the observed NPF events were typically characterized by high particle formation rates and strongly size-dependent growth of newly-formed particles (Kulmala et al., 2016b; Wang et al., 2017b; Chu et al., 2019). Since the first reported sub-3 nm particle measurements in China a few years ago (Xiao et al., 2015), new insight into the formation pathways of molecular clusters and their growth have been obtained, including the relative roles of gaseous sulfuric acid, amines, ammonia and organic vapors in these processes (Yao et al., 2018; Yan et al., 2021). While high pre-existing particle loadings appear to suppress NPF during severe haze periods in Chinese megacities, it is unclear how NPF is possible at all under less but still quite polluted conditions typical for these environments (Kulmala et al., 2017). Overall, the available observations suggest NPF to be a major source of aerosol particles in urban China, with potentially large effects on haze formation (Kulmala et al., 2021) and cloud properties (Chu et al., 2019).

Urban measurements of particle number size distributions give deep understanding into the sources and atmospheric processing of fine particles. The longest urban continuous record is from the SORPES station in the Yangtze River Delta (Qi et al., 2015), covering almost a decade of measurements, whereas the broadest size range (1.5 nm – 1 µm) was measured in the winter Beijing atmosphere (Zhou et al., 2020). The latter study found clear differences in particle sources in different size ranges: NPF was in general the largest source of clusters and nucleation mode (<25 nm) particles, while traffic contributed to all the size ranges and dominated both cluster and nucleation modes on haze days. Aitken mode (25–100 nm) particles originated mainly from local emissions, with additional contributions from regional and transported pollution as well as from the growth of nucleation mode particles. Regional and transported pollution were identified as the main source of accumulation mode (>100 nm) particles.

Air pollution and chemical transformation, including annual and seasonal variations of the concentrations of atmospheric constituents, were analyzed for North China for the period 2005–2015 (Bai et al., 2018a). A photochemical link that related the production of fine PM and O₃ to VOCs was detected, and this mechanism was found to be prominent in summer. An intensive measurement campaign (SORPES station, Yangtze River Delta) was carried out to investigate sulfate formation and associated nitrogen chemistry (Xie et al., 2015). That study highlighted the effect of NO_x in enhancing the atmospheric oxidizing capacity, and indicated a potentially very important impact of increasing NO concentrations on particulate pollution formation and regional climate change in East Asia. In Changzhou, a highly-populated city in the Yangtze River Delta, primary organic aerosol concentrations outweighed secondary ones, indicating an important role

Formatted: Font color: Auto

Formatted: Font color: Auto

Formatted: Font color: Auto

Formatted: Font color: Auto

of local anthropogenic emissions in aerosol pollution (Ye et al., 2017). The measurement also showed the abundance of organic nitrogen compounds in water-soluble organic aerosol, suggesting that these compounds are likely associated with traffic emissions.

Aerosol impacts on warm cloud properties were investigated over three major urban clusters in Eastern China and East China Sea using multi-sensor satellite observations (Liu et al., 2017, 2018). In addition to the amount of aerosol, evidence was provided that aerosol types and environmental conditions need to be considered to understand the relationship between cloud properties and aerosols. Aerosol-cloud interactions were found to be more complex and of greater uncertainty over land than over ocean.

The atmospheric boundary layer (ABL), and especially its dynamic behavior, is central to the evolution of near-surface air pollution. Using atmospheric observations combined with theoretical arguments, Petäjä et al. (2016) proposed a feedback mechanism connecting ABL properties with PM. According to such mechanism, high concentrations of PM enhance the stability of an urban boundary layer (BL) decreasing its height, thus causing further accumulation of pollution inside BL. Ding et al. (2016a) and Wang et al. (2018b) demonstrated an important role of BC aerosols in this feedback using model simulations combined with observations. A tight connection between the BL height and pollutant concentration, and indications of the presence of the above feedback mechanism, was also found based on comprehensive observations made on a 325-m tower in Beijing (Wang et al., 2020). In order to understand these feedbacks, Kulmala (2018) and Hari et al. (2016) emphasized the crucial role of continuous, comprehensive measurements on a network of flagship stations in tackling the air pollution problem in urban China and megacities elsewhere in the world. They also introduced a so-called “Stations for Measuring Atmospheric and Earth surface Relations” (SMEAR) concept, which consists of integrated atmospheric and ecosystem observations allowing the analysis of Earth surface – atmosphere feedbacks and interactions. The first SMEAR-type station in China, the SORPES station located in the Yangtze River Delta, has been operating since 2011 (Ding et al., 2016b).

Anthropogenic emissions and environmental pollution in Russia

In the complex situation of the plurality of emissions, an important research task remains in the Moscow megacity environment for the assessment of the air quality and potential sources through aerosol composition analyses. Moscow aerosol pollution has been studied using a special AeroRadCity-2018 experiment (Chubarova et al., 2019) and satellite data with the application of new MAIAC/MODIS aerosol algorithm with a 1-km resolution (Zhdanova et al., 2020). An advanced source apportionment for this environment was performed using combined Fourier-transform infrared spectroscopy data and statistical principal component analysis (Popovicheva et al., 2020b). The main principal component loadings revealed the source impacts of transport, biomass burning, biogenic, dust and secondary aerosol in spring. Identification of biomass burning-affected periods discriminated the daily aerosol composition change with respect to air mass transport and number of fires detected in the surrounding areas. Measurements of

Formatted: Font color: Auto

Formatted: Font color: Auto

Formatted: Font color: Auto

particulate BC were conducted at an urban background site (Meteorological Observatory of MSU) during the spring period of 2017–2018 (Popovicheva et al., 2020c). The mean BC concentrations displayed significant diurnal variations, with a poorly prominent morning peak and minimum at daytime. BC mass concentrations were higher at nighttime due the shallow boundary layer and intensive diesel traffic. The aerosol optical thickness (AOT) over Moscow showed a pronounced seasonal cycle, with a summer maximum and winter minimum (Chubarova et al., 2016a). It was found that during 2001–2014, the monthly-mean values of AOT declined by 1–5% per year, and this decline was attributed to decreased emissions of aerosols and their precursors.

In general, the atmospheric environment over remote areas of Siberia and Northern Asia is relatively clean compared with other surrounding regions of Asia and Eastern Europe (Baklanov et al., 2013). However, air pollution from Siberian industrial centers poses significant environmental threats. For Siberian cities (e.g., Norilsk, Barnaul, Novokuznetsk), the air quality is among the worst in the Russian and European cities. Similar to Arctic cities, stable atmospheric stratification and temperature inversions dominate for more than half a year. This leads to pollution accumulation near the surface, which influences ecosystems and people. Moreover, not only severe climatic conditions, but also manmade impacts on the environment in industrial areas and large cities have intensified. The impacts manifest themselves as the pollution of environment, land use changes, hydrodynamic regimes and local climate. Ultimately, these impacts feed back to people, affecting their health and well-being.

The Russian part of the Barents Euro-Arctic region includes severe emission ‘hot spots’ for air pollutants. The Kola Peninsula, despite the presence of areas with undisturbed nature in the eastern part, is the most industrially developed and urbanized region in the Russian Arctic. The main polluters are the smelters of the Severonickel (Monchegorsk, central part of the peninsula) and the Pechenganickel (Nickel and Zapolyarnyi near the Russian-Norwegian border) enterprises. For comparison, emissions of SO₂ from the Nickel smelter alone are 5–6 times larger than the total Norwegian emissions (NILU, 2013). In 2015 the Norilsk Nickel in Siberia - the biggest mining and the metallurgical complex - emitted about 1.9 million tons of SO₂ (GGO, 2016). With the nickel factory (located in the southern part of the city), copper factory (just to its north) and metallurgical plant (12 km to the east), the city of Norilsk is influenced by heavy industry no matter which way the wind blows. The Blacksmith Institute declared in 2007 that Norilsk is one of the top 10 worst-polluted places in the world. The impacts of emissions are manifested as deterioration of forest ecosystems and acidification of soils and surface waters (Derome and Lukina, 2011), even at considerable distances from the smelters. Heavy metals and alkaline pollutants contaminate areas around the sources of pollution within a few hundred kilometres, while acid sulphates can be transported over long distances (Mahura et al., 2018).

A recent analysis on the total deposition and loading on the population in North-Western Russia and Scandinavian countries caused by the continuous sulfur emissions from the Cu-Ni smelters in Murmansk indicates the dominance of wet deposition, especially in winter time (Mahura et al., 2018). North-Western

Formatted: Font color: Auto

Russia is influenced more by the Severonikel emissions compared with countries in the Scandinavian Peninsula. The cities of the Murmansk region (Kola Peninsula) are under highest impacts. On a yearly scale, the individual loadings on population are at the largest level (up to 120 kg/person) in the Murmansk region, much lower (15 kg/person) in northern Norway, and the smallest (< 5 kg/person) in eastern Finland, Karelia Republic and Arkhangelsk region. Distinct seasonal variability was identified, with the lowest contribution during summer and the highest contribution during winter-spring in Russia, during spring in Norway, and during autumn in Finland and Sweden.

The annual yearbook "The State of Atmospheric Pollution in Cities on the Territory of Russia" for 2018 (Roshydromet and GGO, 2019) states the highest atmospheric emissions of PM were observed in Siberian and Ural cities. In Novokuznetsk and Omsk, the observed PM was the highest ($> 30\,000$ tons per year) while emissions from other cities such as Angarsk and Chelyabinsk were lower ($< 20\,000$ tons per year). Note that in the 2015-2019 yearbooks, emissions from only stationary sources were provided due to revisions (approved and implemented in November 2019 by the Russian Ministry of Natural Resources and Ecology, MNRE) of methods applied for estimation of emissions into the atmosphere from mobile sources. Depending on a source type, different methods to calculate emissions are applied (MNRE, 2019). For the gaseous compounds, such as SO_2 , the maximum emissions included very high from Siberian cities (e.g. Norilsk, Novosibirsk, Novokuznetsk, Omsk, Ufa, Irkutsk, Angarsk) and from North-West Russia cities (Zapolyarny, Nickel, Monchegorsk). High NO_2 emissions were observed in Novosibirsk, Omsk, Angarsk and Chelyabinsk. The CO integral urban emissions depend on a city size. These varied from less than 10 Gg yr^{-1} (for small regional centers like Vladimir, Kursk, Samara) to 406 and 804 Gg yr^{-1} for large metropolitan areas such as St. Petersburg and Moscow. As a whole, an analysis of spatio-temporal variation of trace gases in the boundary layer over Russian cities indicated significant emission variations between the urban environments and remote sites (Elansky et al., 2016).

Cities, being not isolated systems, may distribute as much pollution to the surrounding areas as they receive it from outside them or from remote regions. The analysis of the transboundary atmospheric transport between Russian Siberia and bordering countries (e.g. China, Kazakhstan, and Mongolia) is part of a mutual risk assessment for urban areas/ cities and their surroundings. For example, the city of Ulaanbaatar (Mongolia) suffers from high levels of pollution due to excessive airborne particulate matter emanating from coal combustion mixed with traffic emissions and resuspended soil dust, resulting in variable chemical source profiles (Gunchin et al., 2019). Long-range transport from remote sources might be an additional contributor. Moreover, there are indications that such transport of biomass burning emissions from Siberia could lead to pollution episodes and impact on surface ozone as far as in western North America (Jaffe et al., 2004).

2.2.3 Weather and atmospheric circulation (Q6)

Formatted: Font color: Auto

The observed evolution of weather and climate represents the combined effects of external forcing (changes in the concentrations of greenhouse gases and aerosols etc.) and internal variability, related to a large extent to the atmospheric circulation. It is also affected by local factors, particularly urban heat islands in cities. Here we discuss these interconnected processes, focusing on cold and warm episodes, cyclone density and atmosphere-ocean interaction, effects of circulation on temperature and moisture, cloudiness in the Arctic, and boundary layer dynamics relevant to the Arctic-boreal region.

Cold and warm episodes

The Arctic warming, and the Arctic amplification, have been associated with changes in atmospheric large-scale circulation together affecting the European winter temperatures. In large parts of Europe, severe cold (warm) winter events are significantly correlated with warm (cold) Arctic episodes (Vihma et al., 2020). Air mass trajectory analysis revealed that air masses associated with extreme cold (warm) events typically originate from over continents (sea areas). Despite Arctic and European-wide warming, winter cooling has occurred in northeastern Europe in cases of air masses arriving from the southeast (Vihma et al., 2020).

Cyclone density dynamics and atmosphere-ocean interaction

Transporting large amounts of heat and moisture from mid-latitudes to the central Arctic, synoptic-scale cyclones are vital for the Arctic climate system. Recent findings, based on atmospheric reanalysis, above all the global ERA-Interim reanalysis available from 1 January 1979 to 31 August 2019, are summarized below. During 1979–2016 in winter (Dec, Jan, Feb), the cyclone density increased in the areas around Svalbard and in northwestern Barents Sea, but decreased in southeastern Barents Sea (Wickström et al., 2020). This is related to a shift to more meridional winter storm tracks in the Norwegian, Barents and Greenland Seas. The shift is favored by a positive trend in the Scandinavian Pattern and, in the areas north of Svalbard, by a significant increase in the Eddy Growth Rate (Wickström et al., 2020).

Numerical model simulations of the storm activity in the White, Baltic and Barents Seas were analyzed for the period 1979–2015 (Myslenkov et al., 2018). A high interannual variability in the storm number was observed for all studied seas. No significant trends in the storm number during the period 1979–2015 were found in the studied sea areas. On average, the connection with global atmospheric circulation is stronger for the Baltic Sea than for the other two seas. Also, the future changes of wind wave climate were analyzed. According to the RCP8.5 scenario, in the second part of the 21st century the number of storm events will rise in the Baltic and Barents Seas.

In the Bjerknes compensation, changes in atmospheric heat transport co-occur with opposing changes in ocean heat transport. Observations and model simulations indicate a central role for ocean-atmosphere heat exchange in the Barents Sea area in maintaining this compensation in the Arctic (Bashmachnikov et al., 2018a, 2018b).

Circulation effect on temperature

The effect of atmospheric circulation on temperature trends in years 1979-2018 was studied by Räisänen (2019, 2021) using a trajectory-based method. He found that circulation trends had reduced the annual mean warming during this period in western and central Siberia locally by over 1°C, with a much larger cooling effect in autumn and winter (Fig. 3). His findings also confirmed a circulation-induced amplification of warming over the Barents and Kara seas particularly in winter. Yet, in most areas the circulation-related temperature trends have varied strongly from month to month, leaving only a relatively small effect on the annual mean temperature trends. The residual warming obtained after subtracting the circulation effect therefore tends to have a smoother seasonal cycle than the observed temperature trends, in better agreement with the multi-model mean trends in the CMIP5 simulations (Taylor et al., 2012).

Circulation effect on moisture

The effects of large-scale circulation on moisture, cloud and longwave radiation occur mostly via the impact of horizontal moisture transport (Nygård et al., 2019). Evaporation is typically not efficient enough to shape those distributions, and much of the moisture evaporated in the Arctic is transported southward (Nygård et al., 2019). Strong moisture transport events avail a large part of the northwards moisture transport. The meridional net transport is only a small part of the water vapor exchange between the Arctic and mid-latitudes (Naakka et al., 2019). When a high-pressure pattern across the Arctic Ocean from Siberia to North America is lacking, the amounts of moisture, clouds and downward longwave radiation are anomalously high near the North Pole (Nygård et al., 2019). Using vertically-integrated water vapor as a metric, the Arctic (north of 70°N) has experienced a robust moistening trend since 1979, and in absolute numbers this trend is the smallest in March and the largest in August (Rinke et al., 2019). However, the relative trends are the largest in winter. Although different atmospheric reanalysis are consistent in spatiotemporal trend patterns, they scatter in the trend magnitudes.

Analysis of moisture and aridity estimated using the web-GIS "CLIMATE" and the ECMWF ERA-Interim reanalysis data for Southern Siberia (50-65 °N, 60-120 °E) from 1979 to 2010 with a $0.75^\circ \times 0.75^\circ$ grid resolution showed that the mountain regions of Eastern Siberia have been come more arid each month during the last 30 years (Ryazanova and Voropay, 2017). In Western Siberia, aridity increased in May and decreased in June, while in the other months positive and negative trends were found. The greatest differences in the trends of the aridity index, air temperature and precipitation were observed in July.

Cloudiness in Arctic

The climatology and inter-annual variability of Arctic cloudiness remains a wildcard in regional climate change projections. Both climate models and satellite data products need *in situ* observations for calibration and validation. Chernokulsky et al. (2017) and Chernokulsky and Esau (2019) collected and processed

manual cloud observations from meteorological stations in the PEEX area. The cloud records in the Arctic are available since the end of the 19th century. Since 1936, cloud observations representatively cover the Eurasian Arctic. This permits reconstructions of cloud type and cloud cover climatologies as well as studies of inter-decadal variability of cloudiness. A problem of a special interest is related to the co-variability of the total cloud cover and sea ice concentration or extent. Both clouds and sea ice affect the surface heat balance through surface albedo, but their feedback mechanisms, dynamical impacts and climate sensitivities are different. Chernokulsky et al. (2017) found that the annual-mean total cloud cover (TCO) decreases during warmer climate periods with a lower sea ice concentration, but increases over sea ice in the Barents Sea as more moisture is transported into the Arctic at higher temperatures. Furthermore, the increasing TCO reduces the deficit of the surface heat, and the intra- and inter-annual variability of TCO over solid ice is higher than that over open water (Chernokulsky et al. 2017). Long-term cloud climatological analysis based on meteorological observations of the total and low cloud cover and cloud types from the Barents Sea to the Chukchi Sea showed that significant transitions between cloud types has been taken place, especially the low-level stratus and stratocumulus types have been transformed to convective cloud types (Chernokulsky and Esau, 2019). Chernokulsky and Esau (2019) addressed that their results are relevant for understanding Arctic cloud processes and feedbacks, and that new knowledge is needed to connect the changes in the Arctic radiation balance with the Arctic cloud cover—cloud type climatology.

Boundary layer dynamics and urban heat islands

On the background of accelerated and amplified Arctic warming, anthropogenic heat release and metabolism of cities add up to persistent warm temperature anomalies in urbanized areas (Fig. 4). Indeed, if the climate change forcing approaches 2 W m^{-2} , the urban heat forcing could be $10\text{--}100 \text{ W m}^{-2}$ (Konstantinov et al., 2018). The urban heating trapped in the shallow PBLs is potent to rise the local temperatures by 1°C to 10°C and even more. This local climate phenomenon is known as the urban heat island (UHI) (Esau et al., 2020). A series of *in situ* and satellite UHI studies in the northern cities revealed strong and persistent warm temperature anomalies in almost all of 28 northern West Siberian cities (Miles and Esau, 2017), in 5 cities covered by the UHIARC network (Konstantinov et al., 2019; Varentsov et al., 2018a) and in 57 Scandinavian cities (Miles and Esau, 2020). The mean wintertime temperature anomalies, the UHI intensity, varied from 0.8 K to 1.4 K and had extreme intensities of up to 7 K during cold anticyclone weather conditions. The complete dataset of surface UHI intensity derived from MODIS LST data products is freely available and published in Miles (2020). Such a UHI induced strong mediation of cold temperature spells might cause significant socio-economic and environmental impacts in the cities (Konstantinov et al. 2018, Fig. 4). A survey of other UHI studies in 11 Arctic cities and towns confirmed that even relatively small cities at high latitudes may exhibit intensive UHIs. A recent analysis confirms the important role of the surrounding temperature in explaining spatial-temporal variation of UHI intensity (Miles and Esau, 2017). The major contribution to the UHI was revealed for water, sparse vegetation, grassland and scrubland. The

mechanisms and pathways of the UHI maintenance requires involvement of numerical experiments with turbulence-resolving models to advance the understanding of the local climate features (Urban Heat Islands - UHIARC dataset see http://urbanreanalysis.ru/uhi_arc.html). We would need a denser meteorological network, especially high quality temperature data, to better understand the urban climatology and the thawing processes in urban soils and to better assess climatic trends relevant to Arctic societies and welfare (Konstantinov et al. 2018).

Urban climate anomalies may cause more extreme weather and climate phenomena in densely populated megacities. The Moscow agglomeration – the largest megacity in the boreal continental climate within the PEEEX domain – demonstrates profound effect of interactions between the UHI and urban winds, known as a cross-over effect (Varentsov et al. 2018b). The UHI creates an urban heat “dome” with near-surface air inflow into the urban central districts and air outflow at higher levels in the atmosphere. The air uplift in the urban dome is connected to the increase in summer rainfall at the lee side and over the central urban districts. Stable atmospheric stratification over rural area is strengthened by the downwind air motions coming from the urban region.

Atmospheric boundary layer over the Arctic Ocean has been studied on the basis of tethered sounding observations over sea ice (Palo et al., 2017) and research aircraft observations over the open ocean and sea ice (Suomi et al., 2016). Palo et al. (2017) found that in spring and summer, the occurrence and properties of temperature inversions were controlled by the surface melt and warm air advection rather than surface net radiation. During snow/ice melt, temperature inversions were frequently surface-based, and equally strong as winter inversions over the Arctic Ocean. To better understand atmospheric boundary layer processes in the Arctic, Suomi et al. (2016) developed a method to measure wind gusts from a research aircraft. It allows wind gust observations at altitudes not reached by traditional weather mast observations. The observed gust factors strongly depended on the surface roughness, which differed for sea ice and the open ocean.

2.3 ARCTIC-BOREAL AQUATIC SYSTEM

We discuss the recent results on Arctic sea ice dynamics and thermodynamics, snow depth and sea ice thickness, sea ice research supporting navigation, and rare elements in snow and the ocean sediments, especially from the perspective of improvements in the observation and modelling methods (Q7, section 3.3.1). We introduce new results on the Arctic marine ecosystem and focus on the primary production and carbon cycle (Q8, section 3.3.2.). In section 3.3.3 for the Arctic – boreal lakes and rivers, we discuss the browning of lakes and lake sediment with a special attention on the Selenga River system of Lake Baikal (Q9).

2.3.1 Changing water systems, snow, sea ice and ocean sediments (Q7)

Sea ice and thermodynamics with atmospheric and ocean dynamics

Referring to the earlier discussion in section 2.2.3 on atmospheric circulation, we address here how the sea ice dynamics closely interacts with the atmospheric and ocean dynamics. A rapid decrease in the Arctic Ocean ice cover, particularly in the Barents and Kara Seas, has been taking place since the late 1970s simultaneously with the cooling of winters in central Eurasia (McCusker et al., 2016). This unexpected winter cooling is related to increasing northeasterly winds over the southeastern flank of an anomalous high that has developed over the northwestern coast of Russia (McCusker et al., 2016; Mori et al., 2019, Räisänen 2021). However, the causality between the atmospheric circulation changes and the Arctic sea ice decrease is debated. Observations suggests a strong correlation between these two, but climate model simulations forced by reduced ice cover produce much weaker circulation changes than observed, resulting in only weak cooling in central Eurasia (Mori et al., 2014, 2019; McCusker et al., 2016). This suggests that either most models are underestimating the sensitivity of the atmospheric circulation to sea ice decrease, supported by Romanowsky et al. (2019), or that the circulation change has not been primarily caused by the decreasing sea ice. In the latter case, the correlation between the reduced ice cover and atmospheric circulation would mainly reflect the effect of circulation on sea ice. In support of this, Blackport et al. (2019) showed that a reduced sea ice coincides with an anomalous heat flux from the atmosphere to the ocean, and that on the sub-seasonal time scale, anomalies in atmospheric circulation tend to precede rather than follow those in sea ice. Thus, while the reduced sea ice might partly explain the observed changes in atmospheric circulation (Mori et al., 2019), the effect of circulation on sea ice appears to be stronger than the effect of sea ice on circulation.

Considering atmosphere-ice interactions, Jakobson et al. (2019) studied the linkages between sea ice concentration (SIC), atmospheric stratification, surface roughness and wind speed at the 10-m height (W10) and 850-hPa level (W850). In all the seasons except summer, a reduction in SIC favored reduced atmospheric stratification and aerodynamic surface roughness, which resulted in a stronger W10. The effect was the strongest in autumn, and positive trends in W10 and its ratio to W850 typically occurred in regions with the strongest negative trends in SIC. The relationships were stronger on inter-annual than on sub-seasonal time scales. Large-scale atmospheric circulation, characterized, e.g., by the Dipole Anomaly (DA), has also contributed to sea ice dynamics. A positive polarity in DA has contributed to the recent rapid loss of summer sea ice in the Pacific part of the Arctic Ocean by bringing warmer air masses from the south and transporting more ice towards the north enhancing the ice-albedo feedback (Lei et al., 2016). Another example of ice dynamics affecting the ice-albedo feedback was the weakened Transpolar Drift Stream in summer 2013. It reduced sea ice transport out of the Arctic Ocean, and restrained ice melt because of the low air temperatures, weakened albedo feedback, and a relative small oceanic heat flux in the central Arctic (Lei et al., 2018).

Solar radiation, being the main forcing factor for a sea ice melt in summer, is difficult to parameterize in thermodynamic models. This is due to the large variability in the optical properties of sea ice in space and

Formatted: Font color: Auto

time. A two-stream model provides a time-efficient parameterization of the apparent optical properties (AOPs) for ponded sea ice, accounting for both absorption and scattering, and has a potential to be implemented into sea-ice thermodynamic models to explain the role of melt ponds in the summer decay of Arctic sea ice (Lu et al. 2016). This model was used to investigate the role of solar radiation in the Arctic sea ice during the melting season considering layers of melt ponds, underlying sea ice, and ocean beneath the ice. It was found that the energy absorption profiles depend strongly on the incident irradiance and ice scattering, but only weakly on the pond depth. It seems that the incident solar energy is largely absorbed by the melt pond rather than by the underlying sea ice (Lu et al., 2018a). The model was further applied to investigate the influence of a surface ice lid on the optical properties of a melt pond. The thickness of the ice lid determines the amount of solar energy absorbed. Visual inspections on the color of refreezing melt ponds also help to judge the significance of the influence of the ice lid. This will allow for an accurate estimation on the role of surface ice lid during field investigations on the optical properties of melt ponds (Lu et al., 2018a). The modelled pond color agrees with field observations from the Arctic sea ice in summer. The analysis of pond color is a new potential method to obtain ice thickness in summer, however, more validation data and improvements to the radiative transfer model would be needed (Lu et al., 2018b).

Snow depth/mass and sea ice thickness

Snowpack on sea ice has a crucial role in insulating the sea ice from the colder atmosphere, accordingly reducing sea ice growth in winter, effectively reflecting the incoming solar radiation, reducing sea ice melt in spring and summer and contributing to its formation. The replacement of snow fall by rain strongly enhances the ice-albedo feedback in the Arctic Ocean (Dou et al., 2019). Shalina and Sandven (2018) refined the description of snow depth on sea ice in the central Arctic, providing new snow depth data for the Arctic marginal seas. High autumn and winter precipitation and thinning Arctic sea ice make snow-ice formation prevalent in the Atlantic sector of the Arctic (Merkouriadi et al., 2017).

Advance has been made in applying thermistor string based autonomous high-resolution Snow and Ice Mass Balance (IMB) Array (SIMBA) buoys to measure snow depth and ice thickness (Figs. 5 and 6.). SIMBA has a lower cost, allowing deployment in large numbers (Lei et al., 2015). The determination of snow depth and ice thickness from SIMBA temperature profiles has so far been largely a manual process. A SIMBA-algorithm was developed to process SIMBA data automatically (Liao et al., 2018), assuming a fixed snow-ice interface. Snow-ice formation results in snow-ice interface moving upward. The SIMBA-algorithm was further developed to tackle the moving interfaces (Cheng et al., 2020). The developed SIMBA-algorithm works well in cold condition for lakes and Polar Oceans. For Polar Oceans, the snow and ice are close to isothermal during summer, which prevents the identification of interfaces on the basis of the temperature gradient. Under such conditions, thermodynamic modelling yields valuable information on snow depth and ice thickness (Tian et al., 2017).

A challenge in sea ice thermodynamic modelling is the uncertainty in the magnitude of the oceanic heat flux at the ice base, especially for land-fast sea ice. Yang et al. (2015) applied a one-dimensional thermodynamic model to investigate impact factors on land-fast sea ice in the East Siberian Sea. The modelled snow cover was less than 10 cm, having a small influence on the ice thickness, but surface albedo and oceanic heat fluxes were critical.

Also in the terrestrial Arctic and boreal zone, there is a need for a better efficiency and coverage of an *in-situ* snow observation network. Snow cover and snow mass are fundamental parameters for global energy and water cycles, and the changes in the regional snowpack have societal impacts like on amount of drinking water or capacity for the hydropower generation (Bormann et al., 2018). Snow depth data in the Arctic region are available from the synoptic weather stations and snow mass data are systematically collected from the snow courses, as demonstrated in Extended Data (fig. 2) by Pulliainen et al. (2020). The use of automatic and cost-effective measurements together with harmonized snow measurement practices is the way forward. A survey on a harmonized snow monitoring in Europe demonstrated that crucial parameters for operational services, such as parameters characterizing precipitating and suspended snow, are measured by 74% of the European snow network contributors (COST Action ES1404), but the parameters characterizing the snow microstructural properties, electromagnetic properties and composition are currently measured by only 41%, 26% and 13%, respectively, of the network contributors (Pirazzini et al., 2018). The observations at the continental scale, so far, demonstrate a widespread snow-cover retreat since the 1970s across the Northern Hemisphere, particularly in the Arctic (Derksen et al., 2012; Bormann et al., 2018). On the contrary, the results from the mountains are mixed and there is no consistent picture of what is happening at the regional scale (Bormann et al., 2018). Pulliainen et al. (2020) provided new insight into the seasonal snow mass and its trend by using a bias-corrected GlobSnow 3.0 estimates. Pulliainen et al. (2020) is now able to demonstrate different continental trends based on the 39-year satellite record: a decrease in North America, a negligible trend in Eurasia, and a high regional variability in both areas.

Sea ice research supporting navigation

Recent research has addressed emerging opportunities for Arctic navigation and the importance of operational sea ice analysis. Lei et al. (2015) showed trends along the Arctic Northeast Passage (NEP) and demonstrated an increase in the spatially-averaged length of the open period (the ice concentration less than 50%) from 84 days in the 1980s to 114 days in the 2000s. The summer sea ice along the High-Latitude Sea Route (HSR) north of the eastern Arctic islands has decreased during the last decade, with the ice-free period reaching 42 days in 2012. The HSR avoids shallow waters along the coast, which easier the access to for deeper-draft vessels (Lei et al., 2015). Considering operational sea ice analyses for the Bohai Sea, work has been done to combine thermodynamic modelling and Earth Observation (EO) data from synthetic aperture radar (SAR) and microwave radiometers (Karvonen et al., 2017). The SAR-based discrimination between sea ice and open-water works well, and areas of thinner and thicker ice can be distinguished. However, a

larger comprehensive training dataset is needed to set up an operational algorithm for the estimation of sea ice concentration and for the weighting scheme for sea ice thickness (Karvonen et al., 2017).

Multi-decadal Arctic sea-ice state estimates are important for the strategic planning of Arctic navigation. These estimates are usually based on climate models with a thermodynamic-dynamic sea-ice models. An up-to-date assessment of large-scale sea-ice models was with the aid of sea-ice models as a climate model component, a comprehensive review was carried out by Leppäranta et al. (2020). Specifically, Uotila et al. (2015) found that a model with the subgrid-scale sea-ice thickness distribution reproduces more realistic sea ice and upper ocean, due to better captured spring evolution, than a model with just single sea-ice thickness category. In terms of validity of initial conditions for multi-decadal predictions, Uotila et al. (2019) analyzed a set of ocean reanalysis products, including Arctic sea ice, and found that the multi-model set mean is a useful product as a state estimate. This finding increases confidence toward the use of the combination of ocean reanalysis for both initialization of multi-decadal predictions and analysis of multi-decadal variability.

Ocean floor and Sediments: composition and fluxes

A significant content of illite and muscovite among layer silicates in most of the ice-rafted sediments samples taken from selected Arctic regions suggests that sources of the sedimentary material are mainly mineralogically similar to modern bottom sediments of the East Siberian and Chukchi seas, as well as presumably sediments of the eastern Laptev Sea. A significant kaolinite fraction in the samples from the North Pole area can be caused by the influx of ice-rafted fine-grained sedimentary material from the Beaufort or Chukchi seas, where kaolinite is supplied from the Bering Sea. The samples contained variable proportions of erosion products of both mafic and felsic magmatic rocks and/or sufficiently mature sedimentary rocks (Maslov et al., 2018a).

Quantification of CH₄ sources is fundamental information for the climate change mitigation (Fletcher and Schaefer 2019). Methane stored in ocean floor reservoirs can reach the atmosphere in the form of bubbles or dissolved in water. Methane hydrates could destabilize with rising temperatures, further increasing greenhouse gas emissions in a warming climate. Subsea permafrost and hydrates in the East Siberian Arctic Shelf (ESAS) are acting as a substantial carbon pool, and source of methane to the atmosphere. Annual methane emissions of the region varies from 0.0 to 4.5 TgCH₄ yr⁻¹ estimated by Berchet et al. (2016). Yasunaka et al. (2018) estimated the monthly air-sea CO₂ fluxes in the Arctic Ocean and adjacent seas located north of 60 degrees N for the period 1997 2014 and ended up to a net annual Arctic Ocean CO₂ uptake of 180 ± 130 TgC per year.

The Zeppelin Observatory data for 2014 suggest that the CH₄ fluxes from the Svalbard continental platform are smaller than 0.2 Tg yr⁻¹. All estimates are in the lower range of values reported earlier (Pisso et al., 2016). Platt et al. (2018) reported a potential region with high ocean-atmosphere CH₄ flux located north of

Svalbard, but addressed that at the time of the measurements the meteorological conditions were unique, including a short episode of the highly sensitive to emissions over an active seep site without a sensitivity to land-based emissions.

River runoff affecting the hydrological processes at coastal marine environments

The Arctic Ocean, including the Hudson Bay, receives 55.6 % of its river inflow from Russia, mostly via 19 large rivers (Shiklomanov and Shiklomanov, 2003). This freshwater inflow of approximately 2920 km³ per year (Shiklomanov, 2008) is associated with large sediment and heat transports, which together affect the hydrography, marine climate and ecosystems across the Siberian shelf seas (Magritsky et al., 2018). A major part of seasonal and interannual variations in the river runoff is anthropogenic, due to regulation in large reservoirs (Georgiadi et al., 2016). In addition, Magritsky et al. (2018) detected an increased runoff trend of 5-10 %, compared to a reference period of 1936 to 1975, in most of the major Russian rivers discharging into the Arctic Ocean. This trend is mostly due to a climate-induced increase since the second half of 1980s (Magritsky et al., 2018). However, due to gaps in the monitoring programs, these estimates have a large uncertainty: focusing on river discharges from the six largest Eurasian rivers to the Arctic Ocean, estimates of the increase range from 7% (Peterson et al., 2002) to 1.5 % (Shiklomanov and Lammers, 2009).

Permafrost thawing has resulted in releases of old carbon storages, but so far there is no clear evidence on the impact of permafrost thawing on the net emissions of CO₂ and CH₄ to the atmosphere (IPCC, 2019). A potential explanation of no or weak net increase is that a fraction of the released methane has been taken by rivers instead of emitted to the atmosphere. Increased amounts of organic carbon in rivers impact the regional and global biochemical and methane cycles (Shakhova et al., 2007; Wild et al., 2019). With the accelerating permafrost thaw, also the atmospheric emissions are expected to increase, in particular for CO₂ but also for CH₄. Expected future changes in river ice regime are consistent with the expected changes in the duration of the cold season and accumulated negative air temperatures. Significant changes are expected for the rivers in the Kola Peninsula and the lower reaches of the rivers Northern Dvina and Pechora, whereas the lowest changes are expected for the central parts of Eastern Siberia (Agafonova et al., 2017). Due to anthropogenic activities (above all industry, municipal services, and filling of reservoirs), water withdrawal from Russian Arctic rivers and related groundwater systems is approximately 20.6 km³ per year, and it is expected to increase to 37 km³ per year by 2025 to 2030 (Magritsky et al., 2018). Features of these changes at the marine margin of the Lena River delta are different compared to changes in the delta head area.

The hydrological representativeness of a glacier is a new characteristic, and of practical importance for basin-wide tasks of hydrology and glaciology. For its evaluation, it is proposed to replace the seasonal air temperatures with the glacier summer mass balance (BS) or to include BS in the multiple regression equations for calculating the runoff of rivers fed by melting of snow and ice. This method can be

recommended for at least of some glaciers in the existing network of the World Glacier Monitoring Service (WGMS) (Kononov et al., 2019).

2.3.2 Marine ecology (Q8)

Living marine organisms weaken or even subdue CO₂ accumulation

The important climatological role of the world's oceans is to reduce the CO₂ accumulation into the atmosphere through its absorption. This mechanism is ordinarily viable as the partial pressure of dissolved CO₂ in marine surface waters is less than the content of CO₂ in the overlying atmosphere. Due to the organic pump, a net draw down of atmospheric CO₂ into the ocean is put into effect. It proceeds in the process of sinking of particulate organic carbon of algal origin: organically bound CO₂ is released through remineralization and further accumulated in the deep ocean. In contrast, owing to the processes of carbonate counter pump, CaCO₃ is exported downward and, at depth, dissolves causing a net release of CO₂ to the atmosphere (Balch et al., 2016). However, there are living marine organisms that are able to weaken or even subdue CO₂ accumulation, at least within their habitat. Among this group of marine organisms, the leading role belongs to coccolithophores. Among marine bio systems, coccolithophores (class Primnesiophyceae) are most productive calcifying algae (Taylor et al., 2017). They both produce particulate inorganic carbon (in the form of calcite) and promote the increase of CO₂ partial pressure ($p\text{CO}_2$) in the ambient marine surface waters. Thus, the biological activity of coccolithophores can exercise a direct influence on both the CO₂ flux exchange at the atmosphere-ocean interface and the marine carbonate chemistry system (CCS). The rain ratio, i.e. the ratio of particulate inorganic carbon to organic carbon, determines the intensity and direction of CO₂ flux at the atmosphere-ocean interface. In the case of coccolithophores, the rain ratio is above unity within their habitat area, which potentially can have climatic consequences but also drive alterations in marine CCSs (Balch 2018).

Emiliania huxleyi is the most widespread coccolithophorid algal species in Earth's oceans, which, in light of the above, naturally explains why this is one of the best-studied marine algae. Of all other coccolithophores, *E. huxleyi* is probably the most successful in forming extensive blooms in world-wide marine waters ranging from oligotrophic to eutrophic. Unlike diatoms and dinoflagellates, this alga is phenomenally immune to both light-limitation and very high light intensities. As high levels of incident light/irradiance enhance calcification (which is predominantly a light-dependent reaction), it is supposed that the calcification machinery enables *E. huxleyi* cells to resist photodamage through dissipating excess energy. This specialty is important in case of nutrient-depleted waters, especially in combination with the high affinity of *E. huxleyi* for nutrients including nitrogen but especially phosphorous. The property of both mixotrophic nutrition, and resistance, at least partial, to zooplankton grazing and virus attacks (due to cell's coverage by calcite scales/coccoliths) contribute to this alga ability to sustain a variety of unfavorable conditions and retain steadfastly its ecological niche (Godrijan et al, 2020). Thus, the elaborate biology of *E. huxleyi* cells imparts to them the intrinsic and rather rare property of pursuing growth-maximizing and loss-minimizing life

strategies. This property reveals itself through multiple manifestations, two of which are vastness and sustainability of *E. huxleyi* bloom areas. A typical bloom surface is not less than thousands of square kilometers, but in many marine environments it is far larger (Kondrik et al., 2018b). For example, in some years, the value of S in the North and Norwegian Sea can be well above 100 000 km², in the Bering Sea maximum bloom area (S) values were registered at 250 000 km², particularly large *E. huxleyi* bloom areas (up to 380 000 km²) were observed in the Barents Sea (Kondrik et al., 2017). Within the subpolar and polar zones of the Northern Hemisphere, in the waters around the Great Britain, in the North, Norwegian, Labrador, Greenland, Barents, and Bering seas *E. huxleyi* blooms occur annually although with largely varying intensity (Pozdnyakov et al., 2017). The duration of blooms in the Northern Atlantic and the Barents Sea is on average about three-four weeks. The moment of onset of the *E. huxleyi* bloom area maximum shifts from June-July to September-October for the seas located at the temperate, subpolar and polar latitudes of the Northern Hemisphere, respectively. This sequence mimics the flow pattern of the Gulf Stream. In the Bering Sea, the temporal pattern of S variations reveals two periods (1998-2001 and 2018-2020) of extraordinary intense *E. huxleyi* outbursts. It is hypothesized that this phenomenon was driven by massive advection of Fe-depleted North Pacific waters due to a significant weakening of the Alaskan Current. The latter is supposed to be a teleconnected aftermath of exceptionally strong El Niño events in 1996-1997 and 2017, respectively (Pozdnyakov et al., 2020).

Satellite-borne estimations made during 1998-2018 showed that *E. huxleyi* outbursts resulted in a release of inorganic carbon (PIC) in the form of CaCO₃ in surface waters in amounts ranging from ~10 to several hundreds of kilotons. In the Barents Sea, the released PIC content varied between ~100 kt and 250-300 kt, whereas in the Bering Sea, during the two periods of exceptional activity, the PIC content was as high as 500 kt (Kondrik et al., 2017). There is ample evidence that the release of PIC was accompanied by a significant increase in CO₂ partial pressure ($\Delta p\text{CO}_2$) within the bloom area: between 1998 and 2016, the mean and maximum values of the ratio $\Delta p\text{CO}_2/(\Delta p\text{CO}_2)_{\text{background}}$, varied in the range ~ (20-40)%, and ~ (30- 60)%. The highest numbers were registered in the Bering and Barents seas (Kondrik et al., 2018a; 2019). Also, there is space borne evidence for the atmospheric columnar ΔCO_2 enhancement (ΔCO_2)_{atm} over *E. huxleyi* blooms: numerous case studies in the aforementioned North Atlantic seas as well as in the Barents and Black seas proved that (ΔCO_2)_{atm} could reach 2-3 ppm (Kondrik et al., 2019; Morozov et al., 2019).

Notwithstanding the remarkable ability of *E. huxleyi* to grow under conditions unfavorable for algae of other functional groups (e.g. diatoms, flagellates, cyanobacteria), a highly irregular pattern of the registered two-decadal (1998-present) time series of S , PIC, and $\Delta p\text{CO}_2$ are indicative of susceptibility of this alga outbursts to environmental conditions (Nissen et al., 2018; Kazakov et al., 2019; Silkin et al., 2019). Statistical prioritization of non-biogenic forcing factors (FFs) shows that the latter are sea- and time-period specific (Pozdnyakov et al., 2019). Thus, in the Barents Sea, sea water temperature (SWT) is the highest-ranked FF, followed by PAR (photosynthetic active radiation). In the Bering Sea, beyond the aforementioned periods (1998-2001 and 2018-present), sea surface salinity (SSS) is the FFs leader, with PAR as a runner up,

whereas SWT is only third in the row. Although these assessments are done without explicitly considered nutrients concentrations (NCs), implicitly NCs were among the FFs. Indeed, arguably, variations in SWT, SSS, CHL, MLD, and surface current speed/advection (tested as FFs) indirectly account for the variations in NCs as well in such CCSs parameters as alkalinity and basicity (Durairaj et al., 2015; Pozdnyakov et al., 2019, and references therein).

In the long run, under the conditions of steady accumulation of CO₂ into the atmosphere, this factor should be closely considered (Rivero-Calle et al., 2015). The action of a rising atmospheric CO₂ concentration is expected to proceed through a number of direct and indirect interactions (Fig. 7), both of which should ultimately cause alterations in the rain ratio. An increase in the atmospheric CO₂ concentration leads to the rising of the global temperature, and further to the strengthening of stratification, intensification of irradiance within the euphotic zone and cutting of nutrient fluxes from below. Although increases in CO₂ fluxes to the surface ocean cause a reduction of pH and CO₃²⁻ levels in water, the large pool of HCO₃⁻ remains to support the calcification machinery. Thus, it will lead to the establishment of environmental conditions unfavorable for non-calcifying phytoplankton (NCP), but beneficial (or at least endurable) for coccolithophores in general and *E. huxleyi* specifically. The reduction of NCP and uncontested growth of *E. huxleyi* drives a further reduction of dissolved CO₂ consumption by other groups of phytoplankton, increase in pCO₂ in the surface ocean and intensification of CO₂ fluxes into the atmosphere. Concurrently, through a system of feedback interactions, alterations in the rain ratio are bound to affect the carbon fluxes at the water-atmosphere interface. Therefore, the scenario of further increases atmospheric CO₂ concentration in the future, in all probability, implies a vaster proliferation of *E. huxleyi* in the world's oceans.

In combination with statistic-based-mathematical models of *E. huxley* blooms (Pozdnyakov et al., 2019), the available IPCC climate models permit mid-term projections of the forthcoming changes (Gnatiuk et al., 2020). However, our knowledge on the reciprocal influence of climate change and both the structure and functioning of marine ecosystems (even at the level of primary producers!) is still insufficient to confidently prognose the future dynamics of the *E. huxleyi* phenomenon. More studies are required even to fully understand the mechanism of intracellular light-dependent reaction of calcification, its dependency on both seawater carbonate chemistry and environmental FFs (Vihma et al., 2019). Creation of respective multidecadal databases (as in Kazakov et al., 2019) as well as further delivery of satellite and *in situ*/shipborne/laboratory data are necessary to improve our capacity to assess with certainty the climatological and ecological role of *E. huxleyi* blooms on regional and global scales (Fig. 7).

2.3.3 Lakes and rivers (Q9)

Organic carbon in lakes

Spatial variability, an essential characteristic of lake ecosystems, has often been neglected in field research and monitoring. The detected spatial "noise" strongly suggests that besides vertical variation also the

horizontal variation should be considered in the ecosystem monitoring and, most importantly when the role of dissolved organic carbon (DOC) on the CO₂ flux is estimated (Manasypov et al., 2015; Leppäranta et al., 2018). In natural waters with increasing level of colored dissolved organic matter (CDOM) concentration, the water color is shifted towards brown. The key "permanent" landscape variables, the coverage by lakes and peatland in the catchment area can be strongly correlated with lake elevation above the sea level. A high lake coverage indicates a low CDOM concentration, while a high peat coverage indicates the opposite (Arvola et al., 2016). For example in Finland, recent results from inland water studies have not shown any overall, consistent large-scale changes in CDOM concentrations over the last 101-year period (Arvola et al., 2017). Rather, CDOM changes in individual lakes have been related to changes in land use in the drainage basin. Manasypov et al. (2015) reported results from Siberian lakes, representing a discontinuous permafrost zone, and addressed that although the concentration of most elements in the lakes are lowest in spring, the maximal water coverage of land made it as an significant reservoir of DOC. The soluble metals in the water column that can be easily mobilized to the hydrological network.

In very shallow freezing lakes, the volume liquid water is much reduced due to ice growth, and rejection of nutrients and pollutants in the ice growth causes major enrichment of the water body. This has major implications to the ecosystem of these lakes (Yang et al., 2016; Song et al., 2019). Freezing rejects some 80-90 % of the impurities in freshwater lakes. On the other hand, ice cover accumulates atmospheric deposition over several months but releases them into the water body within one month's melting phase. Rejection of nutrients and pollutants in lake ice growth causes major enrichment of the water body in shallow lakes and notable increases in nutrient concentrations in a shallow lake during seasonal ice growth (Fang et al., 2015).

Lake carbon balance

Arctic and boreal lakes are an important natural source of CH₄ to the atmosphere (Bastviken et al, 2011). Methane is mainly produced in the bottom sediments and/or hypolimnion, where most of anaerobic decomposition of organic matter take place, and then is either oxidized to CO₂ in the water column or emitted to the atmosphere. At Kuivajärvi, a typical meso humid lake located in Southern Finland, it was found that 91% of available CH₄ was oxidized in the active CH₄ oxidation zone during hypolimnetic hypoxia (Saarela et al., 2020). In warm springs, the early onset of thermal stratification with cold and well-oxygenated hypolimnion delays the period of hypolimnetic hypoxia and thus limiting the production of methane. At Kuivajärvi measured CO₂ fluxes (F-CO₂) showed that the lake acted as net source of carbon during two open-water periods (Mammarella et al., 2015). During daytime, with typically high wind speeds, shear-induced water turbulence controls the water-air gas transfer efficiency, thus enhancing the vertical diffusive fluxes across the water-air interface. However, during calm nighttime conditions, buoyancy-driven turbulent mixing, associated with penetrative cooling of surface water, controls the gas exchange, and simple wind speed-based transfer velocity models strongly underestimate F- CO₂ (Mammarella et al., 2015). Kiuru et al. (2018) developed a model simulating CO₂ dynamics of a boreal lake in warming climate. The

simulations for 2070-2099 showed a 20–35% increase in the CO₂ flux from the lake compared to the reference period 1980–2009.

Lake ice cover

Wei et al. (2016) studied the Lake Inari (67.14 N, 25.73 E), Finnish Lapland, in winters 1980/1981 - 2012/2013, and observed an increasing trend in the air temperature during the freezing season, associated with an increasing trend in the water precipitation during winter. Low temperatures with less precipitation lead to the formation of columnar ice, while strong winds together with heavy snowfall favored granular ice formation. Karetnikov et al., (2017) analyzed long-term ice conditions in Lake Ladoga, Russia, for the period of 1913–2015 and showed that the mean freezing and breakup dates were November 26 and May 15, respectively, and that the annual frequency of complete freeze over of the lake was 0.83. The period from 1990 to present was much milder than the preceding years. The annual increase in the ice concentration depended on the accumulated freezing-degree-days (AFDD) and the hypsographic curve, while the ice thickness increased with the square root of AFDD.

An analysis of a Siberian thermokarst lake located in the Lena River Delta, characterized as a floating ice lake, showed that the temporal dynamics and magnitude of heat fluxes and surface energy balance closures are substantially different depending on lake surface conditions (Franz et al., 2018). Sensible heat and latent heat fluxes, modelled using available heat bulk transfer models (Woolmay et al, 2015; Verburg and Antenucci, 2010; Andreas et al, 2002), tend to underestimate the measured fluxes and show less variability over freezing ice cover, melting ice in Spring, as well as over open water in Summer. However, the performance of these models depends also on the accuracy of meteorological and hydrological input parameters, which should be carefully measured especially during challenging winter conditions.

The seasonal lake ice cover is a sensitive indicator of climate variations in the Arctic (Kirillin et al., 2012; Leppäranta, 2015). To work more on this question, Lake Kilpisjärvi (surface 37.1 km², max depth 57 m), a tundra lake in northern Finland, has been under an intensive ice-related field programs in recent years. The research covered the whole year but was focused on the melting period in May–June. The heat budget over the ice season was dominated by the radiation balance. Turbulent fluxes were significant before the freeze-up in fall, but in the ice season they were small. The evolution of ice thickness served as a very good approximation to the total surface heat flux (Leppäranta et al., 2017) (Fig. 8). In the melting stage, solar radiation, the strongest forcing of the water body beneath ice cover, breaks the stability and initiates convective turbulent mixing. This brings heat from the deeper water to ice, enhancing melting at the ice bottom (Kirillin et al., 2018). Thus, the common assumption of the heat flux from the water to ice to be due to molecular conduction does not hold in the melting stage but it is much higher. The ice–water interaction under lake ice has not been well covered in earlier studies of ice growth and melting.

The ice melting process was studied in detail in Lake Kilpisjärvi. The melting progressed in the upper and lower surfaces and in the interior, with proportions depending on the solar flux and optical properties of the ice, and were therefore case-dependent. About one-third of the solar flux that penetrated the ice returned to ice bottom, providing heat for melting. This was consistent with the under-ice results by Kirillin et al. (2018). In 2013 a rapid ice breakage event completed the ice breakup in a short time interval, with final breakage at the ice porosity 40-50%. A lake ice melting model should include the thickness and porosity of ice, with porosity connected to an ice strength criterion (Leppäranta et al., 2019).

Lake Baikal and Selenga River delta

The Selenga River, the main tributary of Lake Baikal, has a catchment area of 450 000 km² in the boundary region between Northern Mongolia and Southern Siberia. This area is well known by its climate, land use and dynamic socioeconomic changes which might have negative impacts on the ecosystems of Lake Baikal and thus was selected as PEEX field laboratory within PEEX subprogram Selenga-Baikal Network (www.atm.helsinki.fi/peex/index.php/baikal-selenga-network-basenet). In the recent past, hydroclimatic development together with land use changes led to a contaminant influx from mining areas and urban settlements increased. Additional hydrological modifications due to the construction of dams and abstractions/water diversions from the Selenga's Mongolian tributaries could lead to additional alterations (Karte et al., 2017b). In addition to Selenga River, a key issue for an improved understanding of regional impacts of the environmental change is to disentangle the influence of climate change from that of other pressures within the catchment (Lychagin et al., 2017). The PEEX subprogram Selenga-Baikal Network aims at integrated field-based and modeling knowledge to develop basin-wide conceptual framework of riverine fluxes (Kasimov et al., 2017a; Karte et al., 2019).

As a PEEX field laboratory, regional large-scale assessments made it possible to predict the comprehensive nature of hydrological and geochemical changes driven by climatic processes and human impacts. Heavy metals in water and sediments (Kasimov et al., 2020a, 2020b) and fish communities (Kaus et al., 2017) were measured since 2011 in over 50 locations around the catchment. The mining zones are potential hotspots for increasing metal loads to downstream river systems. Several metals (Al, Cd, Fe, Mn, Pb and V) are exported from mining sites to the downstream river system, as shown by net increasing mass flows. Based on a novel partitioning coefficient approach (Fig. 9), contrasting patterns with domination of both particulate and dissolved phases in different parts of the basin were found. Such heterogeneity in the metal partitioning is likely to be found in many large river systems.

Multi-scale modeling ranged from the basin wide (Malsy et al., 2017; Frolova et al., 2017) to specific sub-regions, such as particular segments of the river system (Kaus et al., 2017; Thorslund et al., 2017; Garmaev et al., 2019) or its delta (Chalov et al., 2017a, 2017b; Shinkareva et al., 2019), and identified reactions of hydrogeochemical pathways on climate change. The mean flow reduction in the Selenga River was 3-5% in the 2020s-2030s and 4-25% in the 2080s-2090s, being a crucial driver of ongoing and future

hydrogeochemical changes. Increases in temperatures with permafrost thaw and the expansion of agricultural, mining and urbanization processes may induce up to a 6% increase in the particulate modes and 3% in the dissolved modes of some metals in the river system (Chalov et al., 2018). Possible changes in the number or magnitude of high-flow events, caused by climatic or other anthropogenic factors, could influence the total sediment deposition, which was primarily found to occur during relatively short high-flow events. Such potential changes have important implications to the possible spreading of polluted sediments (Pietron et al., 2015) and their storage in the Selenga River Delta, which is an important wetland region forming the geochemical barrier which mitigate pollution of Lake Baikal by riverine fluxes (Voropay and Kichigina, 2018, Chalov et al., 2015). The Selenga delta region sequester various metals bound to Selenga River sediments (Chalov et al., 2015, Pietron et al., 2018). The water shortage decreases the processes of suspended sediment retention in the delta. The seasonal hydrogeochemical patterns are explained by wetland inundation during floods and channel erosion or Baikal wind surge during low flow periods (Chalov et al., 2017a, 2017b).

Asian water lakes

The largest internal drainage basins in the world are located in Central Asia, with a limited availability of both surface and groundwater (Karthé et al., 2017a). Since the twentieth century, water resources of this region have been over exploited and, for example, from small Mongolian headwater streams to the mighty Aral Sea, surface waters have been partially desiccated. It seems that the implementation of the Integrated Water Resources Management and water-food-energy nexus approaches would lead to a more environmental-friendly future (Karthé et al., 2017). The lake-rich Qinghai-Tibet Plateau (QTP) has recently been identified as the Third Pole of the Earth. Due to its high elevation and unique climate, QTP affects the global and local climate and played an important role on the Central and Southern Asian water cycle (Zhang et al., 2018). Lake-atmosphere interactions have been quantified over open-water periods, yet little is known about the lake ice thermodynamics and heat and mass balance during the ice-covered season. A modelling study for a thermokarst lake in the QTP was performed (Huang et al., 2019a). Strong diurnal cycles were seen for all surface heat fluxes. The ice mass balance was dominated by the growth and melt at the base, but the surface sublimation was also crucial for the ice loss, accounting for up to 40% of the maximum ice thickness and 41% of the lake water loss during the ice-covered period. The strong penetration of solar radiative flux is the dominant contributor to the high value of upward sensible heat flux at ice bottom, resulting in a relatively thin ice cover compared with equivalent high-latitude climate.

2.4 SOCIETY

The anthropogenic impact has been addressed as one of the PEEX themes for the society system. The discussion on the mitigation and adaptation, including urban infrastructure design and risk assessment, are

addressed in this context (Q10, section 2.4.1). The social transformations are discussed in terms how local reindeer grazing interacts with the environment (Q11 section 2.4.2). The adaptive capacity of the Northern societies depends on their environment, demographic structure and economic capacity, and the environmental hazards and environmental health under changing climate are the key research areas in this context (Q12 section 2.4.3.).

2.4.1. Anthropogenic impact (Q10)

Mitigation

Arctic climate change generates a need for long-term planning and development of new socio-economic infrastructures, such as dams, bridges, roads and transnational and regional energy networks. For this task, new climate-based forecasting tools, cost and operational risk estimates as well as other methods and tools for an infrastructure and urban design are needed. As an example, engineering calculations for maximal discharges were provided for the Nadym River in Russia (Shevnina et al., 2017). Badina (2018) introduced a method for the natural risk assessment by using indices based on socioeconomic potential data and spatial distribution of natural hazards. This method has been tested and used to identify the most vulnerable municipalities in South Siberia. Another example of new methods is a “Green Factor tool” to increase the share and effectiveness of green areas in urban environments and cities. An ambitious target set in this tool could encourage or force urban developers to aim higher with the planning of green areas and construction, however the existing regulations challenge the use of this approach (Juhola, 2018).

The energy production is of fundamental importance for the society functions, and new clean energy technologies are needed for hindering the climate change. The potential of hydropower production under probabilistic projections of annual runoff rate and future changes in the potential hydropower production need to be evaluated (Shevnina et al. 2019). All the Nordic countries are vulnerable to various degrees to potential cross-border impacts, due to their energy sectors being highly globalized and interconnected. However, cross-border impacts are not yet properly included in Nordic climate assessments or energy strategies. The EU’s new Green Deal is pivotal in this respect, as for the first time emissions along the whole supply chain (oil, gas, coal, renewables) become under scrutiny and as part of a normative governance. Therefore, policy makers and energy planners should be assisted in making comprehensive vulnerability assessments that address both domestic and international climate risks (Groundstroem and Juhola, 2019).

2.4.2 Environmental impact (Q11)

*Reindeer (*Rangifer tarandus* L.) grazing and ground vegetation structure and biomass*

Reindeer (*Rangifer tarandus* L.) grazing in the North affects the ground vegetation structure and biomass and cover of lichens. It seems that reindeers affect GHG fluxes from the forest field layer. Grazing changes affect

the vegetation composition and thereby emissions (Köster et al., 2018). Köster et al. (2017) provided detailed information on soil CO₂ effluxes, which were mostly affected by the year of measurement, time of measurement, soil temperature and also by the management, resulting in higher CO₂ emissions on the grazed areas. Soil moisture content did not affect the soil CO₂ efflux. For example, in the Finnish Lapland the average soil CO₂ efflux values were significantly higher in 2014 compared with 2013, mainly due to differences in the soil temperature at the beginning of the season (Köster et al., 2017). Furthermore, grazing significantly decreased the biomass and cover of lichens and also the amount of tree regeneration. In a subarctic mature pine forest, grazing did not affect the soil temperature or soil moisture. No statistically significant effect of grazing on the soil CO₂ efflux, soil C stock or soil microbial C biomass was found. The soil microbial N biomass was significantly lower in the grazed areas compared to the non-grazed areas. It seems that in the boreal subarctic coniferous forests, grazing by reindeer can be considered as "C neutral" (Köster et al., 2015). There is also indication that reindeer grazing affects the boreal forest soils e.g. their fungal community structure and litter degradation (Santalahti et al., 2018).

2.4.3 Natural hazards (Q12)

Under this theme, the PEEX research has so far focused on environmental health issues. These include diseases, impact of UV radiation, and air pollution in urban environments. The spread of diseases caused by living pathogens is basically determined by environmental conditions. Medico-geographical assessments are usually based on identification of the links between the spread of diseases and factors of the geographical environment.

Naturally-determined diseases

Climatic factors are deemed among the main determinants for the spread of naturally-determined diseases (Malkhazova et al., 2018). Emerging zoonotic diseases are expected to be particularly vulnerable to climate and biodiversity disturbances. Anthrax is an archetypal zoonosis that manifests its most significant burden on vulnerable pastoralist communities. Ezhova et al. (2021) investigated the dynamics of environmental factors that led to an anthrax outbreak in Yamal Peninsula, Siberia, during 2016. They found that the local permafrost was thawing rapidly for the last 6 years before the outbreak, supporting the hypothesized role of permafrost thaw in triggering this outbreak, and concluded further that the spread of anthrax was likely intensified by the extremely dry summer of 2016 in the region. Overall, the recent findings highlight the significance of warming temperatures for anthrax ecology in northern latitudes, and suggest potential mitigating effects of interventions targeting megafauna biodiversity conservation in grassland ecosystems and animal health promotion among small to midsize livestock herds (Walsh, et al., 2018). Equally important is the monitoring of climatic factors, such warming and precipitation extremes, in Arctic regions previously contaminated by Anthrax (Ezhova et al., 2021).

Formatted: Font color: Auto

UV variations

Different geophysical parameters affecting the UV molecular number density show that especially at high altitudes, the increased surface albedo has a significant effect on the UV growth. The new parameterization of the on-line UV tool (momsu.ru/uv/) for Northern Eurasia allows us to determine the altitude dependence of UV and to estimate the possible effects of UV on human health considering different skin types and various open body fraction for January and April conditions in the Alpine region (Chubarova et al., 2016b). Using UV satellite retrievals, ERA-Interim data and the INM-RSHU chemistry-climate model, the changes in the UV irradiance and UV resources were estimated over Northern Eurasia for the 1979-2015 period, demonstrating significant UV increases over vast areas (Chubarova et al., 2020). Referring to long-term UV measurements and model simulations in Moscow, a statistically significant positive trend of more than 5% per decade since 1979 was evaluated (Chubarova et al., 2018). Related to the connection between UV variation and stratospheric O₃, see also the section 2.2.1 Atmospheric composition and chemistry.

Formatted: Font color: Auto

Examples of air pollution episodes

Street-level urban air pollution is one of the key topics in urban environments. For example, in Norway, Bergen, the most extreme cases of repetitive wintertime air pollution episodes, followed by increased large-scale wind speeds above the valley, were transported by the local re-circulations to other less polluted areas with only slow dilution. This result underlines the need for better described assumptions on transport paths and weak dispersion in classical air pollution models, in order to improve the current air quality forecasts in urban areas (Wolf-Grosse et al., 2017b). A link between the persistence of the flow above the Bergen valley and the occurrence and severity of the local air pollution episodes was found. Analysis of the large-scale circulation over the North Atlantic-European region, with respect to air pollution in Bergen, revealed that the persistence in meteorological conditions connected with air pollution episodes is not necessarily caused by large-scale anomalies of the atmospheric circulation over the Norwegian west coast, but rather connected with anomalies as far away as Greenland (Wolf-Grosse et al., 2017a).

Formatted: Font color: Auto

Formatted: Font color: Auto

In Russia, especially intensive atmospheric pollution episodes have severe impacts on the environment and human health. Popovicheva et al (2019b) analyzed the Tver region, north of Moscow, which was considerably affected the secondary organic aerosol (SOA) formation originating from long-lasting peat bog fires. Spectral absorbance characteristics were similar to peat burning and traffic source emissions during fire and non-fire related days and confirmed the effect of transported peat smoke on air quality in a megacity environment (Popovicheva et al., 2019b). Popovicheva et al. (2019b) also showed that long-term transport from the North-West Russia and Scandinavia influence the local population.

Formatted: Font color: Auto

Local Arctic air pollution alone can seriously affect public health and ecosystems locally, especially in wintertime when the pollution can accumulate under inversion layers (Schmale et al., 2018a). We need more research on the contributing emission sources and the relevant atmospheric pollution mechanisms, and more

detailed epidemiological or toxicological health impact studies in the Arctic. Socioeconomic changes (shipping, tourism, natural resources extraction, increasing number of population) are already taking place in the Arctic, and they will increase in the future. It is also expected that the emission types and magnitudes will increase the number of exposed individuals (Arnold et al., 2016). There is still a large variation in the amount of the location of emissions. Future predictions are even more difficult due to the yet unknown development of the Arctic economic activities and their emissions (Arnold et al., 2016, Schmale et al., 2018a, 2018b).

3. SYNTHESIS AND FUTURE PROSPECTS

3.1 Future research needs from the system perspectives

For the Land ecosystem, the recent progress towards understanding of the Northern Eurasian Arctic - boreal land ecosystems (section 3.1) are dealing with improved methodologies relevant to land processes (Q1), observations on permafrost thawing (Q2), and observed changes in the Northern ecosystems, especially soil conditions (Q3).

Improved satellite-based methods and (validation) data together with better quantification and, especially, the scaling of the gross primary production (GPP) are enabling a better identification and quantification of Earth surface characteristics and ecosystem carbon balance compared with the earlier capacity (Gurchenkov et al., 2017, Rautiainen et al., 2016, Nitzbon et al., 2019, Boike et al., 2019, Terentieva et al., 2016), Zhang et al., 2018, Pulliainen et al., 2017, Matkala et al., 2020; Bondur and Chimitdorzhiev, 2008 a,b). Intensive research has been carried out on the quantification of the GPP, a key variable for biological activity, in different conditions and at different scales (Pulliainen 2017, Kulmala et al., 2019, Matkala et al., 2020). Further investigations are called for a more detailed understanding of the seasonal dynamics of the biological activity.

The Northern Eurasian ecosystems' tipping points are related to multiple simultaneous stress factors. The key stress factors here are the permafrost thawing and factors important for ecosystems, such as the prolongation of the growing season, increase in the mean temperature of the growing season and forest fires (Kukkonen et al. 2020, Biskaborn et al. 2019, Payne et al., 2016. Köster et al. 2016, Miles and Esau 2016, Miles et al., 2019). New evidence on the progress of permafrost thawing in Siberia has been introduced by Kukkonen et al. (2020) and Biskaborn et al. (2019). The permafrost thawing is also triggering yet not clearly-known processes related to changing fluxes, ecosystem processes and dynamics of greenhouse gas sinks and sources (Schuur et al., 2008, Thomson et al., 2017, Commane et al., 2017, Euskirchen et al., 2017, Dean et al., 2018, Thonat et al., 2017). The progress affecting permafrost thawing has not yet been analyzed in detail. For example, we need more information on the dynamics of how the thawing processes vary between soil types due to differences in water movement and, in the winter time, how the snow cover affects ground surface temperatures (Bartsch et al. 2010). In addition to permafrost processes, the recent advances in

observed changes in the Northern ecosystem reveal a significant role of soil processes in biogeochemical cycles, especially the nitrogen cycle (Voigt et al., 2016, Pärn et al., 2018). Knowledge of the soil microbiological composition and the effect of forest fires have been improved (Köster et al., 2015, 2016, Zhang-Turpeinen et al., 2020), but further research is called for vegetation changes influencing the below-ground microbiology, its composition and enzymatic activity (Payne et al., 2016. Köster et al. 2016). The NDVI methods have made it possible to detect vegetation changes (Miles and Esau 2016). A range of vegetation cover changes in Siberia have been reported, such as the Arctic greening and browning processes, but e.g. the greening of Siberian cities remains an issue of intensive research also in the future (Miles and Esau 2016, Miles et al., 2019).

For the Atmospheric system, the recent progress in understanding the Northern Eurasian Arctic - boreal land atmospheric system and the aspects of the megacity air quality (section 3.2) are dealing with atmospheric composition changes (Q4), key feedbacks between climate and air quality (Q5), and synoptic scale weather (Q6). Recent results demonstrate improved quantification of the carbon balance and CO₂ fluxes and concentrations due to land use change, forest fires in Siberia, and new understanding of aerosol sources and properties in the Arctic environment and across the Northern Eurasia (Pulliainen et al., 2017, Karelin et al., 2017, Rakitin et al., 2018, Skorokhod et al., 2017, Alekseychik et al. 2017). However, most of the results deal with atmospheric aerosol chemistry and physics in boreal and Arctic environments originating from measurements in the few flagship stations in Finland and Russia (Kerminen et al., 2018, Wiedensohler et al., 2019, Freud et al., 2017, Paasonen et al., 2018, Östrom et al., 2017, Kalogridis et al., 2018, Bondur et al., 2016, Bondur and Ginzburg 2016, Bondur et al. 2019 c,d, Bondur and Gordo, 2018; Mikhailov et al., 2017, Breider et al., 2017), indicating the need for a comprehensive station network in the PEEX region. Black carbon emitted by the Siberian forest fires and some other sources, and its long range transport to the Arctic, are also widely discussed (Kalogridis et al., 2018, Bondur et al., 2016, Bondur and Ginzburg 2016, Mikhailov et al., 2017, Breider et al., 2017, Shevchenko et al., 2015, Kononov et al., 2018, Marelle et al., 2018). In addition, measurements of ozone in the troposphere and stratosphere provide insight into atmospheric chemistry in urban environments (Skorokhod et al., 2017), UV radiation and human health (Chubarova et al., 2019). Environmental health, including the impacts of air quality and UV radiation, is foreseen as a high momentum research topic in the PEEX domain, and further research is called for in this area.

Related to air pollution, we reported several new results on the dynamics between the haze pollution and boundary layer meteorology in enhancing air pollution in megacity environments (Zhao et al., 2017, Ding et al., 2016a, Wang et al., 2018b, Bai et al., 2018a, Ye et al., 2017). The long-term and comprehensive measurements carried out especially at the SORPES station in Nanjing provide valuable data pools for such studies (Ding et al., 2016a). However, the backbone of the recent progress has been the improved on-line atmospheric measurements and the use of machine learning methods combined with different methodologies, such as back trajectories together with the lidar and radiosonde data. In addition, improved models of emission inventories together with the ECHAM-HAM and GAINS models have led to a better quantification

Formatted: Font color: Auto

of aerosol number emissions. New knowledge has enabled the introduction of new theoretical arguments on the feedbacks between high aerosol concentrations and the urban boundary layer (Petäjä et al. 2016). New measurements have also been obtained from Siberian cities (Elansky et al., 2016, Chubarova et al., 2016a, Mahura et al., 2018). However, we are still in the early phase of having a holistic picture on large-scale feedbacks due to the lack of long-term, comprehensive measurements in these regions.

Changes in the atmospheric dynamics in the North have potential impacts on short-term local/regional and sub-seasonal to seasonal large-scale weather predictions, and on long-term projections on biogeochemical systems. It is therefore crucial to understand changes in boundary-layer processes as well as synoptic- and large-scale circulation in the Arctic and Northern Eurasia. Recent results show potential, but causally arguable, connections between the alarming sea ice decline, evaporation, cloudiness, atmospheric circulation and moisture transport as well as Arctic and European winter temperatures (Nygård et al., 2019, Rinke et al., 2019, McCusker et al., 2016, Mori et al., 2014, Blackport et al., 2019; Cohen et al., 2020). Further investigations are called for atmosphere-ice-ocean interactions, coupling between small-scale processes (such as clouds and turbulence) and synoptic-scale weather, as well as for polar prediction and extreme events. Furthermore, more quantitative knowledge is needed on pan-Arctic energy budgets (Spengler et al., 2016). The urban heat island (UHI) phenomena taking place in Arctic cities has received an increasing attention, and there is a special need for improved forecasting services for Arctic cities (Miles and Esau 2017, Konstantinov et al., 2018, Varentsov et al., 2018b).

For the Water system, we discussed the Arctic sea ice dynamics and thermodynamics, snow depth and sea ice thickness, sea ice research supporting navigation, and rare elements in the snow and the ocean sediments, especially from the perspective of improvements in the observation and modelling methods (Q7, section 3.3.1.). New evidence on atmosphere–Arctic sea ice interactions have been provided by Lei et al. (2018), and Jakobson et al. (2019). Lei et al. (2018) analyzed how the climate warming would affect the winter growth rate of thin and thick ice, and Jakobson et al. (2019) gave new insight into the relation between sea ice concentration and the wind speed. Furthermore, advance has been made in understanding the thermodynamics and metamorphosis of the snowpack on sea ice and their interactions with surface albedo changes (Dou et al., 2019). Operational sea ice analysis is increasingly important for the Arctic shipping and navigation (Lei et al., 2015, Karvonen et al., 2017). New results on rare elements, mineral composition and CO₂ and methane fluxes associated with ocean sediments have been attained (Maslov, et al., 2018, Yasunaka et al., 2018). This serves as an important information for mitigation plans, as well as for new estimates on the river runoff and discharge in Russian rivers into the Arctic seas (Grigoriev and Frolova 2018, Agafonova et al., 2017).

The marine Arctic ecosystems are under a progressive increase of anthropogenic impacts, the main issues calling for better understanding being the integrated effect of Arctic warming, ice and snow melt, ocean freshening, air quality and acidification of the Arctic marine ecosystems, primary production and carbon

cycle (Q8, section 3.3.2). Quantitative information about the CO₂ accumulation into the ocean is having a high momentum. Marine organisms, such as coccolithophrip algae, are influencing the CO₂ flux exchange (Kondrik, et al., 2018b, Pozdnyakov et al., 2017). In addition to changing marine environments, the Arctic – boreal lakes and rivers may undergo changes in flooding, increasing the amount of fresh water and allochthonous materials (Q9, section 3.3.3). In addition to the Arctic Ocean, the ice and snow conditions of Northern lakes are under pressure. Lake Kilpisjärvi (Finland) (Arvola et al., 2017, Leppäranta et al., 2017) and Lake Ladoga (Russia) (Karetnikov et al., 2017) have been under intensive research, and the recent results demonstrate changes in heat fluxes, ice cover periods and stratification. The browning of lakes and lake sediments were discussed, and new results were attained from the Selenga River of the Baikal Lake. Dramatic changes will be expected in the water runoff and in the amount of dissolved modes of metals, also having serious impact on the environmental health (Chalov et al., 2015, 2016, 2017 a, 2017b, Karthe et al., 2017 a, 2017b). As a comparison to the Northern high latitudes, we also discussed freezing lakes in Central Asia, where the climate is cold and arid. There the ice is typically snow-free, or possesses only a thin snow cover, allowing penetration of sunlight into the water body (Huang et al., 2019).

For the Societal system, the anthropogenic impact has been addressed as one of the main themes (Q10). The discussion on the mitigation and adaptation, including the urban infrastructure design (Juhola 2018) and risk assessment, were addressed in this context (section 3.4.1). In social transformations, a special attention was given to one of the most important local livelihoods in Lapland: reindeer grazing and how it interacts with the environment (Q11 section 3.4.2). The adaptive capacity of the Northern societies rest on their environment, demographic structure and economic activities (Q12). Referring to the earlier statement about the future research needs for the Atmospheric system with respect to environmental health, here again we would like to put an increasing attention to environmental health under changing climate, including the spread of diseases and air pollution and their combined effects (section 3.4.3.).

3.2 Feedback mechanisms under changing climate, cryosphere conditions and urbanization

During the recent years, Kulmala et al. (2004, 2020) have focused on the quantification of the COntinental Biosphere-Aerosol-Cloud-Climate (COBACC) feedback loop relevant to the boreal region in Northern Eurasia. Previous results on the COBACC feedback loop addressed the role of BVOC emission dynamics (Arneth et al., 2016). Both higher temperatures and increased CO₂ concentrations are (separately) expected to increase emissions of biogenic volatile organic compounds (BVOCs) to the atmosphere. It also seems that the GPP is controlled by the BVOC effects on the clouds. Sporre et al. (2019) used an Earth System model to estimate aerosol scattering due to enhanced BVOC emissions and estimated the associated negative direct radiative effect (-0.06 W m⁻²). The total global radiative effect associated with this feedback was estimated to be -0.49 W m⁻² (Sporre et al., 2019), indicating that it has the potential to offset about 13 % of the forcing associated with a doubling of CO₂. The direct effect of aerosol on GPP due to an increase in the fraction of

diffuse radiation was estimated between 6 and 14% increase in GPP at maximum observed aerosol loading compared to low aerosol loading in Northern Eurasia forests (Ezhova et al., 2018b).

The results from the Tibetan plateau demonstrate notable feedbacks between vegetation, BVOC emissions and aerosol particles. The historical wetting of the TP region has increased the vegetation cover, allowing for feedback processes via biogenic aerosol formation and aerosol-cloud-precipitation interactions. A significant wetting trend since the early 1980s in Tibetan Plateau is most conspicuous in central and eastern Asia. Fang et al. (2019) hypothesized that the current warming may enhance emissions of biogenic volatile organic compounds (BVOC), which can increase secondary organic aerosols concentrations, contributing to the precipitation increase. The wetting trend can increase the vegetation cover and has a positive feedback on the BVOC emissions. The simulations suggest a significant contribution of increased BVOC emissions to the regional organic aerosol mass, and the simulated increase in BVOC emissions is significantly correlated with the wetting trend in Tibetan Plateau.

To estimate the net effects of various feedback mechanisms on land cover changes, photosynthetic activity, GHG exchange, BVOC emissions, formation of aerosols and clouds, and radiative forcing (Q14) calls for intensive collaboration and integration between the Arctic Ocean sciences and terrestrial sciences across the Pan-Arctic domain and across the Arctic and high-latitude domain. The Arctic greening and browning (section 3.1.3.) call for a multi-disciplinary scientific approach, improved modelling tools and new data to deeply understand the biosphere-atmosphere-anthroposphere interactions and feedbacks. Petäjä et al. (2020a, 2020b) discussed the complexity of feedbacks, especially at the Arctic context, and the interplay between the temperature, GHG, permafrost, land cover and water bodies and between photosynthetic activity, aerosols, clouds and radiation budget. The current downturn of the arctic cryosphere (*section 3.1.2*), together with the changes in sea ice dynamics and glaciers and the permafrost thawing, affect both marine and terrestrial carbon cycles in interconnected ways (section 3.3.1). Parmentier et al. (2017) discussed the changing arctic cryosphere and how the processes in the ocean and on land are too often studied as separate systems, although the sea ice decline connects the rapid warming of the Arctic, Arctic Ocean marine processes and air-sea exchange of CO₂. Thus, the future priorities would be on the development of our modelling tools towards an all-scale modelling approach to cover the feedbacks, processes and interactions at the land-ocean interface and also in urban environments in the Arctic region. We also need to support the further development of the ground-based observation networks.

3.3 Climate scenarios for the Arctic-boreal region

Climate scenarios set the urgency for the mitigation and adaptation actions for the Northern Eurasian region. The Arctic-boreal region combines an area of both amplified climate change (Arctic amplification) and large diversity in the model predictions (Collins et al., 2013, Hoegh-Guldberg et al., 2018). Under the “low-to-medium” RCP4.5 forcing scenario (van Vuuren et al., 2011), the CMIP5 multi-model mean temperature

changes during the 21st century indicate the strongest winter-time warming of >5 °C in the Arctic Ocean, whereas the majority of the terrestrial region will warm by 2–4 °C (Fig. 12). Even during summertime, the continental warming over the region will generally exceed 2 °C. It is important to note that the diversity of model projections is accentuated over the Arctic and Northern Eurasian domain: the mechanisms behind the Arctic amplification are implemented in varying details in the distinct models, and the associated interactions and feedback processes provide a diverse picture of the future in the Arctic-boreal regions.

In addition to considerable trends in atmospheric temperatures, the models further indicate prominent changes in precipitation (Collins et al., 2013; Hoegh-Guldberg et al., 2018). For the Arctic boreal region, this is largely depicted as an increasing rainfall during both winter and summer, extending to 15–25% over most of the terrestrial domain over the winter and somewhat less during summer (Fig. 10). Contemporary warm Arctic temperatures and large sea ice deficits (75% volume loss) demonstrate climate states outside our previous experience. The modeled changes in the Arctic cryosphere demonstrate that even limiting the global temperature increase to 2 °C will leave the Arctic a much different environment by mid-century, with less snow and sea ice, melted permafrost, altered ecosystems, and a projected annual mean Arctic temperature increase of +4 °C. Even under ambitious emission reduction scenarios, high-latitude land ice melt, including Greenland, are foreseen to continue due to internal lags, leading to accelerating global sea level rise throughout the century (Overland et al., 2019).

4. CONCLUDING REMARKS

Only the integration of different observing networks and programs into an inter-operable and integrated observation system can provide data needed for understanding the mechanisms of the Arctic-boreal system. There is a fundamental need for an integrated, comprehensive network of the-state-of-the art *in situ* stations measuring Earth surface – atmosphere interactions (Kulmala et al., 2016a, 2018; Uttal et al., 2016; Hari et al., 2016; Alekseychik et al., 2016; Vihma et al. 2019). The results obtained in the Pan Eurasian Experiment (PEEX) programme in Russian and China introduced in this paper are based on a combination of long-term observations and campaign data. In addition, the Arctic marine regions require comprehensive observations and subsequent synthesis, as these regions are under a lot of environmental stresses. Therefore, we need more *in situ* observations of the Arctic system covering the marine atmosphere, sea ice and ocean. However, there are pronounced technological and logistical challenges to setup such continuous, marine *in situ* observations (e.g. Vihma et al. 2019). Furthermore, improved monitoring is needed for river discharge and associated fluxes of greenhouse gases and other key compounds and more research on the understanding of coastal processes and atmospheric transport and specific regional socioeconomic issues and their interactions with changing environment (Vihma et al., 2019; Petäjä et al., 2020).

The international organizations and bodies like the Arctic Council (SAON's Roadmap for Arctic Observing and Data Systems, ROADS), EU Horizon2020 (Blue Growth INTAROS and APPLICATE projects), GEO-

CRI (high Mountains and cold regions), the Belmont Forum COPERNICUS and WMO are coordinating development of the Arctic data and services. New data products are expected from the large-scale MOSAiC campaign and projects like ERA-PLANET iCUPE (Petäjä et al. 2020b) or ArcticFLUX to monitor the interface between the marine Arctic and Eurasian continent. Also, national-based Arctic observations and research programs like AC³ by German institutes play a significant role. Russia conducts extensive research in the Arctic region, notably on the manned drifting ice stations. These Arctic observation activities are coordinated and carried out by Roshydromet, universities and Russian Academy of Sciences' institutes.

Concerning global energy markets, the Arctic region holds 25 % or more of the world's undiscovered oil and gas (Arctic Oil & Gas, 2008). The plans of China and Russia to build 'Ice Silk Road' along Northern Sea linking the China and Russia to Europe is highlighting the polar region's growing economic and strategic importance, and the increasing pressure on the Arctic environment and local communities. In addition, wide regions of the high latitudes and Arctic regions are under the pressure of the changing economic activities of the Arctic and are also under a high pressure of the changing environment and climate. A comprehensive observation network providing in-situ data in close coordination with satellite observations and ground-based remote sensing is required to monitor the environmental impacts of the envisioned operations.

Over the last few years, Earth system sciences is driven by the need to understand the scientific processes of climate change and air quality, their interrelations with Earth system and their societal impacts. The interplay between science, politics and business, and the analysis of the existing policies and strategies help us to recognize and analyze new and emerging trends of Arctic governance (e.g. protection and resilience vis-a-vis economic activities), geopolitics (e.g. state sovereignty vis-a-vis internationalization), geo-economics (e.g. tourism vis-à-vis reindeer herding), and science (e.g. climate change). The intensive work towards the new Arctic observations and data systems, together with the intensive observations on the land – atmosphere interactions taking place at the high latitudes, will provide the baseline for cross disciplinary research era. PEEX is aimed for these directions.

ACKNOWLEDGEMENTS

We thank the following funding agencies and projects: Academy of Finland contracts: No 280700, 294600, 296302 (Novel Assessment of Black Carbon in the Eurasian Arctic: From Historical Concentrations and Sources to Future Climate Impacts (NABCEA), 307331 (FCoE Atmospheric Sciences), 311932, 314798/99, 315203, 317999, 337549 (Atmosphere and Climate Competence Center (ACCC), Jane and Aatos Erkko Foundation, Russian Government megagrant project № 075-15-2021-574 "Megapolis - heat and pollution island: interdisciplinary hydroclimatic, geochemical and ecological analysis", Russian Foundation for Basic Research (RFBR) projects No. 17-29-05027 (Selenga-Baikal river system), 17-29-05102, 18-05-00306, 18-05-60037, 18-05-60219 (Arctic river), 18-35-20031, 18-44-860017, 18-45-700015, 18-05-60083 (Storm activity in the Barents Sea), 18-60084 (Dangerous impacts of large - scale industrial emissions on aerosol

Formatted: Font color: Auto

pollution and Arctic ecosystem), 19-05-50088, 19-05-00352, 19-55-80021 (MOST and DST studies), the IAO SB RAS supported by RFBR project No. 19-05-50024, Russian Science Foundation (RSF) projects; RSF project 21-17-00181 (Monitoring at Lena River catchment)" No.17-17-01117, 18-17-00076 (Long-term measurement of aerosol chemical composition in Central Siberia, 19-77-20109 (Black carbon emissions from Siberian fires), 19-77-30004 (Moscow environment), 19-77-300-12 (Measurement networks and field sites in Kola Peninsula), Yugra State University grant No.13-01-20/39, Ministry of Science and Higher Education of Russia - Agreement No.13.1902.21.0003, State assignment No. 0148-2019-0006, Project N75295423 launched by St. Petersburg State University, European Research Council (ERC) projects No. 742206 (ATM-GTP), No. 850614 (CHAPAs), EU Horizon 2020 projects No. 727890 (Integrated Arctic Observing System, INTAROS), 689443 (Integrative and Comprehensive Understanding on Polar Environments, iCUPE), 654109 (Aerosol Clouds and Trace Gases Research Infrastructure, ACTRIS-2), EU7 FP MarcoPolo Grant No. 606953, Erasmus+ 561975-EPP-1-2015-1-FI-EPPKA2-CBHE-JP, Norwegian Research Council and the Belmont Forum project SERUS, No. 311986, National Natural Science Foundation of China Grant No. 41275137, ESA-MOST China Dragon Cooperation projects No. 10663 and 32771 (Dragon 3 and 4).

Our special thanks also to Mrs. Alla Borisova, INAR, University of Helsinki, for the technical editing of the manuscript.

REFERENCES

- Andreae, M. O., Andreae, T. W., and Ditas, F.: How frequent is new particle formation in the boundary layer over the remote temperate/boreal forest?, AGU Fall Meeting, San Francisco, USA, doi:10.1002/essoar.10501148.1, 2019.
- Aalto, J., Porcar-Castell, A., Atherton, J., Kolari, P., Pohja, T., Hari, P., Nikinmaa, E., Petäjä, T., and Bäck, J.: Onset of photosynthesis in spring speeds up monoterpene synthesis and leads to emission bursts, *Plant, Cell and Environment.*, 38, 2299-2312, 2015.
- Agafonova, S. A., Frolova, N. L., Surkova, G. V., and Koltermann, K., P.: Modern characteristics of the ice regime of Russian Arctic rivers and their possible changes in the 21st century, *Geogr. Environ. Sustain.*, 10(4), 4-15, doi:10.24057/2071-9388-2017-10-4-4-15, 2017.
- Alekseychik, P., Lappalainen, H.K., Petäjä, T., Zaitseva, N., Heimann, M., Laurila, T., Lihavainen, H., Asmi, E., Arshinov, M., Shevchenko, V., Makshtas, A., Dubtsov, S., Mikhailov, E., Lapshina, E., Kirpotin, S., Kurbatova, Y., Ding, A., Guo, H., Park, S., Lavric, J.V., Reum, F., Panov, A., Prokushkin, A., and Kulmala, M.: Ground-based station network in Arctic and Subarctic Eurasia: An overview, *Geogr. Environ. Sustain.*, 9(2), 75-88, doi:10.24057/2071-9388-2016-9-2-19-35, 2016.

Formatted: Font: 11 pt

Formatted: Font: 11 pt

Formatted: Font: 11 pt

Formatted: Font color: Auto

Formatted: Font: 11 pt

- 2125 Alekseychik, P., Mammarella, I., Karpov, D., Dengel, S., Terentieva, I., Sabrekov, A., Glagolev, M., and
 2126 Lapshina, E.: Net ecosystem exchange and energy fluxes measured with the eddy covariance technique in a
 2127 western Siberian bog, *Atmos. Chem. Phys.*, 17, 9333–9345, doi:10.5194/acp-17-9333-2017, 2017.
- 2128 AMAP, 2017: Arctic Pollution 2017. Arctic Monitoring and Assessment Programme (AMAP), Oslo,
 2129 Norway.
- 2130 Andreae, M. O.: Emission of trace gases and aerosols from biomass burning – an updated assessment,
 2131 *Atmos. Chem. Phys.*, 19, 8523–8546, doi:10.5194/acp-19-8523-2019, 2019.
- 2132 Arneth, A., Harrison, S., Zaehle, S., Tsigaridis, K., Menon, S., Bartlein, P. J., Feichter, J., Korhola, A.,
 2133 Kulmala, M., O'Donnell, D., Schurgers, G., Sorvari, S., and Vesala, T.: Terrestrial biogeochemical feedbacks
 2134 in the climate system. *Nature Geosci.*, 3, 525–532, <https://doi.org/10.1038/ngeo905>, 2010.
- 2135 Arneth, A., Makkonen, R., Olin, S., Paasonen, P., Holst, T., Kajos, M. K., Kulmala, M., Maximov, T.,
 2136 Miller, P. A., and Schurgers, G.: Future vegetation–climate interactions in Eastern Siberia: an assessment of
 2137 the competing effects of CO₂ and secondary organic aerosols, *Atmos. Chem. Phys.*, 16, 5243–5262,
 2138 doi:10.5194/acp-16-5243-2016, 2016.
- 2139 Arnold, S. R., Law, K. S., Brock, C. A., Thomas, J. L., Starkweather, S. M., von Salzen, K., Stohl, A.,
 2140 Sharma S., Lund, M. T., Flanner, M. G., Petaja, T., Tanimoto, H., Gamble, J., Dibb J. E., Melamed M.,
 2141 Johnson, N., Fidel, M., Tynkkynen, V.-P., Baklanov, A., Eckhardt, S., Monks, S. A., Browse, J., and Bozem,
 2142 H.: Arctic air pollution: Challenges and opportunities for the next decade, *Elementa: Science of the*
 2143 *Anthropocene*, 4:000104, <https://dx.doi.org/10.12952/journal.elementa.00010>. 2016.
- 2144 Arvola, L., Äijälä, C., and Leppäranta, M.: CDOM concentrations of large Finnish lakes relative to their
 2145 landscape properties, *Hydrobiologia*, 780(1), 37–46, doi:10.1007/s10750-016-2906-4, 2016.
- 2146 Arvola, L., Leppäranta, M., and Äijälä, C.: CDOM variations in Finnish lakes and rivers between 1913 and
 2147 2014, *Sci. Total Environ.*, 601, 1638–1648, doi:10.1016/j.scitotenv.2017.06.034, 2017.
- 2148 Asmi, E., Kondratyev, V., Brus, D., Laurila, T., Lihavainen, H., Backman, J., Vakkari, V., Aurela, M.,
 2149 Hatakka, J., Viisanen, Y., Uttal, T., Ivakhov, V., and Makshtas, A.: Aerosol size distribution seasonal
 2150 characteristics measured in Tiksi, Russian Arctic, *Atmos. Chem. Phys.*, 16, 1271–1287, doi:10.5194/acp-16-
 2151 1271-2016, 2016.
- 2152 Backman, J., Schmeisser, L., Virkkula, A., Ogren, J. A., Asmi, E., Starkweather, S., Sharma, S.,
 2153 Eleftheriadis, K., Uttal, T., Jefferson, A., Bergin, M., Makshtas, A., Tunved, P., and Fiebig, M.: On
 2154 Aethalometer measurement uncertainties and an instrument correction factor for the Arctic, *Atmos. Meas.*
 2155 *Tech.*, 10, 5039–5062, doi:10.5194/amt-10-5039-2017, 2017.
- 2156 Badina, S. V.: Socio-economic potential of municipalities in the context of natural risk (case study –
 2157 Southern Siberian regions), *IOP Conference Series: Earth and Environmental Science*, 190,
 2158 doi:10.1088/1755-1315/190/1/012001, 2018.

- Bai, J.H.: Estimation of the isoprene emission from the Inner Mongolia grassland, *Atmospheric Pollution Research*, 6, 406-414, doi: 10.5094/APR.2015.045, 2015.
- Bai, J.H.: UV extinction in the atmosphere and its spatial variation in North China, *Atmos. Environ.*, 154, 318-330, doi:10.1016/j.atmosenv.2017.02.002, 2017a.
- Bai, J.H., Guenther, A., Turnipseed, A., Duhl, T., Greenberg J.: Seasonal and interannual variations in whole-ecosystem BVOC emissions from a subtropical plantation in China. *Atmospheric Environment*, 161, 176-190. <http://dx.doi.org/10.1016/j.atmosenv.2017.05.002>, 2017b.
- Bai, J.H., de Leeuw, G., van der Ronald, A., De Smedt, I., Theys, N., Van Roozendael, M., Sogacheva, L., and Chai, W. H.: Variations and photochemical transformations of atmospheric constituents in North China, *Atmos. Environ.*, 189, 213-226, doi:10.1016/j.atmosenv.2018.07.004, 2018a.
- Bai, Y., Zhang, J., Zhang, S., Yao, F., and Magliulo, V.: A remote sensing-based two-leaf canopy conductance model: Global optimization and applications in modeling gross primary productivity and evapotranspiration of crops, *Remote Sensing of Environment*, 215, 411-437, doi:10.1016/j.rse.2018.06.005, 2018b.
- Bai, J. H.: A calibration method of solar radiometers, *Atmos. Pollut. Res.*, 10(4), 1365-1373, doi:10.1016/j.apr.2019.03.011, 2019.
- Bai, J. H.: O₃ Concentration and its relation with BVOC emissions in a subtropical plantation. *Atmosphere*, 12, 711. <https://doi.org/10.3390/atmos12060711>, 2021.
- Baklanov, A., Mahura, A., Nazarenko, L., Tausnev, N., Kuchin, A., and Rigina, O.: *Atmospheric Pollution and Climate Change in Northern Latitudes*, Russ. Acad. Sci., Apatity, Russia, 2012.
- Baklanov, A. A., Penenko, V. V., Mahura, A. G., Vinogradova, A. A., Elansky, N. F., Tsvetova, E. A., Rigina, O. Y., Maksimenkov, L. O., Nuterman, R. B., Pogarskii, F. A., and Zakey, A.: *Aspects of Atmospheric Pollution in Siberia*, in *Regional Environmental Changes in Siberia and Their Global Consequences*, edited by: Groisman P. Y., and Gutman, G., 303-346, Springer, Dordrecht, Netherlands, 2013.
- Baklanov, A., Molina, L.T., and Gauss, M.: Megacities, air quality and climate, *Atmospheric Environment*, 126, 235-249, <https://doi.org/10.1016/j.atmosenv.2015.11.059>, 2016.
- Baklanov, A., Smith Korsholm, U., Nuterman, R., Mahura, A., Nielsen, K. P., Sass, B. H., Rasmussen, A., Zakey, A., Kaas, E., Kurganskiy, A., Sørensen, B., and González-Aparicio, I.: Enviro-HIRLAM online integrated meteorology-chemistry modelling system: strategy, methodology, developments and applications (v7.2), *Geosci. Model Dev.*, 10, 2971-2999, <https://doi.org/10.5194/gmd-10-2971-2017>, 2017.
- Baklanov, A., Brunner, D., Carmichael, G., Flemming, J., Freitas, S., Gauss, M., Hov, O., R. Mathur, R., Schlünzen, K., Seigneur, C., and Vogel, B.: Key issues for seamless integrated chemistry-meteorology modeling, *Bull. Amer. Meteor. Soc.*, doi:10.1175/BAMS-D-15-00166.1., 2018.

Formatted: Font color: Auto

- 2193 Balch, W. M., Bates, N. R., Lam, P. J., Twining, B. S., Rosengard, S. Z., Bowler, B. C., and Rauschenberg,
2194 S.: Factors regulating the Great Calcite Belt in the Southern Ocean, and its biogeochemical significance,
2195 *Global Biogeochem. Cycles*, 30(8), 1124–1144, doi:10.1002/2016GB005414, 2016.
- 2196 Balch, W. M.: The ecology, biogeochemistry, and optical properties of coccolithophores, *Ann. Rev. Mar.*
2197 *Sci.*, 109, 71–98, doi:10.1146/annurev-marine-121916-063319, 2018.
- 2198 Bartsch, A., Kumpula, T., Forbes, B.C. and Stammer F.: Detection of snow surface thawing and refreezing
2199 in the Eurasian Arctic with QuikSCAT: implications for reindeer herding, *Ecol Appl.*, 20, 2346–58., doi:
2200 10.1890/09-1927.1., 2010.
- 2201 Barreira, L. M. F., Duporté, G., Rönkkö, T., Parshintsev, J., Hartonen, K., Hyrsky, L., Heikkinen, E.,
2202 Kulmala, M., and Riekkola, M.-L.: Field measurements of biogenic volatile organic compounds in the
2203 atmosphere using solid-phase microextraction Arrow, *Atmos. Meas. Tech.*, 11, 881–893, 2018.
- 2204 Bashmachnikov, I.L., Yurova, A.Y., Bobylev, L.P., and Vesman, A. V.: Seasonal and Interannual Variations
2205 of Heat Fluxes in the Barents Sea Region, *Izv., Atmos. Ocean. Phys.*, 54, 213–222,
2206 doi:10.1134/S0001433818020032, 2018a.
- 2207 Bashmachnikov, I. L., Yurova, A.Y., Bobylev, L. P., Vesman, A.V.: Seasonal and interannual variations of
2208 the heat fluxes in the Barents Sea region, *Izv. Atmos. Ocean. Phys.*, 54(2), 239–249,
2209 doi:10.7868/S0003351518020149, 2018b.
- 2210 Beer, C., Reichstein, M., Tomelleri, E., Ciais, P., Jung, M., Carvalhais, N., Rödenbeck, C., Altaf Arain,
2211 A., Baldocchi, D., Bonan, G.B., Bondeau, A., Cescatti, A., Lasslop, G., Lindroth, A., Lomas, M.,
2212 Luyssaert, S., Margolis, H., Oleson, K.W., Rouspard, O., Veenendaal, E., Viovy, N., Williams, C., F Ian
2213 Woodward, F.,I., and Papale, D.:Terrestrial gross carbon dioxide uptake: global distribution and covariation
2214 with climate. *Science*, 329, 834–838, doi: 10.1126/science.1184984, 2010.
- 2215 Belikov, D., Arshinov, M., Belan, B., Davydov, D., Fofonov, A., Sasakawa, M., Machida, T.: Analysis of the
2216 Diurnal, Weekly, and Seasonal Cycles and Annual Trends in Atmospheric CO₂ and CH₄ at Tower Network
2217 in Siberia from 2005 to 2016, *Atmosphere*, 10 (11), 689, doi: 10.3390/atmos10110689, 2019.
- 2218 Berchet, A., Bousquet, P., Pison, I., Locatelli, R., Chevallier, F., Paris, J.-D., Dlugokencky, E. J., Laurila, T.,
2219 Hatakka, J., Viisanen, Y., Worthy, D. E. J., Nisbet, E., Fisher, R., France, J., Lowry, D., Ivakhov, V., and
2220 Hermansen, O.: Atmospheric constraints on the methane emissions from the East Siberian Shelf, *Atmos.*
2221 *Chem. Phys.*, 16, 4147–4157, doi:10.5194/acp-16-4147-2016, 2016.
- 2222 Berezina, E., Moiseenko, K., Skorokhod, A., Elansky, N., Belikov, I., and Pankratova, N.: Isoprene and
2223 monoterpenes over Russia and their impacts in tropospheric ozone formation, *Geogr., Environ., Sustain.*,
2224 12(1), 63–74, doi:10.24057/2071-9388-2017-24, 2019.
- 2225 Bezuglaya, E. Y., Ed.: Air quality in largest cities of Russia for 10 years (1988–1997), Hydrometeoizdat, St.
2226 Petersburg, Russia, 1999.

- 2227 Biskaborn, B. K., Smith, S. L., Noetzli, J., Matthes, H., Vieira, G., Streletskiy, D. A., Schoeneich, P.,
 2228 Romanovsky, V. E., Lewkowicz, A. G., Abramov, A., Allard, M., Boike, J., Cable, W. L., Christiansen, H.
 2229 H., Delaloye, R., Diekmann, B., Drozdov, D., Etzelmüller, B., Grosse, G., ... and Lantuit, H.: Permafrost is
 2230 warming at a global scale, *Nat. Commun.*, 10(1), 264, doi: 10.1038/s41467-018-08240-4, 2019.
- 2231 Blackport, R., Screen, J. A., van der Wiel, K., and Bintanja, R.: Minimal influence of reduced Arctic sea ice
 2232 on coincident cold winters in mid-latitudes, *Nat. Clim. Change*, 9, 697–704, doi: 10.1038/s41558-019-0551-
 2233 4, 2019.
- 2234 Bobylev, S.N., Cheresnaya, O.Y., Kulmala, M., Lappalainen, H. K., Petäjä, T., Solov'eva, S.V., Tikunov,
 2235 V.S., and Tynkkynen, V.-P.: Indicators for digitalization of sustainable development goals in PEEX
 2236 program, *J. Geogr. Sust.*, 11, 145-156, 2018.
- 2237 Boike, J., Nitzbon, J., Anders, K., Grigoriev, M., Bolshiyarov, D., Langer, M., Lange, S., Bornemann, N.,
 2238 Morgenstern, A., Schreiber, P., Wille, C., Chadburn, S., Gouttevin, I., Burke, E., and Kutzbach, L.: A 16-
 2239 year record (2002–2017) of permafrost, active-layer, and meteorological conditions at the Samoylov Island
 2240 Arctic permafrost research site, Lena River delta, northern Siberia: an opportunity to validate remote-sensing
 2241 data and land surface, snow, and permafrost models, *Earth Syst. Sci. Data*, 11, 261–299,
 2242 <https://doi.org/10.5194/essd-11-261-2019>, 2019.
 2243
- 2244 Bondur, G., and Vorobev, V. E.: Satellite Monitoring of Impact Arctic Regions, *Izv. Atmos. Ocean. Phys.*,
 2245 51, 949–968, doi: 10.1134/S0001433815090054, 2015.
- 2246 Bondur, V. G., and Ginzburg, A. S.: Emission of carbon-bearing gases and aerosols from natural fires on the
 2247 territory of Russia based on space monitoring, *Dokl. Earth Sci.*, 466(2), 148-152,
 2248 doi:10.1134/s1028334x16020045, 2016.
- 2249 Bondur, V. G.: Satellite monitoring of trace gas and aerosol emissions during wildfires in Russia. *Izv.*
 2250 *Atmos. Ocean. Phys.*, 52(9), 1078-1091, doi:10.1134/s0001433816090103, 2016.
- 2251 Bondur, V. G., Gordo, K. A., and Kladov, V. L.: Spacetime distributions of wildfire areas and emissions of
 2252 carbon-containing gases and aerosols in northern eurasia according to satellite-Monitoring Data, *Izv. Atmos.*
 2253 *Ocean. Phys.*, 53(9), 859-874, doi:10.1134/s0001433817090055, 2017.
- 2254 Bondur, V. G. and Gordo, K. A.: Satellite Monitoring of Burned out Areas and Emissions of Harmful
 2255 Contaminants due to Forest and other Wildfires in Russia, *Izv., Atmos. Ocean. Phys.*, 54 (9),955–965, doi:
 2256 10.1134/S0001433818090104, 2018.
- 2257 Bondur V. G., Chimitdorzhiev T. N., Dmitriev A. V., and Dagurov P. N.: Otsenka prostranstvennoy
 2258 anizotropii neodnorodnostey lesnoy rastitelnosti pri razlichnykh azimutalnykh uglakh radarnogo
 2259 polyarimetricheskogo zondirovaniya (Spatial anisotropy assessment of the forest vegetation heterogeneity at

- 2260 various azimuth angles of the radar polarimetric sensing), *Issledovanie Zemli iz kosmosa*, Russia, 3, 92-103,
2261 doi:10.31857/S0205-96142019392-103, 2019a.
- 2262 Bondur, V. G., Chimitdorzhiev, T. N., Dmitriev, A. V., Dagurov, P. N., Zakharov, A. I., and Zakharova, L.
2263 N.: Metody radarnoj polyarimetrii dlya issledovaniya izmenenij mekhanizmov obratnogo rasseyaniya v
2264 zonah opolznei na primere obrusheniya sklona berega reki Bureya (Using radar polarimetry to monitor
2265 changes in backscattering mechanisms in landslide zones for the case study of the Bureya river bank
2266 collapse), *Issledovanie Zemli iz kosmosa*, Russia, 4, 3-17, doi:10.31857/S0205-9614201943-17, 2019b.
- 2267 Bondur, V. G., Tsidilina, M. N., and Cherepanova, E. V.: Satellite Monitoring of Wildfire Impacts on The
2268 Conditions of Various Types of Vegetation Cover in The Federal Districts of the Russian Federation, *Izv.*
2269 *Atmos. Ocean. Phys.*, 55 (9), 1238–1253, doi:10.1134/s000143381909010X, 2019 (c).
- 2270 Bondur, V. G., Tsidilina, M. N., Kladov, V. L., and Gordo, K. A.: Irregular Variability of Spatiotemporal
2271 Distributions of Wildfires and Emissions of Harmful Trace Gases in Europe Based on Satellite Monitoring
2272 Data // *Doklady Earth Sciences*, Vol. 485, Part 2, pp. 461–464, doi: 10.1134/S1028334X19040202, 2019(d).
- 2273 Bondur, V. G., Zakharova, L. N., and Zakharov, A. I.: Monitoring of the landslide area state on Bureya river
2274 in 2018-2019 according to radar and optical satellite images, *Issledovanie Zemli iz kosmosa*, Russia, No. 6,
2275 26-35, doi:10.31857/S0205-96142019626-35, 2019(e).
- 2276 Bondur, V. G., Zakharova, L. N., Zakharov, A. I., Chimitdorzhiev, T. N., Dmitriev, A. V., and Dagurov,
2277 P. N.: Monitoring of landslide processes by means of L-band radar interferometric observations: Bureya river
2278 bank caving case // *Issledovanie Zemli iz kosmosa*, Russia, No. 5, 3-14, DOI:
2279 <https://doi.org/10.31857/S0205-9614201953-14>. 2019 (f).
- 2280 Bondur, V. G., Tsidilina, M. N., and Kladov, V. L.: Irregular Variability of Spatiotemporal Distributions of
2281 Wildfires and Emissions of Harmful Trace Gases in Europe Based on Satellite Monitoring Data, *Dokl. Earth*
2282 *Sc.*, 485, 461–464, <https://doi.org/10.1134/S1028334X19040202>, 2019.
- 2283 Bondur, V. G., Mokhov, I. I., Voronova, O. S., and Sitnov, S. A.: Satellite Monitoring of Siberian Wildfires
2284 and Their Effects: Features of 2019 Anomalies and Trends of 20-Year Changes, *Doklady Earth Sciences*,
2285 492, 1, 370–375. doi: 10.1134/S1028334X20050049, 2020.
- 2286 Bormann, K. J., Brown, R. D., Derksen, C., and Painter, T. H.: Estimating snow-cover trends from space,
2287 *Nat. Clim. Chang.*, 8, 924-928, 2018.
- 2288 Boy, M., Thomson, E. S., Acosta Navarro, J.-C., Arnalds, O., Batchvarova, E., Bäck, J., Berninger, F., Bilde,
2289 M., Brasseur, Z., Dagsson-Waldhauserova, P., Castarède, D., Dalirian, M., de Leeuw, G., Dragosics, M.,
2290 Duplissy, E.-M., Duplissy, J., Ekman, A. M. L., Fang, K., Gallet, J.-C., Glasius, M., Gryning, S.-E., Grythe,
2291 H., Hansson, H.-C., Hansson, M., Isaksson, E., Iversen, T., Jonsdottir, I., Kasurinen, V., Kirkevåg, A.,
2292 Korhola, A., Krejci, R., Kristjansson, J. E., Lappalainen, H. K., Lauri, A., Leppäranta, M., Lihavainen, H.,
2293 Makkonen, R., Massling, A., Meinander, O., Nilsson, E. D., Olafsson, H., Pettersson, J. B. C., Prisle, N. L.,

- 2294 Riipinen, I., Roldin, P., Ruppel, M., Salter, M., Sand, M., Seland, Ø., Seppä, H., Skov, H., Soares, J., Stohl,
2295 A., Ström, J., Svensson, J., Swietlicki, E., Tabakova, K., Thorsteinsson, T., Virkkula, A., Weyhenmeyer, G.
2296 A., Wu, Y., Zieger, P., and Kulmala, M.: Interactions between the atmosphere, cryosphere, and ecosystems
2297 at northern high latitudes, *Atmos. Chem. Phys.*, 19, 2015–2061, <https://doi.org/10.5194/acp-19-2015-2019>,
2298 2019.
- 2299 Breider, T.J., Mickley, L.J., Jacob, D.J., Ge, C., Wang, J., Sulprizio, M.P., Croft, B., Ridley, D.A.,
2300 McConnell, J.R., Sharma, S., Husain, L., Dutkiewicz, V. A., Eleftheriadis, K., Skov, H., and Hopke, P. K.:
2301 Multidecadal trends in aerosol radiative forcing over the Arctic: Contribution of changes in anthropogenic
2302 aerosol to Arctic warming since 1980, *J. Geophys. Res.: Atmos.*, 122, 3573–3594,
2303 <https://doi.org/10.1002/2016JD025321>, 2017.
- 2304 Burkhard, B., Kroll, F., Müller, F., and Windhorst, W. F., Landscapes' Capacities to Provide Ecosystem
2305 Services – a Concept for Land-Cover Based Assessments, *Landscape Online* 15(1), 1–12, DOI:
2306 10.3097/LO.200915, 2009.
- 2307 Chalov, S. R., Jarsjo, J., Kasimov, N. S., Romanchenko, A. O., Pietron, J., Thorslund, J., and Promakhova,
2308 E. V.: Spatio-temporal variation of sediment transport in the Selenga River Basin, Mongolia and Russia,
2309 *Environ. Earth Sci.*, 73(2), 663–680, doi:10.1007/s12665-014-3106-z, 2015.
- 2310 Chalov, S. R., Bazilova, V. O., and Tarasov, M. K.: Modelling suspended sediment distribution in the
2311 Selenga River Delta using LandSat data, in *Integrating Monitoring and Modelling for Understanding,*
2312 *Predicting and Managing Sediment Dynamics*, edited by: Collins, A., Stone, M., Horowitz, A., and Foster, I.,
2313 Copernicus Gesellschaft, Gottingen, Germany, 375, 19–22, 2017a.
- 2314 Chalov, S., Thorslund, J., Kasimov, N., Aybullaev, D., Ilyicheva, E., Karthe, D., Kositsky, A., Lychagin,
2315 M., Nitttrouer, J., Pavlov, M., Pietron, J., Shinkareva, G., Tarasov, M., Garmaev, E., Akhtman, Y., and Jarsjö,
2316 J.: The Selenga River delta: a geochemical barrier protecting Lake Baikal waters, *Regional Environ. Change*,
2317 17, 2039–2053, doi: 10.1007/s10113-016-0996-1, 2017b.
- 2318 Chalov, S. R., Millionshchikova, T. D., and Moreido, V. M.: Multi-Model Approach to Quantify Future
2319 Sediment and Pollutant Loads and Ecosystem Change in Selenga River System, *Water Resour.*, 45, S22–S34,
2320 doi:10.1134/s0097807818060210, 2018.
- 2321 Che, Y., Xue, Y., Mei, L., Guang, J., She, L., Guo, J., Hu, Y., Xu, H., He, X., Di, A., and Fan, C.: Technical
2322 note: Intercomparison of three AATSR Level 2 (L2) AOD products over China, *Atmos. Chem. Phys.*, 16,
2323 9655–9674, <https://doi.org/10.5194/acp-16-9655-2016>, 2016.
- 2324 Cheng, Y., Cheng, B., Zheng, F., Vihma, T., Kontu, A., Yang, Q. and Liao, Z.: Air/snow, snow/ice and
2325 ice/water interfaces detection from high-resolution vertical temperature profiles measured by ice mass-
2326 balance buoys on an Arctic lake. *Annals of Glaciology*, accepted (2020).

- 2327 Chernokulsky, A. V., Esau, I., Bulygina, O. N., Davy, R., Mokhov, II, Outten, S., and Semenov, V. A.:
 2328 Climatology and interannual variability of cloudiness in the Atlantic Arctic from surface observations since
 2329 the late nineteenth century, *J. Clim.*, 30(6), 2103-2120, doi:10.1175/jcli-d-16-0329.1, 2017.
- 2330 Chernokulsky, A., and Esau, I.: Cloud cover and cloud types in the Eurasian Arctic in 1936–2012. *Int. J.*
 2331 *Climatol.*, **39**(15), 5771–5790, <https://doi.org/10.1002/joc.6187>, 2019
- 2332 Chu, B., Kerminen, V.-M., Bianchi, F., Yan, C., Petäjä, T. and Kulmala, M.: Atmospheric new particle
 2333 formation in China, *Atmos. Chem. Phys.*, 19, 115-138, 2019.
- 2334 Chubarova, N. Y., Poliukhov, A. A., and Gorlova, I. D.: Long-term variability of aerosol optical thickness in
 2335 Eastern Europe over 2001–2014 according to the measurements at the Moscow MSU MO AERONET site
 2336 with additional cloud and NO2 correction, *Atmos. Meas. Tech.*, 9, 313–334, [https://doi.org/10.5194/amt-9-](https://doi.org/10.5194/amt-9-313-2016)
 2337 313-2016, 2016a.
- 2338 Chubarova, N., Zhdanova, Y., and Nezval, Y.: A new parameterization of the UV irradiance altitude
 2339 dependence for clear-sky conditions and its application in the on-line UV tool over Northern Eurasia, *Atmos.*
 2340 *Chem. Phys.*, 16, 11867–11881, <https://doi.org/10.5194/acp-16-11867-2016>, 2016b.
- 2341 Chubarova, N. E., Pastukhova, A. S., and Galin, V. Y.: Long-Term Variability of UV Irradiance in the
 2342 Moscow Region according to Measurement and Modeling Data, *Izv. Atmos. Ocean. Phys.*, 54, 139–146,
 2343 <https://doi.org/10.1134/S0001433818020056>, 2018.
- 2344 Chubarova, N. E., Androsova, E. E., Kirsanov, A. A., Vogel, B., Vogel, H., Popovicheva, O. B., and Rivin,
 2345 G. S.: Aerosol and Its Radiative Effects during the Aeroradcity 2018 Moscow Experiment, *Geography*,
 2346 *Environment, Sustainability*, 12, 114-131, <https://doi.org/10.24057/2071-9388-2019-72> 2019a.
- 2347 Chubarova, N. E., Timofeev, Y. M., Virolainen, Y. A., and Polyakov, A. V.: Estimates of UV indices during
 2348 the periods of reduced ozone content over Siberia in Winter-Spring 2016, *Atmos. Oceanic Opt.*, 32, 177-179,
 2349 doi:10.1134/s1024856019020040, 2019b.
- 2350 Chubarova, N. E., Pastukhova, A.S., Zhdanova, E.Y., Volpert, E.V., Smyshlyaev and S.P., and Galin, V.Y.:
 2351 Effects of Ozone and Clouds on Temporal Variability of Surface UV Radiation and UV Resources over
 2352 Northern Eurasia Derived from Measurements and Modeling., *Atmosphere*, 11, 59, 2020.
- 2353 Cohen, J., X. Zhang, T., Jung, R. Kwok, J., Overland, T., Ballinger, U.S., Bhatt, H. W., Chen, D., Coumou,
 2354 S., Feldstein, H., Gu, D., Handorf, G., Henderson, M., Ionita, M., Kretschmer, F., Laliberte, S., Lee, H. W.,
 2355 Linderholm, W., Maslowski, Y., Peings, K., Pfeiffer, I., Rigor, T., Semmler, J., Stroeve, P.C., Taylor, S.,
 2356 Vavrus, T., Vihma, S., Wang, M., Wendisch, Y., Wu, and Yoon, J.: Divergent consensus on Arctic
 2357 amplification influence on midlatitude severe winter weather. *Nature Climate Change*, 10, 20-29,
 2358 doi:10.1038/s41558-019-0662-y, 2020.
- 2359 Collins, M., Knutti, R., Arblaster, J., Dufresne, J.-L., Fichet, T., Friedlingstein, P., Gao, X., Gutowski,
 2360 W.J., Johns, T., Krinner, G., Shongwe, M., Tebaldi, C., Weaver, A.J., and Wehner, M.: Long-term climate

- change: Projections, commitments and irreversibility, in *Climate Change 2013: The Physical Science Basis. Contribution of Working Group I to the Fifth Assessment Report of the Intergovernmental Panel on Climate Change*, edited by: Stocker, T.F., Quin, D., Plattner, G.-K., Tignor, M., Allen, S.K., Doschung, J., Nauels, A., Xia, Y., Bex, V., and Midgley, P.M., Cambridge University Press, Cambridge, United-Kingdom, 1029-1136, doi:10.1017/CBO9781107415324.024, 2013.
- Commene, R., Lindaas, J., Benmergui, J., Luus K. A., Chang, R. Y.-W., Daube, B. C., Euskirchen, E. S., Henderson, J. M., Karion, A., Miller, J. B., Miller, S. M., Parazoo, N. C., Randerson, J. T., Sweeney, C., Tans, P., Thoning, K., Veraverbeke, S., Miller, C. E., and Wofsy, S. C.: Carbon dioxide sources from Alaska driven by increasing early winter respiration from Arctic tundra, *PNAS*, 114(21), 5361-5366, 2017.
- Coumou, C., Petoukhov, V., Rahmstorf, S., Petri, S., and Schellnhuber, H.-J.: Quasi-resonant circulation regimes and hemispheric synchronization of extreme weather in boreal summer, *Proc. Natl. Acad. Sci.*, 111, 12 331–12336, <https://doi.org/10.1073/pnas.1412797111>, 2014.
- Dada, L., Paasonen, P., Nieminen, T., Buenrostro Mazon, S., Kontkanen, J., Peräkylä, O., Lehtipalo, K., Hussein, T., Petäjä, T., Kerminen, V.-M., Bäck, J. and Kulmala, M.: Long-term analysis of clear-sky new particle formation events and nonevents in Hyytiälä, *Atmos. Chem. Phys.*, 17, 6227-6241, 2017.
- Dada, L., Chellapermal, R., Buenrostro Mazon, S., Paasonen, P., Lampilahti, J., Manninen, H. E., Junninen, H., Petäjä, T., Kerminen, V.-M., and Kulmala, M.: Refined classification and characterization of atmospheric new-particle formation events using air ions, *Atmos. Chem. Phys.*, 18, 17883–17893, <https://doi.org/10.5194/acp-18-17883-2018>, 2018.
- Dagsson-Waldhauserova, P., Meinander, O.: Atmosphere-cryosphere interaction in the Arctic, at high latitudes and mountains with focus on transport, deposition and effects of dust, black carbon, and other aerosols, *Front. Earth Sci.*, 7, 337, <https://www.frontiersin.org/articles/10.3389/feart.2019.00337/full>, 2019.
- Dave, B., and Kobayashi, Y.: China's silk road economic belt initiative in Central Asia: economic and security implications, *Asia Europe Journal*, 16, 1-15. doi:10.1007/s10308-018-0513-x, 2018.
- Davy, R., and Esau, I.: Differences in the efficacy of climate forcings explained by variations in atmospheric boundary layer depth, *Nat. Commun.*, 7, 8, doi:10.1038/ncomms11690, 2016.
- Davy, R., Esau, I., Chernokulsky, A., Outten, S., and Zilitinkevich, S.: Diurnal asymmetry to the observed global warming, *Int. J. Climatol.*, 37, 79-93, doi:10.1002/joc.4688, 2017.
- Dean, J. F., Middelburg, J. J., Röckmann, T., Aerts, R., Blauw, L. G., Egger, M., Jetten, M. S. M., de Jong, A. E. E., Meisel, O. H., Rasigraf, O., Slomp, C. P., in't Zandt, M. H., and Dolman, A. J.: Methane feedbacks to the global climate system in a warmer world, *Rev. Geophys.*, 56(1), 207-250, <https://doi.org/10.1002/2017RG00055>, 2018.
- Derksen, C., and Brown, R.: Spring snow cover extent reductions in the 2008-2012 period exceeding climate model predictions, *Geophys. Res. Lett.*, 39, L19504, 2012.

Formatted: Font color: Auto

- Derome, J., and Lukina, N.: Interaction between environmental pollution and land-cover/land-use change in Arctic areas, in: *Eurasian Arctic Land Cover and Land Use in a Changing Climate*, edited by: Gutman, G., and Reissell, A., 6, 269–290, Springer, Amsterdam, Netherlands, 2011.
- Ding, A. J., Huang, X., Nie, W., Sun, J. N., Kerminen, V.-M., Petäjä, T., Su, H., Chen, Y. F., Yang, X.-Q., Wang, M. H., Chi, X. G., Wang, J. P., Virkkula, A., Guo, W. D., Yuan, J., Wang, S. Y., Zhang, R. J., Wu, Y. F., Song, Y. Zhu, T., Zilitinkevich, S., Kulmala, M., and Fu, C. B.: Enhanced haze pollution by black carbon in megacities in China, *Geophys. Res. Lett.*, 43, 2873–2879, doi:10.1002/2016GL067745, 2016a.
- Ding, A. J., Nie, W., Huang, X., Chi, X., Sun, J., Kerminen, V.-M., Xu, Z., Guo, W., Petäjä, T., Yang, X., Kulmala, M., and Fu, G.: Long-term observation of pollution-weather/climate interactions at the SORPES station: a review and outlook, *Front. Environ. Sci. Eng.*, 10, doi:10.1007/s11783-016-0877-3, 2016b.
- Dou, T., Xiao, C., Liu, J., Han, W., Du, Z., Mahoney, A. R., Jones, J., and Eicken, H.: A key factor initiating surface ablation of Arctic sea ice: earlier and increasing liquid precipitation, *The Cryosphere*, 13, 1233–1246, <https://doi.org/10.5194/tc-13-1233-2019>, 2019.
- Dragosics, M., Meinander, O., Jonsdottir, T., Durig, T., De Leeuw, G., Palsson, F., Dagsson-Waldhauserová, P., and Thorsteinsson, T.: Insulation effects of Icelandic dust and volcanic ash on snow and ice, *Arab. J. Geosci.*, 9, 126, DOI:10.1007/s12517-015-2224-6, 2016.
- Duporte, G., Parshintsev, J., Barreira, L. M. F., Hartonen, K., Kulmala, M., and Riekkola, M. L.: Nitrogen-containing low volatile compounds from pinonaldehyde-dimethylamine reaction in the atmosphere: a laboratory and field study, *Environ. Sci. Technol.*, 50(9), 4693–4700, doi:10.1021/acs.est.6b00270, 2016.
- Durairaj, P., Sarangi, R., Ramalingam, S., Thirunavukarassu, T., and Chauhan, P.: Seasonal nitrate algorithms for nitrate retrieval using OCEANSAT-2 and MODIS-AQUA satellite data, *Environ. Monit. Assess.*, 187, 176–189, doi: 10.1007/s10661-015-4340-x, 2015.
- Dyukarev, E.A., Godovnikov, E.A., Karpov, D.V., Kurakov, S.A., Lapshina, E.D., Filippov, I.V., Filippova, N.V., and Zarov, E.A.: Net ecosystem exchange, gross primary production and ecosystem respiration in ridge-hollow complex at Mukhrino Bog, *Geography, Environment, Sustainability*, 12(2), 227–244, doi:10.24057/2071-9388-2018-77, 2019.
- Elansky, N. F., Lavrova, O. V., Skorokhod, A. I., and Belikov, I. B.: Trace gases in the atmosphere over Russian cities, *Atmos. Environ.*, 143, 108–119, doi:10.1016/j.atmosenv.2016.08.046, 2016.
- Esau, I., Miles, V. V., Davy, R., Miles, M. W., and Kurchatova, A.: Trends in normalized difference vegetation index (NDVI) associated with urban development in northern West Siberia, *Atmos. Chem. Phys.*, 16, 9563–9577, <https://doi.org/10.5194/acp-16-9563-2016>, 2016.
- Esau, I., Varentsov, M., Laruelle, M., Miles, M. W., Konstantinov, P., Soromotin, A., Baklanov, A. A., and Miles, V. V.: Warmer Climate of Arctic Cities, Chapter 3 in the monography “The Arctic: Current Issues and

- Challenges”, Edited by: Pokrovsky, O., NOVA Publishers, ISBN: 978-1-53617-306-2,
<https://novapublishers.com/shop/the-arctic-current-issues-and-challenges/>, 2020.
- Euskirchen, E. S., Bret-Harte, M. S., Shaver, G. R., Edgar, C. W., and Romanovsky, V. E.: Long-term release of carbon dioxide from arctic tundra ecosystems in northern Alaska, *Ecosystems*, 1–15, 2017.
- Evangelidou, N., Shevchenko, V. P., Yttri, K. E., Eckhardt, S., Sollum, E., Pokrovsky, O. S., Kobelev, V. O., Korobov, V. B., Lobanov, A. A., Starodymova, D. P., Vorobiev, S. N., Thompson, R. L., and Stohl, A.: Origin of elemental carbon in snow from western Siberia and northwestern European Russia during winter–spring 2014, 2015 and 2016, *Atmos. Chem. Phys.*, 18, 963–977, <https://doi.org/10.5194/acp-18-963-2018>, 2018.
- Ezhova, E., Orlov, D., Suhonen, E., Kaverin, D., Mahura, A., Gennadinik, V., Kukkonen, I., Drozdov, D., Lappalainen, H. K., Melnikov, V., Petäjä, T., Kerminen, V.-M., Zilitinkevich, S., Malkhazova, S. M., Christensen, T. R., and Kulmala, M.: Climatic Factors Influencing the Anthrax Outbreak of 2016 in Siberia, Russia. *EcoHealth*, <https://doi.org/10.1007/s10393-021-01549-5>, 2021.
- Ezhova, E., Kerminen, V.-M., Lehtinen, K. E. J., and Kulmala, M.: A simple model for the time evolution of the condensation sink in the atmosphere for intermediate Knudsen numbers, *Atmos. Chem. Phys.*, 18, 2431–2442, <https://doi.org/10.5194/acp-18-2431-2018>, 2018a.
- Ezhova, E., Ylivinkka, I., Kuusk, J., Komsaare, K., Vana, M., Krasnova, A., Noe, S., Arshinov, M., Belan, B., Park, S.-B., Lavrič, J. V., Heimann, M., Petäjä, T., Vesala, T., Mammarella, I., Kolari, P., Bäck, J., Rannik, Ü., Kerminen, V.-M., and Kulmala, M.: Direct effect of aerosols on solar radiation and gross primary production in boreal and hemiboreal forests, *Atmos. Chem. Phys.*, 18, 17863–17881, <https://doi.org/10.5194/acp-18-17863-2018>, 2018b.
- Fang, K., Makkonen, R., Guo, Z., and Seppä, H.: An increase in the biogenic aerosol concentration as a contributing factor to the recent wetting trend in Tibetan Plateau. *Sci Rep* 5, 14628, <https://doi.org/10.1038/srep14628>, 2015.
- Fang, Y., Changyou, L., Leppäranta, M., Xiaonghong, S., Shengnan, Z., and Chengfu, Z.: Notable increases in nutrient concentrations in a shallow lake during seasonal ice growth, *Water Science and Technology*, 74(12), 2773–2783, 2016.
- Fang, K., Makkonen, R., Guo, Z., Zhao, Y., and Seppä, H.: An increase in the biogenic aerosol concentration as a contributing factor to the recent wetting trend in Tibetan Plateau, *Scientific Reports*, 5, 14628, DOI: 10.1038/srep14628, 2015.
- Fletcher, S. E. M., and Schaefer, H.: Rising methane: a new climate challenge, *Science*, 364, 932–933, 2019.
- Franz, D., Mammarella, I., Boike, J., Kirillin, G., Vesala, T., Bornemann, N., Larmanou, E., Langer, M., and Sachs, T.: Lake-Atmosphere Heat Flux Dynamics of a Thermokarst Lake in Arctic Siberia, *J. Geophys. Res.: Atmos.*, 123(10), 5222–5239, doi:10.1029/2017jd027751, 2018.

- 2462 Freud, E., Krejci, R., Tunved, P., Leaitch, R., Nguyen, Q. T., Massling, A., Skov, H., and Barrie, L.: Pan-
 2463 Arctic aerosol number size distributions: seasonality and transport patterns, *Atmos. Chem. Phys.*, 17, 8101–
 2464 8128, <https://doi.org/10.5194/acp-17-8101-2017>, 2017.
- 2465 Frolova, N.L., Belyakova, P.A., Grigoriev, V.Y. *et al.* : Runoff fluctuations in the Selenga River Basin, *Reg*
 2466 *Environ Change*, 17, 1965–1976, doi.org/10.1007/s10113-017-1199-0, 2017.
- 2467
- 2468 Fu, B. J., and Forsius, M.: Ecosystem services modeling in contrasting landscapes, *Landscape Ecol.*, 30(3),
 2469 375–379, [doi:10.1007/s10980-015-0176-6](https://doi.org/10.1007/s10980-015-0176-6), 2015.
- 2470 Garmaev, E. Z., Kulikov, A. I., Tsydypov, B. Z., Sodnomov, B. V., and Ayurzhanayev, A. A.: Environmental
 2471 Conditions Of Zakamensk Town (Dzhida River Basin Hotspot), *Geography, Environment,*
 2472 *Sustainability*, 12(3), 224–239, <https://doi.org/10.24057/2071-9388-2019-32>, 2019.
- 2473 Georgiadi, A. G., Koronkevich, N. I., Milyukova, I. P., and Barabanova, E. A.: Integrated projection for
 2474 runoff changes in large Russian river basins in the XXI Century, *Geography, Environment, Sustainability*,
 2475 9(2), 38–46, 2016.
- 2476 GGO: Air quality in cities of Russia during the year 2015, St. Petersburg, Voeikov Main Geophysical
 2477 Observatory, RosHydroMet, 2016.
- 2478 Giamarelou, M., Eleftheriadis, K., Nyeki, S., Tunved, P., Torseth, K., and Biskos, G.: Indirect evidence of
 2479 the composition of nucleation mode atmospheric particles in the high Arctic, *J. Geophys. Res.: Atmos.*,
 2480 121(2), 965–975, [doi:10.1002/2015jd023646](https://doi.org/10.1002/2015jd023646), 2016.
- 2481 Gil, J., Pérez, T., Boering, K., Martikainen, P. J., and Biasi, C.: Mechanisms responsible for high N₂O
 2482 emissions from subarctic permafrost peatlands studied via stable isotope techniques, *Global Biogeochem.*
 2483 *Cycles*, 31(1), 172, [doi:10.1002/2015GB005370](https://doi.org/10.1002/2015GB005370), 2017.
- 2484 Glagolev, M.V., Ilyasov, D. V. I., Terenteva, E., Sabrekov, A. F., Yu Mochenov, S., and Maksutov, S. S.:
 2485 Methane and carbon dioxide fluxes in the waterlogged forests of south and middle taiga of Western Siberia,
 2486 *IOP Conf. Ser.: Earth Environ. Sci.*, 138 012005, 2018.
- 2487 Gnatiuk, N., Radchenko, I., Davy, R., Morozov E., and Bobylev, L.: Simulation of factors affecting
 2488 *Emiliania huxleyi* blooms in Arctic and sub-Arctic seas by CMIP5 climate models: model validation and
 2489 selection, *Biogeosciences*, 17, 1199–1212. [doi: 10.5194/bg-17-1199-2020](https://doi.org/10.5194/bg-17-1199-2020), 2020.
- 2490 Godrikan, J., Drapeau, D., and Balch, W. M.: Mixotrophic uptake of organic compounds by coccolithophores,
 2491 *Limnol. Ocean.*, Early bird publication, <https://doi.org/10.1002/lno.11396>, 2020.
- 2492 Gordov, E.P., Okladnikov, I.G., Titov, A.G., Voropay N.N., Ryazanova A.A., and Lykosov V.N.:
 2493 Development of Information-computational Infrastructure for Modern Climatology, *Russ. Meteorol. Hydrol.*,
 2494 43, 722–728, <https://doi.org/10.3103/S106837391811002X>, 2018.

- 2495 Granath, G., Rydin, H., Baltzer, J. L., Bengtsson, F., Boncek, N., Bragazza, L., Bu, Z.-J., Caporn, S. J. M.,
 2496 Dorrepaal, E., Galanina, O., Galka, M., Ganeva, A., Gillikin, D. P., Goia, I., Goncharova, N., Hájek, M.,
 2497 Haraguchi, A., Harris, L. I., Humphreys, E., Jiroušek, M., Kajukalo, K., Karofeld, E., Koronatova, N. G.,
 2498 Kosykh, N. P., Lamentowicz, M., Lapshina, E., Limpens, J., Linkosalmi, M., Ma, J.-Z., Mauritz, M., Munir,
 2499 T. M., Natali, S. M., Natcheva, R., Noskova, M., Payne, R. J., Pilkington, K., Robinson, S., Robroek, B. J.
 2500 M., Rochefort, L., Singer, D., Stenøien, H. K., Tuittila, E.-S., Vellak, K., Verheyden, A., Waddington, J. M.,
 2501 and Rice, S. K.: Environmental and taxonomic controls of carbon and oxygen stable isotope composition in
 2502 Sphagnum across broad climatic and geographic ranges, *Biogeosciences*, 15, 5189–5202,
 2503 <https://doi.org/10.5194/bg-15-5189-2018>, 2018.
- 2504 Grigoriev, V. Y., and Frolova, N. L.: Terrestrial water storage change of European Russia and its impact on
 2505 water balance, *Geography, Environment, Sustainability*, 11(1), 38–50. [https://doi.org/10.24057/2071-9388-](https://doi.org/10.24057/2071-9388-2018-11-1-38-50)
 2506 2018-11-1-38-50, 2018.
- 2507 Groundstroem, F., and Juhola, S.: A framework for identifying cross-border impacts of climate change on
 2508 the energy sector, *Environment Systems and Decisions*, 39(1), 3–15, doi:10.1007/s10669-018-9697-2, 2019.
- 2509 Gunchin, G., Manousakas, M., Osan, J., Karydas, A. G., Eleftheriadis, K., Lodoysamba, S., Shagjamba, D.,
 2510 Migliori, A., Padilla-Alvarez, R., Strelci, C., and Darby, I.: Three-year long source apportionment study of
 2511 airborne particles in Ulaanbaatar using x-ray fluorescence and positive matrix factorization, *Aerosol and Air*
 2512 *Quality Research*, 19(5), 1056–1067, doi:10.4209/aaqr.2018.09.0351, 2019.
- 2513 Guo, Y., Yan, C., Li, C., Feng, Z., Zhou, Y., Lin, Z., Dada, L., Stolzenburg, D., Yin, R., Kontkanen, J.,
 2514 Daellenbach, K. R., Kangasluoma, J., Yao, L., Chu, B., Wang, Y., Cai, R., Bianchi, F., Liu, Y., and Kulmala,
 2515 M.: Formation of Nighttime Sulfuric Acid from the Ozonolysis of Alkenes in Beijing, *Atmos. Chem. Phys.*
 2516 *Discuss.*, <https://doi.org/10.5194/acp-2019-1111>, in review, 2020.
- 2517 Gurchenkov, A. A., Murynin, A. B., Trekin, A. N., and Ignatyev, V. Y.: Object-oriented classification of
 2518 substrate surface objects in Arctic impact regions aerospace monitoring, *Herald of the Bauman Moscow*
 2519 *State Technical University*, 135–146. doi:10.18698/1812-3368-2017-3-135-146, 2017.
- 2520 Göckede, M., Kittler, F., Kwon, M. J., Burjack, I., Heimann, M., Kolle, O., Zimov, N., and Zimov, S.:
 2521 Shifted energy fluxes, increased Bowen ratios, and reduced thaw depths linked with drainage-induced
 2522 changes in permafrost ecosystem structure, *The Cryosphere*, 11, 2975–2996, [https://doi.org/10.5194/tc-11-](https://doi.org/10.5194/tc-11-2975-2017)
 2523 2975-2017, 2017.
- 2524 Göckede, M., Kwon, M. J., Kittler, F., Heimann, M., Zimov, N., and Zimov, S.: Negative feedback processes
 2525 following drainage slow down permafrost degradation, *Glob. Change Biol.*, 25, 3254–3266,
 2526 <https://doi.org/10.1111/gcb.14744>, 2019.
- 2527 Hao, L., Garmash, O., Ehn, M., Miettinen, P., Massoli, P., Mikkonen, S., Jokinen, T., Roldin, P., Aalto, P.,
 2528 Yli-Juuti, T., Joutsensaari, J., Petäjä, T., Kulmala, M., Lehtinen, K. E. J., Worsnop, D. R., and Virtanen, A.:
 2529 Combined effects of boundary layer dynamics and atmospheric chemistry on aerosol composition during

- new particle formation periods, *Atmospheric Chemistry and Physics*, 18(23), 17705–17716. doi:10.5194/acp-18-17705-2018, 2018.
- Hari, P. & Kulmala, M.: Station for Measuring Ecosystem–Atmosphere Relations (SMEAR II). *Boreal Env. Res.* 10: 315–322, 2005.
- Hari, P., Andreae M., Kabat P., and Kulmala M.: A comprehensive network of measuring stations to monitor climate change. *Boreal Env. Res.* 14: 442–446, 2009.
- Hari, P., Petäjä, T., Bäck, J., Kerminen, V.-M., Lappalainen, H. K., Vihma, T., Laurila, T., Viisanen, Y., Vesala, T., and Kulmala, M.: Conceptual design of a measurement network of the global change, *Atmos. Chem. Phys.*, 16, 1017–1028, doi:10.5194/acp-16-1017-2016, 2016.
- Hari, P., Kerminen, V.-M., Kulmala, L., Kulmala, M., Noe, S., Petäjä, T., Vanhatalo, A., and Bäck, J.: Annual cycle of Scots pine photosynthesis, *Atmos. Chem. Phys.*, 17, 15045–15053, doi:10.5194/acp-17-15045-2017, 2017.
- Heikkilä, A., Makelä, J. S., Lakkala, K., Meinander, O., Kaurola, J., Koskela, T., Karhu, J. M., Karppinen, T., Kyro, E., and De Leeuw, G.: In search of traceability: two decades of calibrated Brewer UV measurements in Sodankyla and Jokioinen, *Geoscientific Instrumentation, Methods and Data Systems*, 5(2), 531–540, doi:10.5194/gi-5-531-2016, 2016.
- Heintzenberg, J., Tunved, P., Galí, M., and Leck, C.: New particle formation in the Svalbard region 2006–2015, *Atmos. Chem. Phys.*, 17, 6153–6175, doi:10.5194/acp-17-6153-2017, 2017.
- Helin, A., Sietiö, O.-M., Heinonsalo, J., Bäck, J., Riekkola, M.-L., and Parshintsev, J.: Characterization of free amino acids, bacteria and fungi in size-segregated atmospheric aerosols in boreal forest: seasonal patterns, abundances and size distributions, *Atmos. Chem. Phys.*, 17, 13089–13101, doi.org/10.5194/acp-17-13089-2017, 2017.
- Hellén, H., Praplan, A. P., Tykkä, T., Ylivinkka, I., Vakkari, V., Bäck, J., Petäjä, T., Kulmala, M., and Hakola, H.: Long-term measurements of volatile organic compounds highlight the importance of sesquiterpenes for the atmospheric chemistry of a boreal forest, *Atmos. Chem. Phys.*, 18, 13839–13863, <https://doi.org/10.5194/acp-18-13839-2018>, 2018.
- Hinzman, L.D., Bettez, N.D., Bolton, W.R. et al. :Evidence and Implications of Recent Climate Change in Northern Alaska and Other Arctic Regions, *Climatic Change*, 72, 251–298, doi.org/10.1007/s10584-005-5352-2, 2005.
- Hoegh-Guldberg, O., Jacob, D., Taylor, M., Bindi, M., Brown, S., Camilloni, I., Diedhiou, A., Djalanter, R., Ebi, K. L., Engelbrecht, F., Guiot, J., Hijjoka, Y., Mehrotra, S., Payne, A., Seneviratne, S. I., Thomas, A., Warren, R., and Zhou, G.: Impacts of 1.5°C Global Warming on Natural and Human Systems,

- in: Global Warming of 1.5°C: An IPCC Special Report on the impacts of global warming of 1.5°C above pre-industrial levels and related global greenhouse gas emission pathways, in the context of strengthening the global response to the threat of climate change, sustainable development, and efforts to eradicate poverty, edited by: Masson-Delmotte, V., Zhai, P., Pörtner, H.-O., Roberts, D., Skea, J., Shukla, P. R., Pirani, A., Moufouma-Okia, W., Péan, C., Pidcock, R., Connors, S., Matthews, J. B. R., Chen, Y., Zhou, X., Gomis, M. I., Lonnoy, E., Maycock, T., Tignor, M., and Waterfield, T., WMO, Geneva, Switzerland, 2018.
- Hong, J., Kim, J., Nieminen, T., Duplissy, J., Ehn, M., Äijälä, M., Hao, L. Q., Nie, W., Sarnela, N., Prisle, N. L., Kulmala, M., Virtanen, A., Petäjä, T., and Kerminen, V.-M.: Relating the hygroscopic properties of submicron aerosol to both gas- and particle-phase chemical composition in a boreal forest environment, *Atmos. Chem. Phys.*, 15, 11999–12009, <https://doi.org/10.5194/acp-15-11999-2015>, 2015.
- Huang, W., Cheng, B., Zhang, J., Zhang, Z., Vihma, T., Li, Z., and Niu, F.: Modeling experiments on seasonal lake ice mass and energy balance in the Qinghai–Tibet Plateau: a case study, *Hydrol. Earth Syst. Sci.*, 23, 2173–2186, 2019a.
- Huang, W., Zhang, J., Leppäranta, M., Li, Z., Cheng, B. and Lin, Z. 2019b. Thermal structure and water-ice heat transfer in a shallow ice-covered thermokarst lake in central Qinghai-Tibet Plateau, *Journal of Hydrology*, 578, [124122], 2019b.
- Hölttä, T., Lintunen, A., Chan, T., Mäkelä, A., and Nikinmaa, E.: A steady state stomatal model of balanced leaf gas exchange, hydraulics and maximal source-sink flux, *Tree Physiology*, 37, 851–868, doi: 10.1093/treephys/tpx011, 2017.
- IPCC: Special Report on the Ocean and Cryosphere in a Changing Climate, edited by Pörtner, H.-O., Roberts, D.C., Masson-Delmotte, V., Zhai, P., Tignor, M., Poloczanska, E., Mintenbeck, K., Alegría, A., Nicolai, M., Okem, A., Petzold, J., Rama, B., and Weyer, N. M., 2019.
- IPCC, 2021: Climate Change 2021: The Physical Science Basis. Contribution of Working Group I to the Sixth Assessment Report of the Intergovernmental Panel on Climate Change [Masson-Delmotte, V., P. Zhai, A. Pirani, S. L. Connors, C. Péan, S. Berger, N. Caud, Y. Chen, L. Goldfarb, M. I. Gomis, M. Huang, K. Leitzell, E. Lonnoy, J.B.R. Matthews, T. K. Maycock, T. Waterfield, O. Yelekçi, R. Yu and B. Zhou (eds.)]. Cambridge University Press. In Press. Summary for Policymakers IPCC, 2021: Summary for Policymakers. In: Climate Change 2021: The Physical Science Basis. Contribution of Working Group I to the Sixth Assessment Report of the Intergovernmental Panel on Climate Change [Masson-Delmotte, V., P. Zhai, A. Pirani, S. L. Connors, C. Péan, S. Berger, N. Caud, Y. Chen, L. Goldfarb, M. I. Gomis, M. Huang, K. Leitzell, E. Lonnoy, J.B.R. Matthews, T. K. Maycock, T. Waterfield, O. Yelekçi, R. Yu and B. Zhou (eds.)]. Cambridge University Press. In Press.
- Ivakhov, V. M., Paramonova, N. N., Privalov, V. I., Zinchenko, A. V., Loskutova, M. A., Makshtas, A. P., Kustov, V. Y., Laurila, T., Aurela, M., and Asmi, E.: Atmospheric Concentration of Carbon Dioxide at Tiksi

Formatted: Font color: Auto

- 2599 and Cape Baranov Stations in 2010-2017, *Russ. Meteorol. Hydrol.*, 44, 291–299,
2600 doi:10.3103/s1068373919040095, 2019.
- 2601 Jaffe, D., Bertschi, I., Jaegle, L., Novelli, P., Reid, J. S., Tanimoto, H., Vingarzan, R. and Westphal, D. L.:
2602 Long-range transport of Siberian biomass burning emissions and impact on surface ozone in western North
2603 America, *Geophys. Res. Lett.*, 31(16), L16106, doi:10.1029/2004GL020093, 2004.
- 2604 Jakobson, L., T. Vihma, and E. Jakobson,: Relationships between Sea Ice Concentration and Wind Speed
2605 over the Arctic Ocean during 1979–2015., *J. Climate*, 32, 7783–7796, [https://doi.org/10.1175/JCLI-D-19-](https://doi.org/10.1175/JCLI-D-19-0271.1)
2606 0271.1, 2019.
- 2607 Juhola, S.: Planning for a green city: The Green Factor tool, *Urban Forestry and Urban Greening*, 34, 254-
2608 258, doi:10.1016/j.ufug.2018.07.019, 2018.
- 2609 Juutinen, S., Virtanen, T., Kondratyev, V., Laurila, T., Linkosalmi, M., Mikola, J., Nyman, J., Räsänen, A.,
2610 Tuovinen, J.-P., and Aurela, M.: Spatial variation and seasonal dynamics of leaf-area index in the arctic
2611 tundra-implications for linking ground observations and satellite images, *Environ. Res. Lett.*, 12(9), 10,
2612 doi:10.1088/1748-9326/aa7f85, 2017.
- 2613 Kalogridis, A.C., Popovicheva, O.B., Engling, G., Diapouli, E., Kawamura, K., Tachibana, E., Ono, K.,
2614 Kozlov, V.S., and Eleftheriadis, K.: Smoke aerosol chemistry and aging of Siberian biomass burning
2615 emissions in a large aerosol chamber, *Atmos. Environ.*, 185,15-28, 2018.
- 2616 Kangasluoma, J., Ahonen, L. R., Laurila, T., Cai, R., Enroth, J., Mazon, S., Korhonen, F., Aalto, P.,
2617 Kulmala, M., Attoui, M. and Petäjä, T.: Laboratory verification of a new high flow differential mobility
2618 particle sizer, and field measurements in Hyytiälä, *J Aerosol Sci*, 124, 1-9, 2018.
- 2619 Karelin, D. V., Goryachkin, S. V., Zamolodchikov, D. G., Dolgikh, A. V., Zazovskaya, E. P., Shishkov, V.
2620 A., and Kraev, G. N.: Human footprints on greenhouse gas fluxes in cryogenic ecosystems, *Dokl. Earth Sc.*,
2621 477, 1467–1469, doi:10.1134/S1028334X17120133, 2017.
- 2622 Karetnikov, S., Leppäranta, M., and Montonen, A.: A time series of over 100 years of ice seasons on Lake
2623 Ladoga, *Journal of Great Lakes Research*, 43(6), 979-988, doi:10.1016/j.jglr.2017.08.010, 2017.
- 2624 Karthe, D., Abdullaev, I., Boldgiv, B., Borchardt, D., Chalov, S., Jarsjö, J., Li, L., and Nitttrouer, J.A.: Water
2625 in Central Asia: an integrated assessment for science-based management, *Environmental Earth Sciences*,
2626 76(20), 15, doi:10.1007/s12665-017-6994-x, 2017a.
- 2627 Karthe, D., Chalov, S., Moreido, V., Pashkina, M., Romanchenko, A., Batbayar, G., Kalugin, A., Westphal,
2628 K., Malsy, M., and Flörke, M.: Assessment of runoff, water and sediment quality in the Selenga River basin
2629 aided by a web-based geoservice, *Water Resources*, 44(3), 399-416, 2017b.
- 2630 Karthe D., Chalov S., Gradel A., and Kusbach A.: Special issue: Environment change on the Mongolian
2631 plateau: atmosphere, forests, soils and water, *Geography, Environment, Sustainability*, 12(3), 60-65,
2632 doi:10.24057/2071-9388-2019-1411, 2019.

- 2633 Karvonen, J., Shi, L., Cheng, B., Similä, M., Mäkynen, M., and Vihma, T.: Bohai Sea ice parameter
 2634 estimation based on thermodynamic ice model and Earth observation data, *Remote Sensing*, 9, 234,
 2635 doi:10.3390/rs9030234, 2017.
- 2636 Kasimov, N., Karthe, D., and Chalov, S.: Environmental change in the Selenga River—Lake Baikal Basin,
 2637 *Reg. Environ. Chang.*, 17, 1945–1949, 2017a.
- 2638 Kasimov, N. S., Kosheleva, N. E., Nikiforova, E. M., and Vlasov, D. V.: Benzo a pyrene in urban
 2639 environments of eastern Moscow: pollution levels and critical loads, *Atmos. Chem. Phys.*, 17(3), 2217–2227,
 2640 doi:10.5194/acp-17-2217-2017, 2017b.
- 2641 Kasimov, N., Shinkareva, G., Lychagin, M., Kosheleva, N., Chalov, S., Pashkina, M., Thorslund, J., and
 2642 Jarsjö, J.: River water quality of the selenga-baikal basin: Part i—spatio-temporal patterns of dissolved and
 2643 suspended metals, *Water*, 12(8), 2137, 2020a.
- 2644
- 2645 Kasimov, N., Shinkareva, G., Lychagin, M., Chalov, S., Pashkina, M., Thorslund, J., and Jarsjö, J.: River
 2646 water quality of the selenga-baikal basin: part ii — metal partitioning under different hydroclimatic
 2647 conditions, *Water*, 12(9), 2392, 2020b.
- 2648
- 2649 Kaus, A., Schäffer, M., Karthe, D., Büttner, O., von Tümpling, W., and Borchardt, D.: Regional patterns of
 2650 heavy metal exposure and contamination in the fish fauna of the Kharaa River basin, Mongolia, *Reg.*
 2651 *Environ. Change*, 17, 2023–2037, doi: 10.1007/s10113-016-0969-4, 2017.
- 2652 Kazakov, E., Kondrik, D., and Pozdnyakov, D.: A synthetic satellite dataset of the spatio-temporal
 2653 distributions of *Emiliana huxleyi* blooms and their impacts on Arctic and sub-Arctic marine environments
 2654 (1998–2016), *Earth Systems Science Data*, 11, 119–128, doi: 10.5194/essd-11-119-2019, 2019.
- 2655 Kecorius, S., Vogl, T., Paasonen, P., Lampilahti, J., Rothenberg, D., Wex, H., Zeppenfeld, S., van Pinxteren,
 2656 M., Hartmann, M., Henning, S., Gong, X., Welti, A., Kulmala, M., Stratmann, F., Herrmann, H., and
 2657 Wiedensohler, A.: New particle formation and its effect on cloud condensation nuclei abundance in the
 2658 summer Arctic: a case study in the Fram Strait and Barents Sea, *Atmos. Chem. Phys.*, 19, 14339–14364, doi:
 2659 10.5194/acp-19-14339-2019, 2019.
- 2660 Kerminen, V.-M., Chen, X., Vakkari, V., Petäjä, T., Kulmala, M., and Bianchi, F.: Atmospheric new particle
 2661 formation and growth: review of field observations, *Environ. Res. Lett.*, 13, 103003, doi: 10.1088/1748-
 2662 9326/aadf3c, 2018.
- 2663 Kim, J., Kim, H. M., Cho, C.-H., Boo, K.-O., Jacobson, A. R., Sasakawa, M., Machida, T., Arshinov, M.,
 2664 and Fedoseev, N.: Impact of Siberian observations on the optimization of surface CO₂ flux, *Atmos. Chem.*
 2665 *Phys.*, 17, 2881–2899, <https://doi.org/10.5194/acp-17-2881-2017>, 2017.

- 2666 Kirillin, G., Leppäranta, M., Terzhevik, A., Bernhardt, J., Engelhardt, C., Granin, N., Golosov, S., Efremova,
2667 T., Palshin, N., Sherstyankin, P., Zdorovenova, G., and Zdorovenov, R.: Physics of seasonally ice-covered
2668 lakes: major drivers and temporal/spatial scales, *Aquatic Ecol.*, 74, 659–682, 2012.
- 2669 Kirillin, G., Aslamov, I., Leppäranta, M., and Lindgren, E.: Turbulent mixing and heat fluxes under lake ice:
2670 the role of seiche oscillations, *Hydrology of Earth System Sciences*, 22(12), 6493–6504, doi:10.5194/hess-
2671 22-6493-2018, 2018.
- 2672 Kirschke, S., Bousquet, P., Ciais, P., Saunio, M., Canadell, J. G., Dlugokencky, E. J., Bergamaschi, P.,
2673 Bergmann, D., Blake, D. R., Bruhwiler, L., Cameron-Smith, P., Castaldi, S., Chevallier, F., Feng, L., Fraser,
2674 A., Heimann, M., Hodson, E. L., Houweling, S., Josse, B., Fraser, P. J., Krummel, P. B., Lamarque, J.-F.,
2675 Langenfelds, R. L., Le Quere, C., Naik, V., O'Doherty, S., Palmer, P. I., Pison, I., Plummer, D., Poulter, B.,
2676 Prinn, R. G., Rigby, M., Ringeval, B., Santini, M., Schmidt, M., Shindell, D. T., Simpson, I. J., Spahni, R.,
2677 Steele, L. P., Strode, S. A., Sudo, K., Szopa, S., van der Werf, G.R., Voulgarakis, A., van Weele, M., Weiss,
2678 R. F., Williams, J. E., and Zeng, G.: Three decades of global methane sources and sinks, *Nature Geoscience*,
2679 6(10), 813–823, doi: 10.1038/ngeo1955, 2013.
- 2680 Kiselev, M. V., Voropay, N. N., and Cherkashina, A. A.: influence of anthropogenic activities on the
2681 temperature regime of soils of the South-Western Baikal region, *IOP Conf. Ser.: Earth Environ. Sci.*, 381,
2682 012043, doi: 10.1088/1755-1315/381/1/012043, 2019.
- 2683 Kittler, F., Heimann, M., Kolle, O., Zimov, N., Zimov, S., and Göckede, M.: Long-term drainage reduces
2684 CO₂ uptake and CH₄ emissions in a Siberian permafrost ecosystem, *Global Biogeochemical Cycles*, 31,
2685 1704–1717. doi: 10.1002/2017GB005774, 2017.
- 2686 Kiuru, P., Ojala, A., Mammarella, I., Heiskanen, J., Kämäräinen, M., Vesala, T. and Huttula, T.: Effects of
2687 Climate Change on CO₂ Concentration and Efflux in a Humic Boreal Lake: A Modeling Study, *Journal of*
2688 *Geophysical Research, Biogeosciences*, 123, 7, 2212–2233, 2018.
- 2689 Kondrik, D., Pozdnyakov, D., and Pettersson, L.: Particulate inorganic carbon production within *E. huxleyi*
2690 blooms in subpolar and polar seas: a satellite time series study (1998–2013), *International Journal of Remote*
2691 *Sensing*, 38:22, 6179–6205, doi: 10.1080/01431161.2017.1350304, 2017.
- 2692 Kondrik, D. V., Pozdnyakov, D. V., and Johannessen, O. M.: Satellite evidence that *E. huxleyi*
2693 phytoplankton blooms weaken marine carbon sinks, *Geophys. Res. Lett.*, 5, 846–854. doi:
2694 10.1002/2017GL076240, 2018a.
- 2695 Kondrik, D. V., Pozdnyakov, D. V., and Pettersson, L. H.: Tendencies in Coccolithophorid Blooms in Some
2696 Marine Environments of the Northern Hemisphere according to the Data of Satellite Observations in 1998–
2697 2013. *Izv. Atmos. Ocean. Phys.*, 53, 955–964, doi: 10.1134/S000143381709016X, 2018b.
- 2698 Kondrik, D. V., Kazakov, E. E., Pozdnyakov, D. V., and Johannessen, O. M.: Satellite evidence for
2699 enhancement of the column mixing ratio of atmospheric CO₂ over *E. huxleyi* blooms, *Transactions of the*

- 2700 Karelian Research Centre of the Russian Academy of Sciences, *Limnologia i Oceanologia* series, 9, 1-11,
2701 doi: 10.17076/lim1107, 2019.
- 2702 Konovalov, I. B., Lvova, D. A., Beekmann, M., Jethva, H., Mikhailov, E. F., Paris, J.-D., Belan, B. D.,
2703 Kozlov, V. S., Ciaia, P., and Andreae, M. O.: Estimation of black carbon emissions from Siberian fires using
2704 satellite observations of absorption and extinction optical depths, *Atmos. Chem. Phys.*, 18, 14889–14924,
2705 doi: 10.5194/acp-18-14889-2018, 2018.
- 2706 Konovalov V., Rets E., and Pimankina N.: Interrelation between glacier summer mass balance and runoff in
2707 mountain river basins, *Geography, Environment, Sustainability*, 12(1), 23-33, doi: 10.24057/2071-9388-
2708 2018-26, 2019.
- 2709 Konstantinov, P. I., Grishchenko, M. Y., and Varentsov, M. I.: Mapping urban heat islands of arctic cities
2710 using combined data on field measurements and satellite images based on the example of the city of Apatity
2711 (Murmansk Oblast), *Izv. Atmos. Ocean. Phys.*, 51(9), 992-998, doi:10.1134/s000143381509011x, 2015.
- 2712 Konstantinov, P., Varentsov, M., and Esau, I.: A high density urban temperature network deployed in several
2713 cities of Eurasian Arctic, *Environ. Res. Lett.*, 13(7), 12, doi:10.1088/1748-9326/aacb84, 2018.
- 2714 Kontkanen, J., Paasonen, P., Aalto, J., Back, J., Rantala, P., Petäjä, T., and Kulmala, M.: Simple proxies for
2715 estimating the concentrations of monoterpenes and their oxidation products at a boreal forest site, *Atmos.*
2716 *Chem. Phys.*, 16(20), 13291-13307, doi:10.5194/acp-16-13291-2016, 2016.
- 2717 Kontkanen, J., Deng, C., Fu, Y., Dada, L., Zhou, Y., Cai, J., Daellenbach, K.R., Hakala, S., Kokkonen, T.V.,
2718 Lin, Z., Liu, Y., Wang, Y., Yan, C., Petäjä, T., Jiang, J., Kulmala, M. and Paasonen, P. : Size-resolved
2719 particle number emissions in Beijing determined from measured particle size distributions, *Atmos. Chem.*
2720 *Phys.* 20, 11329-11348, 2020.
- 2721 Kooijmans, L. M. J., Sun, W., Aalto, J., Erkkilä, K.M., Maseyk, K., Seibt, U., Vesala, T., Mammarella, I.,
2722 and Chen, H.: Influences of light and humidity on carbonyl sulfide-based estimates of photosynthesis,
2723 *Proceedings of the National Academy of Sciences*, 116 (7), 2470-2475, doi:10.1073/pnas.1807600116, 2019.
- 2724 Korneykova, M. V., and Evdokimova, G. A.: Microbiota of the ground air layers in natural and industrial
2725 zones of the Kola Arctic, *J Environ. Sci. Health A*, 53(3), 271-277, doi:10.1080/10934529.2017.1397444,
2726 2018a.
- 2727 Korneykova, M. V., Redkina, V. V., and Shalygina, R. R.: Algological and mycological characterization of
2728 soils under pine and birch forests in the Pasvik Reserve, *Eurasian Soil Science*, 51(2), 211-220,
2729 doi:10.1134/s1064229318020047, 2018b.
- 2730 Koronatova, N. G., & Milyaeva, E. V.: Plant community succession in post-mined quarries in the northern-
2731 taiga zone of West Siberia. *Contemporary Problems of Ecology*, 4(5), 513–518, 2011.

- 2732 Kukkonen, I., Ezhova, E., Suhonen, E. A. J., Lappalainen, H. K., Gennadinik, V., Ponomareva, O., Gravis,
2733 A., Miles, V., Kulmala, M., Melnikov, V., and Drozdov, D.: Observations and modelling of ground
2734 temperature evolution in the discontinuous permafrost zone in Nadym, North-West Siberia, *Permafrost and*
2735 *Periglacial Processes*, 1–17, doi:10.1002/ppp.2040, 2020.
- 2736 Kulmala, M., Vehkamäki, H., Petäjä, T., Dal Maso, M., Lauri, A., Kerminen, V.-M., Birmili, W., and
2737 McMurry, P.H.: Formation and growth rates of ultrafine atmospheric particles: a review of observations,
2738 *Journal of Aerosol Science*, 35, 143–176, doi:10.1134/S1995425511050, 2004.
- 2739 Kulmala, M.: Atmospheric chemistry: China’s choking cocktail, *Nature*, 526, 497–499,
2740 doi:10.1038/526497a, 2015a.
- 2741 Kulmala, M., Lappalainen, H. K., Petäjä, T., Kurten, T., Kerminen, V.-M., Viisanen, Y., Hari, P., Sorvari, S.,
2742 Bäck, J., Bondur, V., Kasimov, N., Kotlyakov, V., Matvienko, G., Baklanov, A., Guo, H. D., Ding, A.,
2743 Hansson, H.-C., and Zilitinkevich, S.: Introduction: The Pan-Eurasian Experiment (PEEX) –
2744 multidisciplinary, multiscale and multicomponent research and capacity-building initiative, *Atmos. Chem.*
2745 *Phys.*, 15, 13085–13096, doi:10.5194/acp-15-13085-2015, 2015b.
- 2746 Kulmala, M., Lappalainen, H. K., Petäjä, T., Kerminen, V.-M., Viisanen, Y., Matvienko, G., Melnikov, V.,
2747 Baklanov, A., Bondur, V., Kasimov, N., and Zilitinkevich, S.: Pan-Eurasian Experiment (PEEX) Program:
2748 Grant Challenges in the Arctic-boreal context, *J. Geography Environment Sustainability*, 2, 5–18, 2016a.
- 2749 Kulmala, M., Petäjä, T., Kerminen, V. M., Kujansuu, J., Ruuskanen, T., Ding, A., Nie, W., Hu, M., Wang,
2750 Z., Wu, Z., and Wang, L.: On secondary new particle formation in China, *Front. Environ. Sci. Eng.*, 10, 8,
2751 doi:10.1007/s11783-016-0850-1, 2016b.
- 2752 Kulmala, M., Kerminen, V.-M., Petäjä, T., Ding, A. J., and Wang L.: Atmospheric gas-to-particle
2753 conversion: why NPF events are observed in megacities?, *Faraday Discuss.*, 200, 271–288,
2754 doi:10.1039/c6fd00257a, 2017.
- 2755 Kulmala, M.: Build a global Earth observatory, *Nature*, 553, 21–23, doi: 10.1038/d41586-017-08967-y, 2018.
- 2756 Kulmala, L., Pumpanen, J., Kolari, P., Dengel, S., Berninger, F., Köster, K., Matkala, L., Vanhatalo, A.,
2757 Vesala, T., and Bäck, J.: Inter- and intra-annual dynamics of photosynthesis differ between forest floor
2758 vegetation and tree canopy in a subarctic Scots pine stand, *Agricultural and Forest Meteorology*, 271, 1–11,
2759 doi: 10.1016/j.agrformet.2019.02.029, 2019.
- 2760 Kulmala, M., Dada, L., Daellenbach, K. R., Yan, C., Stolzenburg, D., Kontkanen, J., Ezhova, E., Hakala, S.,
2761 Tuovinen, S., Kokkonen, T. V., Kurppa, M., Cai, R., Zhou, Y., Yin, R., Baalbaki, R., Chan, T., Chu, B.,
2762 Deng, C., Fu, Y., Ge, M., He, H., Heikkinen, L., Junninen, H., Liu, Y., Lu, Y., Nie, W., Rusanen, A.,
2763 Vakkari, V., Wang, V., Yang, G., Yao, L., Zheng, J., Kujansuu, J., Kangasluoma, J., Petäjä, T., Paasonen, P.,
2764 Järvi, L., Worsnop, D., Ding, A., Liu, Y., Wang, L., Jiang, J., Bianchi, F., and Kerminen, V.-M.: Is reducing

- new particle formation a plausible solution to mitigate particulate air pollution in Beijing and other Chinese megacities?, *Faraday Discussions*, doi: 10.1039/D0FD00078G.2021.
- Kwon, M. J., Beulig, F., Ilie, I., Wildner, M., Küsel, K., Merbold, L., Mahecha, M. D., Zimov, N., Zimov, S. A., Heimann, M., Schuur, E. A. G., Kostka, J. E., Kolle, O., Hilke, I. and Göckede, M.: Plants, microorganisms, and soil temperatures contribute to a decrease in methane fluxes on a drained Arctic floodplain, *Glob. Change Biol.*, 23, 2396-2412, doi:10.1111/gcb.13558, 2017.
- Kwon, M. J., Natali, S. M., Hicks Pries, C. E., Schuur, E. A., Steinhof, A., Crummer, K. G., Zimov, N., Zimov, S. A., Heimann, M., Kolle, O., and Göckede, M.: Drainage enhances modern soil carbon contribution but reduces old soil carbon contribution to ecosystem respiration in tundra ecosystems, *Glob. Change Biol.*, 25, 1315– 1325, doi: 10.1111/gcb.14578, 2019.
- Kühn, T., Kupiainen, K., Miinalainen, T., Kokkola, H., Paunu, V.-V., Laakso, A., Tonttila, J., Van Dingenen, R., Kulovesi, K., Karvosenoja, N., and Lehtinen, K. E. J.: Effects of black carbon mitigation on Arctic climate, *Atmos. Chem. Phys.*, 20, 5527–5546, doi: 10.5194/acp-20-5527-2020, 2020.
- Köster, E., Köster, K., Berninger, F., and Pumpanen, J.: Carbon dioxide, methane and nitrous oxide fluxes from podzols of a fire chronosequence in the boreal forests in Värriö, Finnish Lapland, *Geoderma Regional*, 5, 181-187, doi:10.1016/j.geodrs.2015.07.001, 2015.
- Köster, E., Köster, K., Berninger, F., Prokushkin, A., Aaltonen, H., Zhou, X., and Pumpanen, J.: Changes in fluxes of carbon dioxide and methane caused by fire in Siberian boreal forest with continuous permafrost, *Journal of Environmental Management*, 228, 405-415, doi:10.1016/j.jenvman.2018.09.051, 2018.
- Köster, K., Berninger, F., Köster, E., and Pumpanen, J.: Influences of reindeer grazing on above- and belowground biomass and soil carbon dynamics, *Arctic Antarctic and Alpine Res.*, 47(3), 495-503, doi:10.1657/aaar0014-062, 2015.
- Köster, K., Berninger, F., Heinonsalo, J., Lindén, A., Köster, E., Ilvesniemi, H., and Pumpanen J.: The long-term impact of low-intensity surface fires on litter decomposition and enzyme activities in boreal coniferous forests, *Int. J Wildland Fire*, 25(2), 213-223, doi:10.1071/wf14217_co, 2016.
- Köster, K., Köster, E., Berninger, F., Heinonsalo, J., and Pumpanen, J.: Contrasting effects of reindeer grazing on CO₂, CH₄, and N₂O fluxes originating from the northern boreal forest floor. *Land Degradation and Development*, 29(2), 374-381, doi:10.1002/ldr.2868, 2018.
- Köster, K., Köster, E., Kulmala, L., Berninger, F., and Pumpanen, J.: Are the climatic factors combined with reindeer grazing affecting the soil CO₂ emissions in subarctic boreal pine forest? *Catena*, 149, 616-622, doi:10.1016/j.catena.2016.06.011, 2017.
- Lan, H., Holopainen, J., Hartonen, K., Jussila, M., Ritala, M. and Riekkola, M.-L.: Fully automated online dynamic in-tube extraction for continuous sampling of volatile organic compounds in air, *Anal. Chem.*, 91, 8507, 2019.

- 2799 Lappalainen, H.K., Kulmala, M. and Zilitinkevich, S. (Eds.): Pan Eurasian Experiment (PEEX) Science Plan,
 2800 web: www.atm.helsinki.fi/peex, ISBN 978-951-51-0587-5 (printed), ISBN 978-951-51-0588-2 (online),
 2801 2015.
- 2802 Lappalainen H.K., Petäjä T., Kujansuu J., Kerminen V., Shvidenko A., Bäck J., Vesala T., Vihma T., De
 2803 Leeuw G., Lauri A., Ruuskanen T., Lapshin V.B., Zaitseva N., Glezer O., Arshinov M., Spracklen D.V.,
 2804 Arnold S.R., Juhola S., Lihavainen H., Viisanen Y., Chubarova N., Chalov S., Filatov N., Skorokhod A.,
 2805 Elansky N., Dyukarev E., Esau I., Hari P., Kotlyakov V., Kasimov N., Bondur V., Matvienko G., Baklanov
 2806 A., Mareev E., Troitskaya Y., Ding A., Guo H., Zilitinkevich S., and Kulmala M.: Pan-Eurasian Experiment
 2807 (PEEX) –a research initiative meeting the grand challenges of the changing environment of the northern Pan-
 2808 Eurasian arctic-boreal areas, *J. Geography Environment Sustainability*, 2(7), 13-48, doi:10.24057/2071-
 2809 9388-2014-7-2-13-48, 2014.
- 2810 Lappalainen, H. K., Kerminen, V.-M., Petäjä, T., Kurten, T., Baklanov, A., Shvidenko, A., Bäck, J., Vihma,
 2811 T., Alekseychik, P., Andreae, M. O., Arnold, S. R., Arshinov, M., Asmi, E., Belan, B., Bobylev, L., Chalov,
 2812 S., Cheng, Y., Chubarova, N., de Leeuw, G., Ding, A., Dobrolyubov, S., Dubtsov, S., Dyukarev, E., Elansky,
 2813 N., Eleftheriadis, K., Esau, I., Filatov, N., Flint, M., Fu, C., Glezer, O., Gliko, A., Heimann, M., Holtslag, A.
 2814 A. M., Hörrak, U., Janhunen, J., Juhola, S., Järvi, L., Järvinen, H., Kanukhina, A., Konstantinov, P.,
 2815 Kotlyakov, V., Kieloaho, A.-J., Komarov, A. S., Kujansuu, J., Kukkonen, I., Duplissy, E.-M., Laaksonen, A.,
 2816 Laurila, T., Lihavainen, H., Lisitzin, A., Mahura, A., Makshtas, A., Mareev, E., Mazon, S., Matishov, D.,
 2817 Melnikov, V., Mikhailov, E., Moisseev, D., Nigmatulin, R., Noe, S. M., Ojala, A., Pihlatie, M., Popovicheva,
 2818 O., Pumpanen, J., Regerand, T., Repina, I., Shcherbinin, A., Shevchenko, V., Sipilä, M., Skorokhod, A.,
 2819 Spracklen, D. V., Su, H., Subetto, D. A., Sun, J., Terzhevik, A. Y., Timofeyev, Y., Troitskaya, Y.,
 2820 Tynkkynen, V.-P., Kharuk, V. I., Zaytseva, N., Zhang, J., Viisanen, Y., Vesala, T., Hari, P., Hansson, H. C.,
 2821 Matvienko, G. G., Kasimov, N. S., Guo, H., Bondur, V., Zilitinkevich, S., and Kulmala, M.: Pan-Eurasian
 2822 Experiment (PEEX): towards a holistic understanding of the feedbacks and interactions in the land–
 2823 atmosphere–ocean–society continuum in the northern Eurasian region, *Atmos. Chem. Phys.*, 16, 14421–
 2824 14461, <https://doi.org/10.5194/acp-16-14421-2016>, 2016.
- 2825 Lappalainen, H.K., Kulmala, M., Kujansuu, J., Petäjä, T., Mahura, A., de Leeuw, G., Zilitinkevich, S.,
 2826 Juustila, M., Kerminen, V.M., Bornstein, B. and Jiahua, Z.: The Silk Road agenda of the Pan-Eurasian
 2827 Experiment (PEEX) program, *Big Earth Data*, 2(1), 8-35, doi:10.1080/20964471.2018.1437704, 2018.
- 2828 Lei, R. B., Xie, H. J., Wang, J., Leppäranta, M., Jonsdóttir, I., and Zhang, Z. H.: Changes in sea ice
 2829 conditions along the Arctic Northeast Passage from 1979 to 2012, *Cold Regions Science and Technology*,
 2830 119, 132-144. doi:10.1016/j.coldregions.2015.08.004, 2015.
- 2831 Lei, R., Tian-Kunze, X., Leppäranta, M., Wang, J., Kaleschke, L., and Zhang, Z.: Changes in summer sea
 2832 ice, albedo, and partitioning of surface solar radiation in the Pacific sector of Arctic Ocean during 1982-2009,
 2833 *J. Geophys. Res.: Oceans*, 121(8), 5470-5486, doi:10.1002/2016jc011831, 2016.

- 2834 Lei, R. B., Cheng, B., Heil, P., Vihma, T., Wang, J., Ji, Q., and Zhang, Z. H.: Seasonal and interannual
2835 variations of sea ice mass balance from the Central Arctic to the Greenland Sea, *J. Geophys. Res.: Oceans*,
2836 123(4), 2422-2439, doi:10.1002/2017jc013548, 2018.
- 2837 Leino, K., Nieminen, T., Manninen, H. E., Petäjä, T., Kerminen, V.-M., and Kulmala, M.: Intermediate ions
2838 as a strong indicator of new particle formation bursts in a boreal forest, *Boreal Environ. Res.*, 21(3-4), 274-
2839 286, 2016.
- 2840 Leppäranta, M.: Structure and properties of lake ice. Freezing of Lakes and the Evolution of their Ice Cover,
2841 Springer, Berlin/Heidelberg, Germany, 51–90. doi: 10.1007/978-3-642-29081-7_3, 2015.
- 2842 Leppäranta, M., Lindgren, E., and Shirasawa, K.: The heat budget of Lake Kilpisjärvi in the Arctic tundra,
2843 *Hydrol. Res.*, 48(4), 969-980, doi:10.2166/nh.2016.171, 2017.
- 2844 Leppäranta, M., Lewis, J. E., Heini, A., and Arvola, L.: Spatial statistics of hydrography and water chemistry
2845 in a eutrophic boreal lake based on sounding and water samples, *Environ. Monit. Assess.*, 190(7), 378,
2846 doi:10.1007/s10661-018-6742-z, 2018.
- 2847 Leppäranta, M., Lindgren, E., Wen, L. and Kirillin, G.: Ice cover decay and heat balance in Lake Kilpisjärvi
2848 in Arctic tundra, *Journal of Limnology*, 78(2). doi: 10.4081/jlimnol.2019.1879, 2019.
- 2849 Leppäranta, M., Meleshko, V., Uotila, P., and Pavlova, T.: Sea ice modelling, 315-387, *Sea Ice in the Arctic*
2850 (Springer, Cham), 2020.
- 2851 Li, H., Välranta, M., Mäki, M., Kohl, L., Sannel, B., Pumpanen, J., Koskinen, M., Bäck, J. and Bianchi, F.:
2852 Overlooked organic vapor emissions from thawing Arctic permafrost, *Environmental Research Letters* 15,
2853 Issue 10, id.104097, 12 pp., 2020a.
- 2854 Li, M., Wang, L., Liu, J., Gao, W., Song, T., Sun, Y., Li, L., Li, X., Wang, Y., Liu, L. and Daellenbach,
2855 K.R., Paasonen, P.J., Kerminen, V.-M., Kulmala, M., and Wang Y.: Exploring the regional pollution
2856 characteristics and meteorological formation mechanism of PM_{2.5} in North China during 2013–2017,
2857 *Environment international*, 134, 105283, 2020b.
- 2858 Liao, Z., Cheng, B., Zhao, J., Vihma, T., Jackson, K., Yang, Q., Yang, Y., Zhang, L., Li, Z., Qiu, Y., and
2859 Cheng, X.: Snow depth and ice thickness derived from SIMBA ice mass balance buoy data using an
2860 automated algorithm, *Int. J. Digital Earth*, 12(8), 962-979, doi:10.1080/17538947.2018.1545877, 2018.
- 2861 Lin, X., Rogers, B. M., Sweeney, C., Chevallier, F., Arshinov, M., Dlugokencky, E., Machida, T., Motoki
2862 Sasakawa, Tans, P., Keppel-Aleks, G.: Siberian and temperate ecosystems shape Northern Hemisphere
2863 atmospheric CO₂ seasonal amplification, *PNAS*, 117 (35), 21079-21087, doi:10.1073/pnas.1914135117 ,
2864 2020.
- 2865 Lintunen, A., Paljakka, T., Salmon, Y., Dewar, R., Riikonen, A, and Hölttä, T.: The influence of soil
2866 temperature and water content on belowground hydraulic conductance and leaf gas exchange in mature trees
2867 of three boreal species, *Plant, Cell and Environment*, 43, 532-547, doi: 10.1111/pce.13709, 2020.

- 2868 Liu, Y.C., Yan, C., Feng, Z., Zheng, F., Fan, X., Zhang, Y., Li, C., Zhou, Y., Lin, Z., Guo, Y., Zhang, Y.,
2869 Ma, L., Zhou, W., Liu, Z., Dada, L., Dällenbach, K., Kontkanen, J., Cai, R., Chan, T., Chu, B., Du, W., Yao,
2870 L., Wang, Y., Cai, J., Kangasluoma, J., Kokkonen, T., Kujansuu, J., Rusanen, A., Deng, C., Fu, Y., Yin, R.,
2871 Li, X., Lu, Y., Liu, Y., Lian, C., Yang, D., Wang, W., Ge, M., Wang, Y., Worsnop, D.R., Junninen, H., He,
2872 H., Kerminen, V.-M., Zheng, J., Wang, L., Jiang, J., Petäjä, T., Bianchi, F. and Kulmala, M. : Continuous
2873 and comprehensive atmospheric observation in Beijing: a station to understand the complex urban
2874 atmospheric environment, *Big Earth Data*, 4, 295-321, 2020.
- 2875 Liu, J., Wang, L., Li, M., Liao, Z., Sun, Y., Song, T., Gao, W., Wang, Y., Li, Y., Ji, D., Hu, B., Kerminen,
2876 V.-M., Wang, Y., and Kulmala, M.: Quantifying the impact of synoptic circulation patterns on ozone
2877 variability in northern China from April to October 2013–2017, *Atmos. Chem. Phys.*, 19, 14477–14492,
2878 doi:10.5194/acp-19-14477-2019, 2019 a.
- 2879 Liu, W., Atherton, J., Möttö, M., Gastellu-Etchegorry, J.P., Malenovsky, Z., Raunonen, P., Åkerblom, M.,
2880 Mäkipää, R. and Porcar-Castell, A.: Simulating solar-induced chlorophyll fluorescence in a boreal forest
2881 stand reconstructed from terrestrial laser scanning measurements, *Remote Sensing of Environment*, 232,
2882 111274, 2019b.
- 2883 Liu, Y., de Leeuw, G., Kerminen, V.-M., Zhang, J., Zhou, P., Nie, W., Qi, X., Hong, J., Wang, Y., Ding, A.,
2884 Guo, H., Krüger, O., Kulmala, M., and Petäjä, T.: Analysis of aerosol effects on warm clouds over the
2885 Yangtze River Delta from multi-sensor satellite observations, *Atmos. Chem. Phys.*, 17, 5623–5641,
2886 doi:10.5194/acp-17-5623-2017, 2017.
- 2887 Liu, Y., Zhang, J., Zhou, P., Lin, T., Hong, J., Shi, L., Yao, F., Wu, J., Guo, H., and de Leeuw, G.: Satellite-
2888 based estimate of the variability of warm cloud properties associated with aerosol and meteorological
2889 conditions, *Atmos. Chem. Phys.*, 18, 18187–18202, doi:10.5194/acp-18-18187-2018, 2018.
- 2890 López-Blanco, E., Exbrayat, J.-F., Lund, M., Christensen, T. R., Tamstorf, M. P., Slevin, D., Hugelius, G.,
2891 Bloom, A. A., and Williams, M.: Evaluation of terrestrial pan-Arctic carbon cycling using a data-
2892 assimilation system, *Earth Syst. Dynam.*, 10, 233–255, doi:10.5194/esd-10-233-2019, 2019.
- 2893 Lu, P., Leppäranta, M., Cheng, B., and Li, Z.: Influence of melt-pond depth and ice thickness on Arctic sea-
2894 ice albedo and light transmittance, *Cold Regions Science and Technology*, 124, 1-10,
2895 doi:10.1016/j.coldregions.2015.12.010, 2016.
- 2896 Lu, P., Cheng, B., Leppäranta, M., and Li, Z. J.: Partitioning of solar radiation in Arctic sea ice during melt
2897 season, *Oceanologia*, 60(4), 464-477, doi:10.1016/j.oceano.2018.03.002, 2018a.
- 2898 Lu, P., Leppäranta, M., Cheng, B., Li, Z., Istomina, L., and Heygster, G.: The color of melt ponds on Arctic
2899 sea ice, *The Cryosphere*, 12, 1331–1345, doi:10.5194/tc-12-1331-2018, 2018b.
- 2900 Lu, Y., Yan, C., Fu, Y., Chen, Y., Liu, Y., Yang, G., Wang, Y., Bianchi, F., Chu, B., Zhou, Y., Yin, R.,
2901 Baalbaki, R., Garmash, O., Deng, C., Wang, W., Liu, Y.C., Petäjä, T., Kerminen, V.-M., Jiang, J., Kulmala,

- 2902 M. and Wang, L. : A proxy for atmospheric daytime gaseous sulfuric acid concentration in urban Beijing,
2903 *Atmos. Chem. Phys.* 19, 1971-1983, 2019.
- 2904 Luoma, K., Virkkula, A., Aalto, P.P, Petäjä, T., and Kulmala, M.: Over a 10-year record of aerosol optical
2905 properties at SMEAR II, *Atmos. Chem. Phys.*, 19, 11363–11382, doi:10.5194/acp-19-11363-2019, 2019.
- 2906 Lychagin, M., Chalov, S., Kasimov, N., Shinkareva, G., Jarsjo, J., and Thorslund, J.: Surface water pathways
2907 and fluxes of metals under changing environmental conditions and human interventions in the Selenga River
2908 system, *Environ. Earth Sci.*, 76(1), 14, doi:10.1007/s12665-016-6304-z, 2017.
- 2909 Ma,J., Yan, X., Dong, W. et al.: Gross primary production of global forest ecosystems has been
2910 overestimated, *Sci Rep* 5, 10820, doi:10.1038/srep10820, 2015.
- 2911 Magritsky, D. V., Frolova, N. L. , Evstigneev, V. M. , Povalishnikova, E. S. , Kireeva, M. B., and
2912 Pakhomova, O. M.: Long-term changes of river water inflow into the seas of the Russian Arctic sector,
2913 *Polarforschung*, 87(2),177-194, doi: 10.2312/polarforschung.87.2.177, 2018.
- 2914 Mahura A., Baklanov A., Sørensen, J. H., Svetlov, A., and Koshkin, V.: Assessment of Long-Range
2915 Transport and Deposition from Cu-Ni Smelters of Russian North. In "Air, Water and Soil Quality Modelling
2916 for Risk and Impact Assessment", *Security Through Science, Series C - Environmental Security*. Eds. A.
2917 Ebel, T. Davitashvili, Springer Elsevier Publishers, pp. 115-124, 2007.
- 2918 Mahura, A., Gonzalez-Aparacio, I., Nuterman, R., and Baklanov, A.: Seasonal Impact Analysis on
2919 Population due to Continuous Sulphur Emissions from Severonikel Smelters of the Kola Peninsula.
2920 *Geography, Environment, Sustainability*, 11(1), 130-144, doi:10.24057/2071-9388-2018-11-1-130-144,
2921 2018.
- 2922 Malkhazova, S. M., Mironova, V. A., Orlov, D. S., and Adishcheva, O. S.: Influence of climatic factor on
2923 naturally determined diseases in a regional context, *Geography, Environment, Sustainability*, 11(1), 157-170,
2924 doi:10.24057/2071-9388-2018-11-1-157-170, 2018.
- 2925 Malsy, M., Flörke, M., and Borchardt, D.:What drives the water quality changes in the Selenga basin:
2926 climate change or socio-economic development?, *Reg Environ Chang.*, 17, 1977–1989 doi:10.1007/s10113-
2927 016-1005-4, 2017.
- 2928 Mammarella, I., Nordbo, A., Rannik, Ü., Haapanala, S., Levula, J., Laakso, H., Ojala, A., Peltola, O.,
2929 Heiskanen, J., Pumpanen, J. and Vesala, T.: Carbon dioxide and energy fluxes over a small boreal lake in
2930 Southern Finland, *J. Geophys. Res.: Biogeosciences*, 120(7), 1296-1314, doi:10.1002/2014jg002873, 2015.
- 2931 Manasypov, R. M., Vorobyev, S. N., Loiko, S. V., Krivtsov, I. V., Shirokova, L. S., Shevchenko, V. P.,
2932 Kirpotin, S. N., Kulizhsky, S. P., Kolesnichenko, L. G., Zemtsov, V. A. and Sinkinov, V. V.: Seasonal
2933 dynamics of thermokarst lake chemical composition in discontinuous permafrost zone of Western Siberia,
2934 *Biogeosciences*, 12, 3009-3028, 2015.

- 2935 Marelle, L., Raut, J. C., Law, K. S., and Duclaux, O.: Current and future arctic aerosols and ozone from
 2936 remote emissions and emerging local sources-modeled source contributions and radiative effects, *J.*
 2937 *Geophys. Res.: Atmos.*, 123(22), 12942-12963, doi:10.1029/2018jd028863, 2018.
- 2938 Maslov, A. V., Shevchenko, V. P., Bobrov, V. A., Belogub, E. V., Ershova, V. B., Vereshchagin, O. S., and
 2939 Khvorov, P. V.: Mineralogical-geochemical features of ice-rafted sediments in some arctic regions,
 2940 *Lithology and Mineral Resources*, 53(2), 110-129, doi:10.1134/s0024490218020037, 2018a.
- 2941 Maslov, A. V., Shevchenko, V. P., Kuznetsov, A. B., and Stein, R.: Geochemical and Sr-Nd-Pb-isotope
 2942 characteristics of ice-rafted sediments of the Arctic Ocean, *Geochem. Int.*, 56(8), 751-765,
 2943 doi:10.1134/s0016702918080050, 2018b.
- 2944 Matkala, L., Kulmala, L., Kolari, P., Aurela, M., and Bäck, J.: Resilience of carbon dioxide and water
 2945 exchange to extreme weather events in subarctic Scots pine and Norway spruce stands, *Agricultural and*
 2946 *Forest Meteorology*, 296, 108239, 2020.
- 2947 McCusker, K., Fyfe, J., and Sigmond, M.: Twenty-five winters of unexpected Eurasian cooling unlikely due
 2948 to Arctic sea-ice loss, *Nature Geoscience* 9, 838–842, doi:10.1038/ngeo2820, 2016.
- 2949 Meinander, O., Heikkinen, E., Aurela, M., and Hyvärinen, A.: Sampling, Filtering, and Analysis Protocols to
 2950 Detect Black Carbon, Organic Carbon, and Total Carbon in Seasonal Surface Snow in an Urban Background
 2951 and Arctic Finland (>60° N), *Atmosphere*, 11, 923. doi:10.3390/atmos11090923, 2020a.
- 2952 Meinander, O., Kontu, A., Kouznetsov, R., Sofiev, M.: Snow Samples Combined with Long-Range
 2953 Transport Modeling to Reveal the Origin and Temporal Variability of Black Carbon in Seasonal Snow in
 2954 Sodankylä (67° N), *Front. Earth Sci.*, 8, 13,
 2955 <https://www.frontiersin.org/articles/10.3389/feart.2020.00153/full>, 2020b.
- 2956 Merkouriadi, I., Cheng, B., Graham, R. M., Rösel, A., and Granskog, M. A.: Critical role of snow on sea ice
 2957 growth in the Atlantic sector of the Arctic Ocean. *Geophysical Research Letters*, 44,
 2958 doi:10.1002/2017GL075494, 2017
- 2959 Merkouriadi, I., Cheng, B., Graham, R. M., Rösel, A., and Granskog, M. A.: Critical role of snow on sea ice
 2960 growth in the Atlantic sector of the Arctic Ocean, *Geophys. Res. Lett.*, 44, doi: 10.1002/2017GL075494,
 2961 2018.
- 2962 Mikhailov, E. F., Mironova, S. Y., Makarova, M. V., Vlasenko, S. S., Ryshkevich, T. I., Panov, A. V., and
 2963 Andreae, M. O.: Studying seasonal variations in carbonaceous aerosol particles in the atmosphere over
 2964 central Siberia, *Izv. Atmos. Oceanic Phys.*, 51(4), 423-430, doi:10.1134/s000143381504009x, 2015a.
- 2965 Mikhailov, E. F., Mironov, G. N., Pöhlker, C., Chi, X., Krüger, M. L., Shiraiwa, M., Förster, J.-D., Pöschl,
 2966 U., Vlasenko, S. S., Ryshkevich, T. I., Weigand, M., Kilcoyne, A. L. D., and Andreae, M. O.: Chemical
 2967 composition, microstructure, and hygroscopic properties of aerosol particles at the Zotino Tall Tower

- Observatory (ZOTTO), Siberia, during a summer campaign, *Atmos. Chem. Phys.*, 15, 8847–8869, doi:10.5194/acp-15-8847-2015, 2015b.
- Mikhailov, E. F., Mironova, S., Mironov, G., Vlasenko, S., Panov, A., Chi, X., Walter, D., Carbone, S., Artaxo, P., Heimann, M., Lavric, J., Pöschl, U., and Andreae, M. O.: Long-term measurements (2010–2014) of carbonaceous aerosol and carbon monoxide at the Zotino Tall Tower Observatory (ZOTTO) in central Siberia, *Atmos. Chem. Phys.*, 17, 14365–14392, doi:10.5194/acp-17-14365-2017, 2017.
- Mikola, J., Virtanen, T., Linkosalmi, M., Vähä, E., Nyman, J., Postanogova, O., Räsänen, A., Kotze, D. J., Laurila, T., Juutinen, S., Kondratyev, V., and Aurela, M.: Spatial variation and linkages of soil and vegetation in the Siberian Arctic tundra – coupling field observations with remote sensing data, *Biogeosciences*, 15, 2781–2801, doi:10.5194/bg-15-2781-2018, 2018.
- Miles, V. V., and Esau, I.: Spatial heterogeneity of greening and browning between and within bioclimatic zones in northern West Siberia, *Environ. Res. Lett.*, 11(11), 12, doi:10.1088/1748-9326/11/11/115002, 2016.
- Miles, V., and Esau, I.: Seasonal and Spatial Characteristics of Urban Heat Islands (UHIs) in Northern West Siberian Cities., *Remote Sens.*, 9, 989, 2017.
- Miles, M. W., Miles, V., and Esau, I.: Varying climate response across the tundra, forest–tundra and boreal forest biomes in northern West Siberia, *Environ. Res. Lett.*, 14, 075008, doi:10.1088/1748-9326/ab2364, 2019.
- Miles, V., and Esau, I.: Surface urban heat islands in 57 cities across different climates in northern Fennoscandia, *Urban Climate*, 31, 10.1016/j.uclim.2019.100575, 2020.
- Miles, V.: [Arctic surface Urban Heat Island \(UHI\), MODIS Land Surface Temperature \(LST\) data, 2000–2016](#). Arctic Data Center. doi:10.18739/A2TB0XW4T, 2020.
- MNRE (2019): Methods for calculating emissions of pollutants into the atmosphere from stationary sources. Ministry of Natural Resources and Ecology. In Russian ([www.mnr.gov.ru/docs/metodiki_rascheta_vybrosov_vrednykh_zagryaznyayushchikh_veshchestv_v_atmosf_ernyy_vozdukh_statsionarn/perechen](#)), 2019.
- Mori, M., Watanabe, M., Shiogama, H., Inoue, J., and Kimoton, M.: Robust Arctic sea-ice influence on the frequent Eurasian cold winters in past decades, *Nat. Geosci.*, 7, 869–873, doi:10.1038/ngeo2277, 2014.
- Mori, M., Kosaka, Y., Watanabe, M., Nakamura, H., and Kimoto, M.: A reconciled estimate of the influence of Arctic sea-ice loss on recent Eurasian cooling, *Nat. Clim. Change*, 9, 123–129, doi: 10.1038/s41558-018-0379-3, 2019.
- Morozov, E. A., Kondrik, D. V., Chepikova, S. S., and Pozdnyakov, D. V.: Atmospheric columnar CO₂ enhancement over *E. huxleyi* blooms: case studies in the North Atlantic and Arctic waters. *Transactions of*

Formatted: Font color: Auto

Field Code Changed

Formatted: Font color: Auto

Formatted: Font color: Auto

Formatted: Font color: Auto

- the Karelian Research Centre of the Russian Academy of Sciences, *Limnologia i Oceanologia* series, 3, 1-6.
doi:10.17076/lim989, 2019.
- Myslenkov S., Medvedeva A., Arkhipkin V., Markina M., Surkova G., Krylov A., Dobrolyubov S.,
Zilitinkevich S., and Koltermann P.: Long-term statistics of storms in the Baltic, Barents and White Seas and
their future climate projections., *Geography, environment, sustainability*, 11, 93-112, doi:10.24057/2071-
9388-2018-11-1-93-112, 2018.
- Mäki, M., Krasnov, D., Hellén, H., Noe, S. M., and Bäck, J.: Stand type affects fluxes of volatile organic
compounds from the forest floor in hemiboreal and boreal climates, *Plant Soil*, 441, 363–381,
doi:10.1007/s11104-019-04129-3, 2019.
- Naakka, T., Nygård, T., Vihma, T., Graversen, R., and Sedlar, J.: Atmospheric moisture transport between
mid-latitudes and the Arctic: regional, seasonal and vertical distributions, *Int. J. Climatol.*, 32, 1–18,
doi:10.1002/joc.5988, 2019.
- Natali, S.M., Watts, J.D., Rogers, B.M., Potter, S., Ludwig, S. M., Selbmann, A. K., Sullivan, P.F. Abbott, B.
W., Arndt, K. A., Birch, L., Björkman, M.P., Bloom, A., Celis, G., Christensen, T. R., Christiansen, C. T.,
Commene, R., Cooper, E. J., Crill, P., Czimczik, C., Davydov, S., Du, J., Egan, J.E., Elberling, B.,
Euskirchen, B.S., Friborg, T., Genet, H., Göckede, M., Goodrich, J.P., Grogan, P., Helbig, M., Jafarov, E.E.,
Jastrow, J. D., Kalhori, A.A.M., Kim, Y Kimball, J. S., Kutzbach, L., Lara, M. J, Larsen, K., S., Lee, B.-Y.,
Liu, Z., Loranty, M. M., Lund, M., Lupascu, M., Madani, N., Malhotra, A., Matamala, R., McFarland, J.,
McGuire, A. D., Michelsen, A., Minions, C., Oechel, W., Olefeldt, D., Parmentier, F.-J., Pirk, N., Poulter,
B., Quinton, W., Rezanezhad, F., Risk, D., Sachs, T., Schaefer, K., Schmidt, N. M., Schuur, E., Semenchuk,
P. R., Shaver, G., Sonntag, O., Starr, G., Treat, C. C., Waldrop, M. P., Wang, Y., Welker, J., Wille, C., Xu,
X., Zhang, Z., Zhuang, Q., and Zona, D.: Large loss of CO₂ in winter observed across the northern
permafrost region, *Nat. Clim. Chang.*, 9, 852–857, doi:10.1038/s41558-019-0592-8, 2019.
- Nikandrova, A., Tabakova, K., Manninen, A., Väänänen, R., Petäjä, T., Kulmala, M., Kerminen, V.-M., and
O'Connor, E.: Combining airborne in situ and ground-based lidar measurements for attribution of aerosol
layers, *Atmos. Chem. Phys.*, 18, 10575–10591, doi:10.5194/acp-18-10575-2018, 2018.
- NILU, 2013: Sandanger, T.M., Anda, E., Berglen, T.F., Evenset, A., Christensen, G., and Heimstad, E.S.:
Health and environmental impacts in the Norwegian border area related to local Russian industrial emissions.
Knowledge status, 40/2013, 2013.
- Nissen, C., Munnich, M., Grube, M., and Haumann, N.: Factors controlling coccolithophore biogeography in
the Southern Ocean, *Biogeosciences*, 15(22), 6997-7024, doi:10.5194/bg-15-6997-2018, 2018.
- Nitzbon, J., Langer, M., Westermann, S., Martina, L., Aas, K. S., and Boike, J.: Pathways of ice-wedge
degradation in polygonal tundra under different hydrological conditions, *Cryosphere*, 13(4), 1089-1123,
doi:10.5194/tc-13-1089-2019, 2019.

- 3035 Nygård, T., Graversen, R. G., Uotila, P., Naakka, T., and Vihma, T.: Strong dependence of wintertime Arctic
 3036 moisture and cloud distributions on atmospheric large-scale circulation, *J. Climate*, 32, 8771-8790, doi:
 3037 10.1175/JCLI-D-19-0242.1, 2019.
- 3038 Overland, J., Dunlea, E., Box, J. E., Corell, R., Forsius, M., Kattsov, V., Olsen, M. S., Pawlak, J., Reiersen,
 3039 L. O., and Wang, M.: The urgency of Arctic change, *Polar Science*, 21, 6-13,
 3040 doi:10.1016/j.polar.2018.11.008, 2019.
- 3041 Paasonen, P., Peltola, M., Kontkanen, J., Junninen, H., Kerminen, V.-M., and Kulmala, M.: Comprehensive
 3042 analysis of particle growth rates from nucleation mode to cloud condensation nuclei in boreal forest, *Atmos.*
 3043 *Chem. Phys.*, 18, 12085–12103, doi:10.5194/acp-18-12085-2018, 2018.
- 3044 Palo, T., Vihma, T., Jaagus, J., and Jakobson, E.: Observations on temperature inversion over central Arctic
 3045 sea ice in summer, *Q. J. R. Meteorol. Soc.*, 143(708), 2741-2754, doi:10.1002/qj.3123, 2017.
- 3046 Panov, A. V., Prokushkin, A. S., Bryukhanov, A. V., Korets, M. A., Ponomarev, E. I., Sidenko, N. V.,
 3047 Zrazhevskaya, G. K., Timokhina, A. V., and Andreae, M. O.: A complex approach for the estimation of
 3048 carbonaceous emissions from wildfires in Siberia, *Russian Meteorol. Hydrol.*, 43(5), 295-301, 2018.
- 3049 Parmentier, F. W., Christensen, T. R., Rysgaard, S., Bendtsen, J., Glud, R. N., Else, B., van Huissteden, J.,
 3050 Sachs, T., Vonk, J. E., and Sejr, M. K.: A synthesis of the arctic terrestrial and marine carbon cycles under
 3051 pressure from a dwindling cryosphere, *Ambio*, 46, 53–69, doi:10.1007/s13280-016-0872-8, 2017.
- 3052 Parshintsev, J., Vaikkinen, A., Lipponen, K., Vrkoslav, V., Cvačka, J., et al. : Desorption atmospheric
 3053 pressure photoionization high-resolution mass spectrometry: a complementary approach for the chemical
 3054 analysis of atmospheric aerosols, *Rapid Commun. Mass Spectrom.*, 29, 1233–1241, 2015.
- 3055 Passananti, M., Zapadinsky, E., Zanca, T., Kangasluoma, J., Myllys, N., Rissanen, M.P., Kurtén, T., Ehn,
 3056 M., Attoui, M., and Vehkamäki, H.: How well can we predict cluster fragmentation inside a mass
 3057 spectrometer? *Chem. Commun.*, 55, 5946-5949, 2019.
- 3058 Payne, R. J., Creevy, A., Malysheva, E., Ratcliffe, J., Andersen, R., Tsyganov, A. N., Rowson, J., Marcisz,
 3059 K., Zielinska, M., Lamentowicz, M., Lapshina, E. D., and Mazei, Y.: Tree encroachment may lead to
 3060 functionally-significant changes in peatland testate amoeba communities. *Soil Biology & Biochemistry*, 98,
 3061 18-21. doi:10.1016/j.soilbio.2016.04.002, 2016.
- 3062 Peltola, O., Vesala, T., Gao, Y.; Rätty, O. et al. : Monthly gridded data product of northern wetland methane
 3063 emissions based on upscaling eddy covariance observations, *Earth System Science Data*, 11, 1263-1289,
 3064 doi:10.5194/essd-11-1263-2019, 2019.
- 3065 Peltoniemi, J. I., Gritsevich, M., Hakala, T., Dagsson-Waldhauserová, P., Arnalds, Ó., Anttila, K., Hannula,
 3066 H.-R., Kivekäs, N., Lihavainen, H., Meinander, O., Svensson, J., Virkkula, A., and de Leeuw, G.: Soot on

- 3067 Snow experiment: bidirectional reflectance factor measurements of contaminated snow, *The Cryosphere*, 9,
3068 2323–2337, doi:10.5194/tc-9-2323-2015, 2015.
- 3069 Peterson, B. J., Holmes, R. M., McClelland, J. W., Vörösmarty, C. J., Lammers, R. B., Shiklomanov, A. I.,
3070 Shiklomanov, I. A., and Rahmstorf, S.: Increasing river discharge to the Arctic Ocean, *Science*, 80, 298,
3071 2171–2173, doi: 10.1126/science.1077445, 2002.
- 3072 Petäjä, T., Järvi, L., Kerminen, V.-M., Ding, A. J., Sun, J. N., Nie, W., Kujansuu, J., Virkkula, A., Yang, X.-
3073 Q., Fu, C. B., Zilitinkevich, S., and Kulmala M.: Enhanced air pollution via aerosol-boundary layer feedback
3074 in China, *Scientific Reports*, 6, 18998, doi:10.1038/srep18998, 2016.
- 3075 Petäjä, T., Duplissy, E.-M., Tabakova, K., Schmale, J., Altstädter, B., Ancellet, G., Arshinov, M., Balin, Y.,
3076 Baltensperger, U., Bange, J., Beamish, A., Belan, B., Berchet, A., Bossi, R., Cairns, W. R. L., Ebinghaus, R.,
3077 El Haddad, I., Ferreira-Araujo, B., Franck, A., Huang, L., Hyvärinen, A., Humbert, A., Kalogridis, A.-C.,
3078 Konstantinov, P., Lampert, A., MacLeod, M., Magand, O., Mahura, A., Marelle, L., Masloboev, V.,
3079 Moiseev, D., Moschos, V., Neckel, N., Onishi, T., Osterwalder, S., Ovaska, A., Paasonen, P., Panchenko,
3080 M., Pankratov, F., Pernov, J. B., Platis, A., Popovicheva, O., Raut, J.-C., Riandet, A., Sachs, T., Salvatori, R.,
3081 Salzano, R., Schröder, L., Schön, M., Shevchenko, V., Skov, H., Sonke, J. E., Spolaor, A., Stathopoulos, V.,
3082 K., Strahlendorff, M., Thomas, J. L., Vitale, V., Vratolis, S., Barbante, C., Chabrilat, S., Dommergue, A.,
3083 Eleftheriadis, K., Heilimo, J., Law, K. S., Massling, A., Noe, S. M., Paris, J.-D., Prévôt, A. S. H., Riipinen,
3084 I., Wehner, B., Xie, Z., and Lappalainen, H. K.: Overview: Integrative and Comprehensive Understanding on
3085 Polar Environments (iCUPE) – concept and initial results, *Atmos. Chem. Phys.*, 20, 8551–8592,
3086 doi:10.5194/acp-20-8551-2020, 2020a.
- 3087 Petäjä, T., Ganzei, K. S., Lappalainen, H. K., Tabakova, K., Makkonen, R., Räisänen, J., Chalov, S.,
3088 Kulmala, M., Zilitinkevich, S. S., Baklanov, P., Shakirov, R. B., Mishina, N.V., Egidarev, E.G., and
3089 Kondrat'ev, I. I.: Research agenda for the Russian Far East and utilization of multi-platform comprehensive
3090 environmental observations, *J. Big Data*, 5:3, 277-305, doi:10.1080/17538947.2020.1826589 , 2020b.
- 3091 Pietron, J., Jarsjo, J., Romanchenko, A. O., and Chalov, S. R.: Model analyses of the contribution of in-
3092 channel processes to sediment concentration hysteresis loops, *Journal of Hydrology*, 527, 576-589.
3093 doi:10.1016/j.jhydrol.2015.05.009, 2015.
- 3094 Pietron, J., Nittrouer, J. A., Chalov, S. R., Dong, T. Y., Kasimov, N., Shinkareva, G., and Jarsjö, J.:
3095 Sedimentation patterns in the Selenga River delta under changing hydroclimatic conditions, *Hydrological*
3096 *Processes*, 32(2), 278-292, doi:10.1002/hyp.11414, 2018.
- 3097 Pirazzini, R., Leppanen, L., Picard, G., Lopez-Moreno, J. I., Marty, C., Macelloni, G., Kontu, A., Von
3098 Lerber, A., Tanis, C.M., Schneebeli, M., De Rosnay, P., Arslan, A. N.: European in-situ snow measurements:
3099 practices and purposes, *Sensors*, 18(7), 51, doi:10.3390/s18072016, 2018.
- 3100 Pissó, I., Myhre, C. L., Platt, S. M., Eckhardt, S., Hermansen, O., Schmidbauer, N., Mienert, J.,
3101 Vadakkepuliymbatta, S., Bauguitte, S., Pitt, J., Allen, G., Bower, K. N., O'Shea, S., Gallagher, M. W.,

Formatted: Font color: Auto

- Percival, C. J., Pyle, J., Cain, M., and Stohl, A.: Constraints on oceanic methane emissions west of Svalbard from atmospheric in situ measurements and Lagrangian transport modeling, *J. Geophys. Res. Atmos.*, 121(23), 14188-14200, doi:10.1002/2016jd025590, 2016.
- Platt, S. M., Eckhardt, S., Ferré, B., Fisher, R. E., Hermansen, O., Jansson, P., Lowry, D., Nisbet, E. G., Pissó, I., Schmidbauer, N., Silyakova, A., Stohl, A., Svendby, T. M., Vadakkepuliambatta, S., Mienert, J., and Lund Myhre, C.: Methane at Svalbard and over the European Arctic Ocean, *Atmos. Chem. Phys.*, 18, 17207–17224, doi:10.5194/acp-18-17207-2018, 2018.
- Ponomarev, Evgenii I., Kharuk, Viacheslav I., and Ranson, Kenneth J.: Wildfires Dynamics in Siberian Larch Forests, *Forests*, 7(6), 125, 2016.
- Popovicheva O., Evangeliou N., Eleftheriadis K., Kalogridis A. C., Sitnikov V. N., Eckhardt S., Stohl A.: Black carbon sources constrained by observations and modeling in the Russian high Arctic, *Environmental Science Technology*, 51(7), 3871-3879, 2017.
- Popovicheva, O., Diapouli, E., Makshtas, A., Shonija, N., Manousakas, M., Saraga, D., Uttal, T., and Eleftheriadis, K.: East Siberian Arctic background and black carbon polluted aerosols at HMO Tiksi, *Science of the Total Environment*, 655, 924-938, doi:10.1016/j.scitotenv.2018.11.165, 2019a.
- Popovicheva, O. B., Engling, G., Ku, I. T., Timofeev, M. A., and Shonija, N. K.: Aerosol emissions from long-lasting smoldering of boreal peatlands: chemical composition, markers, and microstructure, *Aerosol and Air Quality Research*, 19(3), 484-503, doi:10.4209/aaqr.2018.08.0302, 2019b.
- Popovicheva, O. B., Padoan, S., Schnelle-Kreis, J., Nguyen, D. L., Adam, T.W., Kistler, M., Steinkogler, T., Kasper-Giebl, A., Zimmermann, R., and Chubarova, N. E.: Spring aerosol in urban atmosphere of megacity: analytical and statistical assessment for source impacts, *Aerosol and Air Quality Research*, 20, 702–719, 2020a.
- Popovicheva O., Ivanov A., and Vojtisek M.: Functional Factors of Biomass Burning Contribution to Spring Aerosol Composition in a Megacity: Combined FTIR-PCA Analyses, *Atmosphere*, 11, 319-339, 2019b.
- Popovicheva, O., Volpert, E., Sitnikov, N., Chichayeva, M., and Padoan, S.: Black carbon in spring aerosols of Moscow urban background, *Geography, Environment, Sustainability*, 13, 1, 233-243, 2020c.
- Pozdnyakov D. V., Pettersson L. H., and Korosov A. A.: Exploring the Marine Ecology from Space. Springer, Switzerland, 2017.
- Pozdnyakov, D. V., Kondrik, D.V., Kazakov, E. E., and Chepikova, S.: Environmental conditions favoring coccolithophore blooms in subarctic and arctic seas: a 20-year satellite and multi-dimensional statistical study, *Proc. SPIE 11150, Remote Sensing of the Ocean, Sea Ice, Coastal Waters, and Large Water Regions*, 111501W, 14 October 2019, doi: 10.1117/12.2547868, 2019.

- 3134 Pozdnyakov D., Kondrik D., and Chepikova S.: Origination of *E. huxleyi* extraordinary bloom outbursts in
 3135 the Bering Sea between the late 1990s and early 2000s, and in 2018-2019: A hypothesis, *Fisheries*
 3136 *Oceanography*, submitted, 2020.
- 3137 Preis, Y. I., Simonova, G. V., Voropay, N. N., and Dyukarev, E. A.: Estimation of the influence of
 3138 hydrothermal conditions on the carbon isotope composition in *Sphagnum* mosses of bogs of Western Siberia,
 3139 *IOP Conf. Series: Earth Environ. Sci.*, 211, doi:10.1088/1755-1315/211/1/012031, 2018.
- 3140 Pugach S. P., Pipko I. I., Shakhova, N. E., Shirshin, E. A., Perminova, I. V., Gustafsson, O., Bondur, V. G.,
 3141 Ruban, A. S., and Semiletov, I. P.: Dissolved organic matter and its optical characteristics in the Laptev and
 3142 East Siberian seas: spatial distribution and interannual variability (2003–2011), *Ocean Sci.*, 14, 87–103,
 3143 doi:10.5194/os-14-87-2018, 2018.
- 3144 Pulliainen, J., Aurela, M., Laurila, T., Aalto, T., Takala, M., Salminen, M., Kulmala, M., Barr, A., Heimann,
 3145 M., Lindroth, A., Laaksonen, A., Derksen, C., Mäkelä, A., Markkanen, T., Lemmetyinen, J., Susiluoto, J.,
 3146 Dengel, S., Mammarella, I., Tuovinen, J.-P., and Vesala, T.: Early snowmelt significantly enhances boreal
 3147 springtime carbon uptake, *PNAS*, 114(42), 11081–11086, doi:10.1073/pnas.1707889114, 2017.
- 3148 Pulliainen, J., Luojus, K., Derksen, C., Mudryk, L., Lemmetyinen, J., Salminen, M., Ikonen, J., Takala, M.,
 3149 Cohen, J., Smolander, T., and Norberg, J.: Patterns and trends of Northern Hemisphere snow mass from
 3150 1980 to 2018, *Nature* 581, 294–298, doi:10.1038/s41586-020-2258-0, 2020.
- 3151 Pärn, J., Verhoeven, J.T., Butterbach-Bahl, K., Dise, N.B., Ullah, S., Aasa, A., Egorov, S., Espenberg, M.,
 3152 Järveoja, J., Jauhiainen, J. and Kasak, K.: Nitrogen-rich organic soils under warm well-drained conditions
 3153 are global nitrous oxide emission hotspots, *Nat. Commun.*, 9, 1135, doi:10.1038/s41467-018-03540-1, 2018.
- 3154 Qi, X. M., Ding, A. J., Nie, W., Petäjä, T., Kerminen, V.-M., Herrmann, E., Xie, Y. N., Zheng, L. F.,
 3155 Manninen, H., Aalto, P., Sun, J. N., Xu, Z. N., Chi, X. G., Huang, X., Boy, M., Virkkula, A., Yang, X.-Q.,
 3156 Fu, C. B., and Kulmala, M.: Aerosol size distribution and new particle formation in the western Yangtze
 3157 River Delta of China: 2 years of measurements at the SORPES station, *Atmos. Chem. Phys.*, 15, 12445–
 3158 12464, doi:10.5194/acp-15-12445-2015, 2015.
- 3159 Rakitin, V. S., Elansky, N. F., Wang, P., Wang, G., Pankratova, N. V., Shtabkin, Y. A., Skorokhod A.I.,
 3160 Safronov A.N., Makarova M.V., and Grechko E.I.: Changes in trends of atmospheric composition over urban
 3161 and background regions of Eurasia: estimates based on spectroscopic observations, *Geography*,
 3162 *Environment, Sustainability*, 11(2), 84–96, doi:10.24057/2071-9388-2018-11-2-84-96, 2018.
- 3163 Rautiainen, K., Parkkinen, T., Lemmetyinen, J., Schwank, M., Wiesmann, A., Ikonen, J., Derksen, C.,
 3164 Davydov, S., Davydova, A., Boike, J., Langer, M., Druschg, M., and Pulliainen, J.: SMOS prototype
 3165 algorithm for detecting autumn soil freezing, *Remote Sensing of Environment*, 180, 346–360,
 3166 doi:10.1016/j.rse.2016.01.012, 2016.

- Rinke, A., Segger, B., Crewell, S., Maturilli, M., Naakka, T., Nygård, T., Vihma, T., Alshawaf, F., Dick, G., Wickert, J., and Keller, J.: Trends of vertically integrated water vapor over the Arctic during 1979-2016: Consistent moistening all over?, *J. Climate*, 32, 6097–6116, doi:10.1175/JCLI-D-19-0092.1, 2019.
- Ripple, W. J., Wolf, C., Newsome, T. M., Galetti, M., Alamgir, M., Crist, E., Mahmoud, M. I., Laurance, W. F., and 15,364 scientist signatories from 184 countries. World scientists' warning to humanity: A second notice, *BioScience*, 67(12), 1026-1028, 2017.
- Rivero-Calle, S., Gnanadesikan, A., Del Castillo, C., Balch, W., and Guikema, S.: Multidecadal increase in North Atlantic coccolithophores and the potential role of rising CO₂, *Science*, 350 (6267), 1533-1537, doi: 10.1126/science.aaa8026, 2015.
- Romanowsky, E., Handorf, D., Jaiser, R., Wohltmann, I., Dorn, W., Ukita, J., Cohen, J., Dethloff, K., and Rex, M.: The role of stratospheric ozone for Arctic-midlatitude linkages, *Sci. Rep.* 9, 7962, doi:10.1038/s41598-019-43823-1, 2019.
- Romanovsky, V. E., and Osterkamp, T. E.: Effects of unfrozen water on heat and mass transport processes in the active layer and permafrost, *Permafrost Periglac. Process*, 11, 219–39, 2000.
- Roshydromet & GGO (2019): The State of Atmospheric Pollution in Cities on the Territory of Russia for 2018. Yearbook. Federal Service on Hydrometeorology and Monitoring Environment, Roshydromet & A.I. Voeikov Main Geophysical Observatory, ISBN 978-5-9500883-8-4, St.Petersburg, 250 p., In Russian (http://voeikovmgo.ru/images/stories/publications/2019/ejegodnik_zagr_atm_2018+.pdf)
- Rost, B., and Riebesell, U.: Coccolithophores and the biological pump: responses to environmental changes, in: *Coccolithophores, from molecular processes to global impact*, edited by: Thierstein, H. R., Young, J. R., 99–125, Springer, Heidelberg, Germany, 2004.
- Ryazanova, A., and Voropay, N. N.: Droughts and Excessive Moisture Events in Southern Siberia in the Late XXth - Early XXIst Centuries, *IOP Conf. Ser.: Earth Environ. Sci.*, 96, 012015, 2017.
- Räisänen, J.: Effect of atmospheric circulation on recent temperature changes in Finland, *Clim. Dyn.*, 53, 5675–5687, doi:10.1007/s00382-019-04890-2, 2019.
- Räisänen, J.: Effect of atmospheric circulation on surface air temperature trends in years 1979–2018. *Clim. Dyn.*, 56, 2303–2320, doi:10.1007/s00382-020-05590-y, 2021.
- Saarela, T., Rissanen, A. J., Ojala, A. et al.: CH₄ oxidation in a boreal lake during the development of hypolimnetic hypoxia, *Aquat Sci*, 82, 19, /doi.org/10.1007/s00027-019-0690-8, 2020.
- Salmon, Y., Lintunen, A., Dayet, A., Chan, T., Dewar, R., Vesala, T. and Hölttä, T.: Leaf carbon and water status control stomatal and non-stomatal limitations of photosynthesis in trees, *New Phytologist* 226, 690-703. doi: 10.1111/nph.16436, 2020.

Formatted: Font color: Auto

Formatted: Font color: Auto

Field Code Changed

Formatted: Font color: Auto

Formatted: Font color: Auto

- 3200 Santalahti, M., Sun, H., Sietiö, O.M., Köster, K., Berninger, F., Laurila, T., Pumpanen, J., and Heinonsalo,
3201 J.: Reindeer grazing alter soil fungal community structure and litter decomposition related enzyme activities
3202 in boreal coniferous forests in Finnish Lapland, *App. Soil Ecol.*, 132, 74-82,
3203 doi:10.1016/j.apsoil.2018.08.013, 2018.
- 3204 Schallhart, S., Rantala, P., Kajos, M. K., Aalto, J., Mammarella, I., Ruuskanen, T. M., and Kulmala, M.:
3205 Temporal variation of VOC fluxes measured with PTR-TOF above a boreal forest, *Atmospheric Chemistry
3206 and Physics*, 18(2), 815-832. doi:10.5194/acp-18-815-2018, 2018.
- 3207 Schmale, J., Arnold, S. R., Law, K. S., Thorp, T., Anenberg, S., Simpson, W. R., Mao, J. and Pratt, K. A.:
3208 Local Arctic air pollution: a neglected but serious problem, *Earths Future*, 6(10), 1385-1412,
3209 doi:10.1029/2018ef000952, 2018a.
- 3210 Schmale, J., Henning, S., Decesari, S., Henzing, B., Keskinen, H., Sellegri, K., Ovadnevaite, J., Pöhlker, M.
3211 L., Brito, J., Bougiatioti, A., Kristensson, A., Kalivitis, N., Stavroulas, I., Carbone, S., Jefferson, A., Park,
3212 M., Schlag, P., Iwamoto, Y., Aalto, P., Äijälä, M., Bukowiecki, N., Ehn, M., Frank, G., Fröhlich, R.,
3213 Frumau, A., Herrmann, E., Herrmann, H., Holzinger, R., Kos, G., Kulmala, M., Mihalopoulos, N., Nenes,
3214 A., O'Dowd, C., Petäjä, T., Picard, D., Pöhlker, C., Pöschl, U., Poulain, L., Prévôt, A. S. H., Swietlicki, E.,
3215 Andreae, M. O., Artaxo, P., Wiedensohler, A., Ogren, J., Matsuki, A., Yum, S. S., Stratmann, F.,
3216 Baltensperger, U., and Gysel, M.: Long-term cloud condensation nuclei number concentration, particle
3217 number size distribution and chemical composition measurements at regionally representative observatories,
3218 *Atmos. Chem. Phys.*, 18, 2853–2881, doi:10.5194/acp-18-2853-2018, 2018b.
- 3219 Schmeisser, L., Backman, J., Ogren, J. A., Andrews, E., Asmi, E., Starkweather, S., Uttal, T., Fiebig, M.,
3220 Sharma, S., Eleftheriadis, K., Vratolis, S., Bergin, M., Tunved, P., and Jefferson, A.: Seasonality of aerosol
3221 optical properties in the Arctic, *Atmos. Chem. Phys.*, 18, 11599–11622, doi:10.5194/acp-18-11599-2018,
3222 2018.
- 3223 Schuur, E. A. G., Bockheim, J., Canadell, J. G., Euskirchen, E., Field, C. B., Goryachkin, S. V., Hagemann,
3224 S., Kuhry, P., Lafleur, P.M., Lee, H., Mazhitova, G., Nelson, F. E., Rinke, A., Romanovsky, V. E.,
3225 Shiklomanov, N., Tarnocai, C., Venevsky, S., Vogel, J. G., and Zimov, S. A.: Vulnerability of permafrost
3226 carbon to climate change: implications for the global carbon cycle, *BioScience*, 58(8), 701–714,
3227 doi:10.1641/B580807, 2008.
- 3228 Schuur, E. A. G., McGuire, A. D., Romanovsky, V., Schädel, C., and Mack, M.: Chapter 11: Arctic and
3229 boreal carbon, in: *Second State of the Carbon Cycle Report (SOCCR2): A Sustained Assessment Report*,
3230 edited by: Cavallaro, N., Shrestha, G., Birdsey, R., Mayes, M. A., Najjar, R. G., Reed, S. C., Romero-
3231 Lankao, P., and Zhu, Z., U.S. Global Change Research Program, Washington, DC, USA, 428-468,
3232 doi:10.7930/SOCCR2.2018.Ch11, 2018.
- 3233 Scott, C. E., Monks, S. A., Spracklen, D. V., Arnold, S. R., Forster, P. M., Rap, A., Äijälä, M., Artaxo, P.,
3234 Carslaw, K. S., Chipperfield, M. P., Ehn, M., Gilardoni, S., Heikkinen, L., Kulmala, M., Petäjä, T.,

- 3235 Reddington, C. L. S., Rizzo, L. V., Swietlicki, E., Vignati, E., and Wilson, C.: Impact on short-lived climate
3236 forcers increases projected warming due to deforestation, *Nat. Commun.*, 9, 9, doi:10.1038/s41467-017-
3237 02412-4, 2018.
- 3238 Shakhova, N., Semiletov, I., and Belcheva, N.: The great Siberian rivers as a source of methane on the
3239 Russian Arctic shelf, *Dokl. Earth Sci.*, 415, 734–736, doi: 10.1134/S1028334X07050169, 2007.
- 3240 Shalina, E. V., and Sandven, S.: Snow depth on Arctic sea ice from historical in situ data, *Cryosphere*, 12(6),
3241 1867–1886, doi:10.5194/tc-12-1867-2018, 2018.
- 3242 Shen, Y., Virkkula, A., Ding, A., Wang, J., Chi, X., Nie, W., Qi, X., Huang, X., Liu, Q., Zheng, L., Xu, Z.,
3243 Petäjä, T., Aalto, P. P., Fu, C., and Kulmala, M.: Aerosol optical properties at SORPES in Nanjing, east
3244 China, *Atmos. Chem. Phys.*, 18, 5265–5292, doi: 10.5194/acp-18-5265-2018, 2018.
- 3245 Shen, Y., Virkkula, A., Ding, A., Luoma, K., Keskinen, H., Aalto, P. P., Chi, X., Qi, X., Nie, W., Huang, X.,
3246 Petäjä, T., Kulmala, M., and Kerminen, V.-M.: Estimating cloud condensation nuclei number concentrations
3247 using aerosol optical properties: role of particle number size distribution and parameterization, *Atmos.*
3248 *Chem. Phys.*, 19, 15483–15502, doi:10.5194/acp-19-15483-2019, 2019.
- 3249 Shestakova, T. A., Gutierrez, E., Valeriano, C., Lapshina, E., and Voltas, J.: Recent loss of sensitivity to
3250 summer temperature constrains tree growth synchrony among boreal Eurasian forests, *Agr. Forest Meteorol.*,
3251 268, 318–330, doi:10.1016/j.agrformet.2019.01.039, 2019.
- 3252 Shevchenko, V. P., Starodymova, D. P., Vinogradova, A. A., Lisitzin, A. P., Makarov, V. I., Popova, S. A.,
3253 Sivonen, V. V., and Sivonen, V. P.: Elemental and organic carbon in atmospheric aerosols over the
3254 northwestern coast of Kandalaksha Bay of the White Sea, *Dokl. Earth Sci.*, 461(1), 242–246,
3255 doi:10.1134/s1028334x1503006x, 2015.
- 3256 Shevchenko, V. P., Maslov, A. V., and Stein, R.: Distribution of some rare and trace elements in ice-rafted
3257 sediments in the Yermak Plateau area, the Arctic Ocean, *Oceanol.*, 57(6), 855–863,
3258 doi:10.1134/s0001437017060157, 2017a.
- 3259 Shevchenko, V. P., Pokrovsky, O. S., Vorobyev, S. N., Krickov, I. V., Manasypov, R. M., Politova, N. V.,
3260 Kopysov, S. G., Dara, O. M., Auda, Y., Shirokova, L. S., Kolesnichenko, L. G., Zemtsov, V. A., and
3261 Kirpotin, S. N.: Impact of snow deposition on major and trace element concentrations and elementary fluxes
3262 in surface waters of the Western Siberian Lowland across a 1700 km latitudinal gradient, *Hydrol. Earth Syst.*
3263 *Sci.*, 21, 5725–5746, doi:10.5194/hess-21-5725-2017, 2017b.
- 3264 Shevchenko, V. P., Kopeikin, V. M., Novigatsky, A. N., and Malafeev, G. V.: Black carbon in the
3265 atmospheric boundary layer over the North Atlantic and the Russian Arctic seas in June–September 2017,
3266 *Oceanol.*, 59(5), doi:10.1134/S0001437019050199, 692–696, 2019.

- 3267 Shevnina, E., Kourzeneva, E., Kovalenko, V., and Vihma, T.: Assessment of extreme flood events in a
 3268 changing climate for a long-term planning of socio-economic infrastructure in the Russian Arctic, *Hydrol.*
 3269 *Earth Syst. Sci.*, 21(5), 2559-2578, doi:10.5194/hess-21-2559-2017, 2017.
- 3270 Shevnina, E., Silaev, A., and Vihma, T.: Probabilistic projections of annual runoff and potential hydropower
 3271 production in Finland, *Universal Journal of Geoscience*, 7(2), 43-55, doi:10.13189/ujg.2019.070201, 2019.
- 3272 Shiklomanov, A.I., and Lammers, R.B.: Record Russian river discharge in 2007 and the limits of analysis,
 3273 *Environ. Res. Lett.*, 4, doi: 10.1088/1748-9326/4/4/045015, 2009.
- 3274 Shinkareva G. L., Lychagin M. Y., Tarasov M. K., Pietroni J., Chichayeva M. A., and Chalov S. R.:
 3275 Biogeochemical specialization of macrophytes and their role as a biofilter in the Selenga delta, *Geography,*
 3276 *Environment, Sustainability*, 12(3), 240-263, 2019.
- 3277 Silkin, V. A., Pautova, L., Giordano, M., Chasovnikov, V., Vostokov, S., Podymov, O., Parkhomova, S., and
 3278 Moskalenko, L.: Drivers of phytoplankton blooms in the northeastern Black Sea, *Mar. Pollution Bull.*, 138,
 3279 274-284, doi:10.1016/j.marpolbul.2018.11.042, 2018.
- 3280 Sizov O. S., and Lobotrosova S. A.: Features of revegetation of drift sand sites in the northern taiga subzone
 3281 of Western Siberia. *Earth Cryosphere*, (3), 3–13, doi:10.21782/kz1560-7496-2016-3(3-13), 2016.
- 3282 Skorokhod, A. I., Berezina, E. V., Moiseenko, K. B., Elansky, N. F., and Belikov, I. B.: Benzene and toluene
 3283 in the surface air of northern Eurasia from TROICA-12 campaign along the Trans-Siberian Railway, *Atmos.*
 3284 *Chem. Phys.*, 17(8), 5501-5514, doi:10.5194/acp-17-5501-2017, 2017.
- 3285 Slukovskaya, M. V., Vasenev, V. I., Ivashchenko, K. V., Morev, D. V., Drogobuzhskaya, S. V., Ivanova, L.
 3286 A., and Kremenetskaya, I. P.: Technosols on mining wastes in the subarctic: Efficiency of remediation under
 3287 Cu-Ni atmospheric pollution, *Int. Soil Water Conserv. Res.*, 7(3), 297-307, doi:10.1016/j.iswcr.2019.04.002,
 3288 2019.
- 3289 Smith, L.: The new north: The world in 2050, Profile Books, London, UK, 2011.
- 3290 Song, S., Li, C., Shi, X., Zhao, S., Li, Z., Bai, Y., Cao, X., Wang, Q., Huotari, J., Tulonen, T., Uusheimo, S.,
 3291 Leppäranta, M., and Arvola, L.: Under-ice metabolism in a shallow lake (Wuliangsuhai) in Inner Mongolia,
 3292 in cold and arid climate zone, *Freshw. Biol.*, 1–11, 2019.
- 3293 Spengler, T., Renfrew, I. A., Terpstra, A., Tjernström, M., Screen, J., Brooks, I. M., Andrew Carleton, A.,
 3294 Chechin, D., Chen, L., Doyle, J., Esau, I., Hezel, P. J., Jung, T., Kohyama, T., Lüpkes, C., McCusker, C. E.,
 3295 Nygård, T., Sergeev, D., Shupe, M. D., Sodemann, H., and Vihma, T.: High-latitude dynamics of
 3296 atmosphere–ice–ocean interactions, *Bull. Am. Meteorol. Soc.*, 97(9), ES179-ES182, doi:10.1175/bams-d-15-
 3297 00302.1, 2016.
- 3298 Sporre, M. K., Blichner, S. M., Karset, I. H. H., Makkonen, R., and Berntsen, T. K.: BVOC–aerosol–climate
 3299 feedbacks investigated using NorESM, *Atmos. Chem. Phys.*, 19, 4763–4782, doi:10.5194/acp-19-4763-
 3300 2019, 2019.

- 3301 Starodymova, D. P., Shevchenko, V. P., Sivonen, V. P., and Sivonen, V. V.: Material and elemental
 3302 composition of surface aerosols on the north-western coast of the Kandalaksha Bay of the White Sea, *Atmos.*
 3303 *Oceanic Opt.*, 29(6), 507-511, doi:10.1134/s1024856016060154, 2016.
- 3304 Sun, H., Santalahti, M., Pumpanen, J., Koster, K., Berninger, F., Raffaello, T., Asiegbu, F. O., and
 3305 Heinonsalo, J.: Bacterial community structure and function shift across a northern boreal forest fire
 3306 chronosequence, *Scientific Rep.*, 6, 12, doi:10.1038/srep32411, 2016.
- 3307 Sun, Y., Frankenberg C., Wood JD, Schimel DS., Jung, M., Guanter L., Drewry, DT., Verma, M., Porcar-
 3308 Castell, A., Griffis, TJ., Gu, L., Magney, S., Köhler P., Evans B., and Yuen, K.: OCO-2 advances
 3309 photosynthesis observation from space via solar-induced chlorophyll fluorescence, *Science* 358, 189,
 3310 doi:10.1126/science.aam5747, 2017.
- 3311 Suomi, I., Gryning, S-E. , O'Connor E.J., and Vihma, T.: Methodology for obtaining wind gusts
 3312 using Doppler lidar, *Quarterly Journal of the Royal Meteorological Society*, 143, 2061-2072,
 3313 doi.org/10.1002/qj.3059, 2016.
- 3314 Svensson, J., Virkkula, A., Meinander, O., Kivekäs, N., Hannula, H.-R., Järvinen, O., Peltoniemi, J.I.,
 3315 Gritsevich, M., Heikkilä, A., Kontu, A., Neitola, K., Brus, D., DagssonWaldhauserova, P., Anttila, K.,
 3316 Vehkamäki, M., Hienola, A., de Leeuw, G., and Lihavainen, H.: Soot-doped natural snow and its albedo —
 3317 results from field experiments, *Boreal Environment Research*, 21, 481-503, 2016.
- 3318 Svensson, J., Ström, J., Kivekäs, N., Dkhar, N. B., Tayal, S., Sharma, V. P., Jutila, A., Backman, J.,
 3319 Virkkula, A., Ruppel, M., Hyvärinen, A., Kontu, A., Hannula, H.-R., Leppäranta, M., Hooda, R. K., Korhola,
 3320 A., Asmi, E., and Lihavainen, H.: Light absorption of dust and elemental carbon in snow in the Indian
 3321 Himalayas and the Finnish Arctic, *Atmos. Meas. Tech.*, 11, 1403-1416, doi:10.5194/amt-11-1403-2018,
 3322 2018.
- 3323 Svensson, J., Ström, J., and Virkkula, A.: Multiple-scattering correction factor of quartz filters and the effect
 3324 of filtering particles mixed in water: implications for analyses of light absorption in snow samples, *Atmos.*
 3325 *Meas. Tech.*, 12, 5913-5925, doi:10.5194/amt-12-5913-2019, 2019.
- 3326 Taylor, K. E., Stouffer, R. J., and Meehl, G. A.: An overview of CMIP5 and the experiment design, *Bull.*
 3327 *Am. Meteorol. Soc.*, 93, 485-498, doi: 10.1175/BAMS-D-11-00094.1, 2012.
- 3328 Taylor, A., Brownlee, C., and Wheeler, G.: Coccolithophore cell biology: chalking up progress, *Ann. Rev.*
 3329 *Mar. Sci.*, 9, 283-310, doi:10.1146/annurev-marine-122414-034032, 2017.
- 3330 Terentieva, I. E., Glagolev, M. V., Lapshina, E. D., Sabrekov, A. F., and Maksyutov, S.: Mapping of West
 3331 Siberian taiga wetland complexes using Landsat imagery: implications for methane emissions,
 3332 *Biogeosciences*, 13, 4615–4626, doi:10.5194/bg-13-4615-2016, 2016.

- 3333 Thompson, R. L., Sasakawa, M., Machida, T., Aalto, T., Worthy, D., Lavric, J. V., Lund Myhre, C., and
 3334 Stohl, A.: Methane fluxes in the high northern latitudes for 2005–2013 estimated using a Bayesian
 3335 atmospheric inversion, *Atmos. Chem. Phys.*, 17, 3553–3572, doi:10.5194/acp-17-3553-2017, 2017.
- 3336 Thonat, T., Saunio, M., Bousquet, P., Pison, I., Tan, Z., Zhuang, Q., Crill, P. M., Thornton, B. F., Bastviken,
 3337 D., Dlugokencky, E. J., Zimov, N., Laurila, T., Hatakka, J., Hermansen, O., and Worthy, D. E. J.:
 3338 Detectability of Arctic methane sources at six sites performing continuous atmospheric measurements,
 3339 *Atmos. Chem. Phys.*, 17, 8371–8394, doi:10.5194/acp-17-8371-2017, 2017.
- 3340 Thorslund, J., Jarsjo, J., Wallstedt, T., Morth, C. M., Lychagin, M. Y., and Chalov, S. R.: Speciation and
 3341 hydrological transport of metals in non-acidic river systems of the Lake Baikal basin: Field data and model
 3342 predictions, *Reg. Environ. Chang.*, 17(7), 2007–2021, doi:10.1007/s10113-016-0982-7, 2017.
- 3343 Tian, Z. X., Cheng, B., Zhao, J. C., Vihma, T., Zhang, W. L., Li, Z. J., and Zhang, Z. H.: Observed and
 3344 modelled snow and ice thickness in the Arctic Ocean with CHINARE buoy data, *Acta Oceanologica Sinica*,
 3345 36(8), 66–75, doi:10.1007/s13131-017-1020-4, 2017.
- 3346 Tillman, H., Yang, J. and Nielsson, E.: The Polar Silk Road: China's New Frontier of International
 3347 Cooperation, *China Quarterly of International Strategic Studies*, 4, 10.1142/S2377740018500215, 2018.
- 3348 Timokhina, A. V., Prokushkin, A. S., Onuchin, A. A., Panov, A. V., Kofman, G. B., and Heimann, M.:
 3349 Variability of ground CO₂ concentration in the middle taiga subzone of the Yenisei region of Siberia, *Russ.*
 3350 *J. Ecol.*, 46, 143–151, doi:10.1134/s1067413615020125, 2015a.
- 3351 Timokhina, A. V., Prokushkin, A. S., Onuchin, A. A., Panov, A. V., Kofman, G. B., Verkhovets, S. V., and
 3352 Heimann, M.: Long-term trend in CO₂ concentration in the surface atmosphere over Central Siberia, *Russ.*
 3353 *Meteorol. Hydrol.*, 40, 186–190, 2015b.
- 3354 Tsuruta, A., Aalto, T., Backman, L., Hakkarainen, J., ... and Peters, W.: Global methane emission estimates
 3355 for 2000–2012 from CarbonTracker Europe-CH₄ v1.0. *Geosci. Model Dev.*, 10, 1261–1289, 2017.
- 3356 Tuovinen, J-P., Aurela, M., Hatakka, J., Räsänen, A., ... Laurila, T.: Interpreting eddy covariance data from
 3357 heterogeneous Siberian tundra: land-cover-specific methane fluxes and spatial representativeness,
 3358 *Biogeosciences*, 16, 255–274, 2019.
- 3359 Uotila, P., Vihma, T., and Haapala, J.: Atmospheric and oceanic conditions and the extremely low Bothnian
 3360 Bay sea ice extent in 2014/2015, 42, 7740–7749, *Geophysical Research and Letters*, 2015.
- 3361 Uotila, P., Iovino, D., Vancoppenolle, M., Lensu, M., and Rousset, C., Comparing sea ice, hydrography and
 3362 circulation between NEMO3.6 LIM3 and LIM2, *Geosci. Model Dev.*, 10, 1009–1031, doi:10.5194/gmd-10-
 3363 1009-2017, 2017.
- 3364 Uotila, P., Goosse, H., Haines, K., Chevallier, M., Barthélemy, A., Bricaud, C., Carton, J., Fučkar, N.,
 3365 Garric, G., Iovino, D., Kauker, F., Korhonen, M., Lien, V. S., Marnela, M., Massonnet, F., Mignac, D.,

- Peterson, K. A., Sadikni, R., Shi, L., Tietsche, S., Toyoda, T., Xie, J., and Zhang, A.: An assessment of ten ocean reanalyses in the polar regions, *Clim Dyn* 52, 1613–1650, doi:10.1007/s00382-018-4242-z, 2019.
- Uttal, T., Starkweather, S., Drummond, J. R., Vihma, T., Makshtas, A. P., Darby, L. S., Burkhart, J. F., Cox, C. J., Schmeisser, L. N., Haiden, T., Maturilli, M., Shupe, M. D., De Boer, G., Saha, A., Grachev, A. A., Crepinsek, S. M., Bruhwiler, L., Goodison, B., McArthur, B., Walden, V. P., Dlugokencky, E. J., P. Persson, O., Lesins, G., Laurila, T., Ogren, J. A., Stone, R., Long, C. N., Sharma, S., Massling, A., Turner, D. D., Stanitski, D. M., Asmi, E., Aurela, M., Skov, H., Eleftheriadis, K., Virkkula, A., Platt, A., Førland, E. J., Iijima, Y., Nielsen, I. E., Bergin, M. H., Candlish, L., Zimov, N. S., Zimov, S. A., O'Neill, N. T., Fogal, P. F., Kivi, R., Konopleva-Akish, E. A., Verlinde, J., Kustov, V. Y., Vasek, B., Ivakhov, V. M., Viisanen Y., and Intrieri, J. M.: International Arctic Systems for Observing the Atmosphere: An International Polar Year Legacy Consortium, *Bull. Amer. Meteor. Soc.*, 97, 1033–1056, doi:10.1175/BAMS-D-14-00145.1, 2016.
- Vanhatalo, A., Ghirardo, A., Juurola, E., Schnitzler, J.-P., Zimmer, I., Hellén, H., Hakola, H., and Bäck, J.: Long-term dynamics of monoterpene synthase activities, monoterpene storage pools and emissions in boreal Scots pine, *Biogeosciences*, 15, 5047–5060, doi:10.5194/bg-15-5047-2018, 2018.
- Varentsov, M., Konstantinov, P., Baklanov, A., Esau, I., Miles, V., and Davy, R.: Anthropogenic and natural drivers of a strong winter urban heat island in a typical Arctic city, *Atmos. Chem. Phys.*, 18(23), 17573–17587, doi:10.5194/acp-18-17573-2018, 2018a.
- Varentsov, M., Wouters, H., Platonov, V., and Konstantinov, P.: Megacity-induced mesoclimatic effects in the lower atmosphere: a modeling study for multiple summers over Moscow, Russia, *Atmos.*, 9(2), 24, doi:10.3390/atmos9020050, 2018b.
- Vasileva, A., Moiseenko, K., Skorokhod, A., Belikov, I., Kopeikin, V., and Lavrova, O.: Emission ratios of trace gases and particles for Siberian forest fires on the basis of mobile ground observations, *Atmos. Chem. Phys.*, 17(20), 12303–12325, doi:10.5194/acp-17-12303-2017, 2017.
- Vestenius, M., Hellén, H., Levula, J., Kuronen, P., Helminen, K. J., Nieminen, T., Kulmala, M., and Hakola, H.: Acidic reaction products of monoterpenes and sesquiterpenes in atmospheric fine particles in a boreal forest, *Atmos. Chem. Phys.*, 14, 7883–7893, doi:10.5194/acp-14-7883-2014, 2014.
- Vihma, T., Uotila, P., Sandven, S., Pozdnyakov, D., Makshtas, A., Pelyasov, A., Pirazzini, R., Danielsen, F., Chalov, S., Lappalainen, H. K., Ivanov, V., Frolov, I., Albin, A., Cheng, B., Dobrolyubov, S., Arkhipkin, V., Myslenkov, S., Petäjä, T., and Kulmala, M.: Towards an advanced observation system for the marine Arctic in the framework of the Pan-Eurasian Experiment (PEEX), *Atmos. Chem. Phys.*, 19, 1941–1970, doi:10.5194/acp-19-1941-2019, 2019.
- Vihma, T., Graversen, R., Chen, L., Dörthe H., Skific, N., Francis, J.A., Tyrrell, N., Hall, R., Hanna, E., Uotila, P., Dethloff, K., Karpechko, A. Y., Björnsson, H. and Overland, J. E.: Effects of the tropospheric large-scale circulation on European winter temperatures during the period of amplified Arctic warming, *Int J Climatol.*, 40, 509– 529, doi:10.1002/joc.6225, 2020

Formatted: Font color: Auto

- 3401 Virkkula, A., Chi, X., Ding, A., Shen, Y., Nie, W., Qi, X., Zheng, L., Huang, X., Xie, Y., Wang, J., Petäjä,
 3402 T., and Kulmala, M.: On the interpretation of the loading correction of the aethalometer, *Atmos. Meas.*
 3403 *Tech.*, 8, 4415–4427, doi:10.5194/amt-8-4415-2015, 2015.
- 3404 Voigt, C., Marushchak, M.E., Lamprecht, R.E., et al.: Nitrous oxide emissions from thawing permafrost,
 3405 *PNAS* May 2017, 201702902; DOI: 10.1073/pnas.1702902114.
- 3406 Voigt, C., Lamprecht, R. E., Marushchak, M. E., Lind, S. E., Novakovskiy, A., Aurela, M., Martikainen, P. J.
 3407 and Biasi, C.: Warming of subarctic tundra increases emissions of all three important greenhouse gases -
 3408 carbon dioxide, methane, and nitrous oxide, *Glob. Change Biol.*, 23(8), 3121–3138, doi:10.1111/gcb.13563,
 3409 2016.
- 3410 Voropay, N. N., Kichigina, N. V.: Long-term changes in the hydroclimatic characteristics in the Baikal
 3411 region, *IOP Conf. Ser.: Earth Environ. Sci.*, 107, 012042, 2018.
- 3412 Voropay N.N., Ryazanova A.A., Dyukarev E.A. Variability of vegetation index NDVI during periods of
 3413 drought in the Tomsk Region, *IOP Conf. Series: Earth Environ. Sci.*, 381, 012096, doi:10.1088/1755-
 3414 1315/381/1/012096, 2019.
- 3415 Walker, X. J., Baltzer, J. L., Cumming, S. G., Day, N. J., Ebert, C., Goetz, S., Johnstone, J. F., Potter, S.,
 3416 Rogers, B. M., Schuur, E. A. G., Turetsky, M. R., and Mack, M. C., Increasing wildfires threaten historic
 3417 carbon sink of boreal forest soils, *Nature*, 572, 520–523, doi:10.1038/s41586-019-1474-y, 2019.
- 3418 Walsh, M. G., de Smalen, A. W., and Mor, S. M.: Climatic influence on anthrax suitability in warming
 3419 northern latitudes, *Sci Rep*, 8(1), 9269, doi:10.1038/s41598-018-27604-w, 2018.
- 3420 van Vuuren, D. P., Edmonds, J., Kainuma, M., Riahi, K., Thomson, A., Hibbard, K., Hurtt, G. C., Kram, T.,
 3421 Krey, V., Lamarque, J. F., Masui, T., Meinshausen, M., Nakicenovic, N., Smith, S. J., and Rose, S. K.: The
 3422 representative concentration pathways: an overview, *Clim. Chang.*, 109, 5–31, doi:10.1007/s10584-011-
 3423 0148-z, 2011.
- 3424 Wang, J., Ge, X., Chen, Y., Shen, Y., Zhang, Q., Sun, Y., Xu, J., Ge, S., Yu, H., and Chen, M.: Highly time-
 3425 resolved urban aerosol characteristics during springtime in Yangtze River Delta, China: insights from soot
 3426 particle aerosol mass spectrometry, *Atmos. Chem. Phys.*, 16, 9109–9127, doi:10.5194/acp-16-9109-2016,
 3427 2016.
- 3428 Wang, J., Zhao, B., Wang, S., Yang, F., Xing, J., Morawska, L., Ding, A., Kulmala, M., Kerminen, V.-M.,
 3429 Kujansuu, J., Wang, Z., Ding, D., Zhang, X., Wang, H., Tian, M., Petäjä, T., Jiang, J., and Hao J.: Particulate
 3430 matter pollution over China and the effects of control policies, *Sci. Total Environ.*, 584–585, 426–447, 2017a.
- 3431 Wang, Z. B., Wu, Z. J., Yue, D. L., Shang, D. J., Guo, S., Sun, J. Y., Ding, A. J., Wang, L., Jiang, J. K., Guo,
 3432 H., Gao, J., Cheung, H. C., Morawska, L., Keywood, M., and Hu, M.: New particle formation in China:
 3433 Current knowledge and further directions, *Sci. Total Environ.*, 577, 258–266,
 3434 doi:10.1016/j.scitotenv.2016.10.177, 2017b.

- Wang, Z., Huang, X., and Ding, A.: Dome effect of black carbon and its key influencing factors, *Atmos. Chem. Phys.*, 18, 2821-2834, 2018b.
- Wang, P. C., Elansky, N. F., Timofeev, Y. M., Wang, G. C., Golitsyn, G. S., Makarova, M. V., Rakitin, V. S., Shtabkin, Yu., Skorokhod, A. I., Grechko, E. I., Fokeeva, E. V., Safronov, A. N., Ran, L., and Wang, T.: Long-term trends of carbon monoxide total columnar amount in urban areas and background regions: ground- and satellite-based spectroscopic measurements, *Adv. Atmos. Sci.*, 35(7), 785-795, doi:10.1007/s00376-017-6327-8, 2018a.
- Wang, Y., Wang, Y., Wang, L., Petäjä, T., Zha, Q., Gong, C., Li, S., Pan, Y., Hu, B., Xin, J., and Kulmala, M.: Increased inorganic aerosol fraction contributes to air pollution and haze in China, *Atmos. Chem. Phys.*, 19, 5881–5888, doi:10.5194/acp-19-5881-2019, 2019.
- Wang, Y.H., Yu, M., Wang, Y., Tang, G., Song, T., Zhou, P., Liu, Z., Hu, B., Ji, D.S., Wang, L., Zhu, X., Yan, C., Ehn, M., Gao, W.K., Pan, Y.P., Xin, J.Y., Sung, Y., Kerminen, V.-M., Kulmala, M. and Petäjä, T.: Rapid formation of intense haze episode via aerosol-boundary layer feedback in Beijing, *Atmos. Chem. Phys.*, 10, 45-53, 2020.
- Wei, L. X., Deng, X. H., Cheng, B., Vihma, T., Hannula, H. R., Qin, T., and Pulliainen, J.: The impact of meteorological conditions on snow and ice thickness in an Arctic lake, *Tellus A: Dyn. Meteorol. Oceanogr.*, 68, 12, doi:10.3402/tellusa.v68.31590, 2016.
- Wickström, S., Jonassen, M., Vihma, T., and Uotila, P.: Trends in cyclones in the high latitude North Atlantic during 1979-2016, *Q. J. R. Meteorol. Soc.*, 146, 762– 779, doi:10.1002/qj.3707, 2020.
- Wiedensohler, A., Ma, N., Birmili, W., Heintzenberg, J., Ditas, F., Andreae, M. O., and Panov, A.: Infrequent new particle formation over the remote boreal forest of Siberia, *Atmos. Environ.*, 200, 167-169, doi:10.1016/j.atmosenv.2018.12.013, 2019.
- Wild, B., Andersson, A., Bröder, L., Vonk, J., Hugelius, G., McClelland, J.W., Song, W., Raymond, P.A., and Gustafsson, Ö.: Rivers across the Siberian Arctic unearth the patterns of carbon release from thawing permafrost *Proceedings of the National Academy of Sciences*, 116 (21) 10280-10285., 2019.
- Williams, P. J., and Smith, M. W.: *The Frozen Earth: Fundamentals of Geocryology*, Cambridge University Press, Cambridge, UK, 1989.
- WMO, 2019 Guidance on Integrated Urban Hydrometeorological, Climate and Environmental Services. Volume 1: Concept and Methodology, Grimmond, S., Bouchet, S., Molina, L., Baklanov, A., Joe, P. et al., WMO-No. 1234, https://library.wmo.int/doc_num.php?explnum_id=9903, 2019.
- Wolf-Grosse, T., Esau, I., and Reuder, J.: The large-scale circulation during air quality hazards in Bergen, Norway, *Tellus A: Dyn. Meteorol. Oceanogr.*, 69, 16, doi:10.1080/16000870.2017.1406265, 2017a.

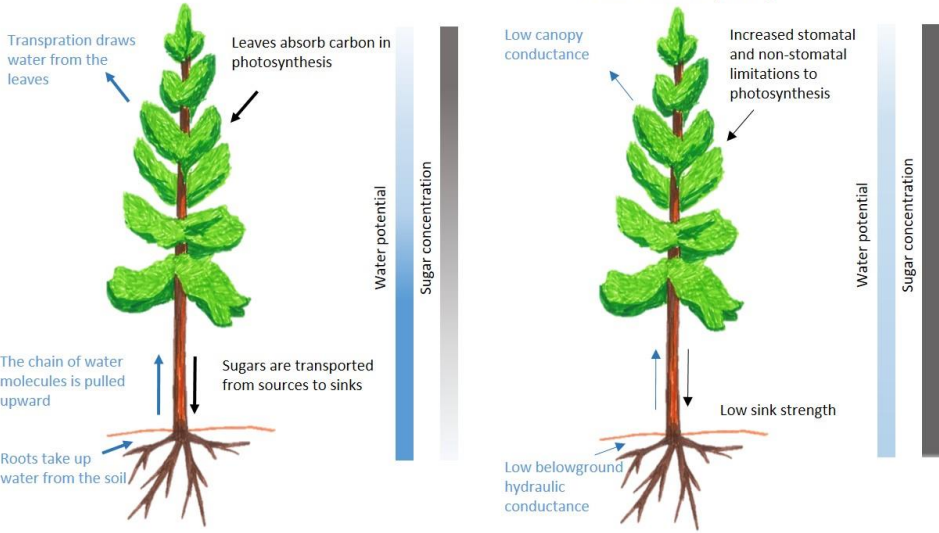
- Wolf-Grosse, T., Esau, I., and Reuder, J.: Sensitivity of local air quality to the interplay between small- and large-scale circulations: a large-eddy simulation study, *Atmos. Chem. Phys.*, 17(11), 7261–7276, doi:10.5194/acp-17-7261-2017, 2017b.
- Xausa, F., Paasonen, P., Makkonen, R., Arshinov, M., Ding, A., Denier Van Der Gon, H., Kerminen, V.-M., and Kulmala, M.: Advancing global aerosol simulations with size-segregated anthropogenic particle number emissions, *Atmos. Chem. Phys.*, 18, 10039–10054, doi:10.5194/acp-18-10039-2018, 2018.
- Xiao, S., Wang, M. Y., Yao, L., Zhou, B., Yang, X., Chen, J. M., Wang, D. F., Fu, Q. Y., Worsnop, D. R. and Wang, L.: Strong atmospheric new particle formation in winter in urban Shanghai, China, *Atmos. Chem. Phys.*, 15, 1769–1781, 2015.
- Xie, Y. N., Ding, A. J., Nie, W., Mao, H. T., Qi, X. M., Huang, X., Xu, Z., Kerminen, V. K., Petäjä, T., Chi, X., Virkkula, A., Boy, M., Xue, L., Guo, J., Sun, J., Yang, X., Kulmala, M., and Fu, C. B.: Enhanced sulfate formation by nitrogen dioxide: Implications from in situ observations at the SORPES station, *J Geophys. Res.: Atmos.*, 120(24), 12679–12694, doi:10.1002/2015jd023607, 2015.
- Yan, C., Yin, R., Lu, Y., Dada, L., Yang, D., Fu, Y., Kontkanen, J., Deng, C., Garmash, O., Ruan, J., Baalbaki, R., Schervish, M., Cai, R., Bloss, M., Chan, T., Chen, T., Chen, Q., Chen, X., Chen, Y., Chu, B., Dällenbach, K., Foreback, B., He, X., Heikkinen, L., Jokinen, T., Junninen, H., Kangasluoma, J., Kokkonen, T., Kurppa, M., Lehtipalo, K., Li, H., Li, H., Li, X., Liu, Y. Ma, Q., Paasonen, P., Rantala, P., Pileci, R. E., Rusanen, A., Sarnela, N., Simonen, P., Wang, S., Wang, W., Wang, Y. Xue, M., Yang, G., Yao, L., Zhou, Y., Kujansuu, J., Petäjä, T., Nie, W., Ma, N., Ge, M., He, H., Donahue, N. M., Worsnop, D. R., Kerminen, V.-M., Wang, L., Liu, Y., Zheng, J., Kulmala, M., Jiang, J. and Bianchi, F. (2021) The synergistic role of sulfuric acid, bases, and oxidized organics governing new-particle formation in Beijing. *Geophys. Res. Lett.* (in press).
- Yang, F., Li, C., Leppäranta, M., Shi, X., Zhao, S. and Zhang, C.: Notable increases in nutrient concentrations in a shallow lake during seasonal ice growth, *Water Sci. Technol.*, 74(12), 2773–2883, 2016.
- Yang, Y., Leppäranta, M. J., Ki, Z., Cheng, B., Zhai, M., and Demchev, D.: Model simulations of the annual cycle of the landfast ice thickness in the East Siberian Sea, *Advances in Polar Sciences*, 26(2), 168–178, doi:10.13679/j.advps.2015.2.00168, 2015.
- Yao, L., Garmash, O., Bianchi, F., Zheng, J., Yan, C., Kontkanen, J., Junninen, H., Mazon, S.B., Ehn, M., Paasonen, P., Sipilä, M., Wang, M.Y., Wang, X.K., Xiao, S., Chen, H.F., Lu, Y.Q., Zhang, B.W., Wang, D.F., Fu, Q.Y., Geng, F.H., Li, L., Wang, H.L., Qiao, L.P., Yang, X., Chen, J.M., Kerminen, V.-M., Petäjä, T., Worsnop, D.R., Kulmala, M. and Wang, L.: Atmospheric new particle formation from sulfuric acid and amines in a Chinese megacity, *Science*, 361, 278–281, 2018.
- Yasunaka, S., Siswanto, E., Olsen, A., Hoppema, M., Watanabe, E., Fransson, A., Chierici, M., Murata, A., Lauvset, S. K., Wanninkhof, R., Takahashi, T., Kosugi, N., Omar, A. M., van Heuven, S., and Mathis, J. T.:

- 3501 Arctic Ocean CO₂ uptake: an improved multiyear estimate of the air–sea CO₂ flux incorporating chlorophyll
3502 a concentrations, *Biogeosciences*, 15, 1643–1661, doi:10.5194/bg-15-1643-2018, 2018.
- 3503 Ye, Z., Liu, J., Gu, A., Feng, F., Liu, Y., Bi, C., Xu, J., Li, L., Chen, H., Chen, Y., Dai, L., Zhou, Q., and Ge,
3504 X.: Chemical characterization of fine particulate matter in Changzhou, China, and source apportionment with
3505 offline aerosol mass spectrometry, *Atmos. Chem. Phys.*, 17, 2573–2592, doi:10.5194/acp-17-2573-2017,
3506 2017.
- 3507 Ylivinkka, I., Kaupinmäki, S., Virman, M., Peltola, M., Taipale, D., Petäjä, T., Kerminen, V.-M., Kulmala,
3508 M., and Ezhova, E.: Clouds over Hyttiälä, Finland: an algorithm to classify clouds based on solar radiation
3509 and cloud base height measurements, *Atmos. Meas. Tech.*, 13, 5595–5619, 2020.
- 3510 He, Y., Chen, F., Jia, H., and Valery, G.: Bondur: Different Drought Legacies between Rain-fed and
3511 Irrigated Croplands in a Typical Russian Agricultural Region, *Remote Sens.*, 12(11), 1700,
3512 doi:10.3390/rs12111700, 2020
- 3513 Zaidan, M. A., Haapasilta, V., Relan, R., Junninen, H., Aalto, P. P., Kulmala, M., Laurson, L., and Foster, A.
3514 S.: Predicting atmospheric particle formation days by Bayesian classification of the time series features,
3515 *Tellus B: Chem. Phys. Meteorol.*, 70, 10, doi:10.1080/16000889.2018.1530031, 2018a.
- 3516 Zaidan, M. A., Haapasilta, V., Relan, R., Paasonen, P., Kerminen, V.-M., Junninen, H., Kulmala, M., and
3517 Foster, A. S.: Exploring non-linear associations between atmospheric new-particle formation and ambient
3518 variables: a mutual information approach, *Atmos. Chem. Phys.*, 18, 12699–12714, doi:10.5194/acp-18-
3519 12699-2018, 2018b.
- 3520 Zanatta, M., Laj, P., Gysel, M., Baltensperger, U., Vratolis, S., Eleftheriadis, K., Kondo, Y., Dubuisson, P.,
3521 Winiarek, V., Kazadzis, S., Tunved, P., and Jacobi, H.-W.: Effects of mixing state on optical and radiative
3522 properties of black carbon in the European Arctic, *Atmos. Chem. Phys.*, 18, 14037–14057, doi:10.5194/acp-
3523 18-14037-2018, 2018.
- 3524 Zapadinsky, E., Passananti, M., Myllys, N., Kurten, T., and Vehkamäki, H.: Modeling on Fragmentation of
3525 Clusters inside a Mass Spectrometer, *Journal of Physical Chemistry, A* 123 (2), 611–624,
3526 <https://doi.org/10.1021/acs.jpca.8b10744>, 2019.
- 3527 Zha, Q., Yan, C., Junninen, H., Riva, M., Sarnela, N., Aalto, J., Quéléver, L., Schallhart, S., Dada, L.,
3528 Heikkinen, L., Peräkylä, O., Zou, J., Rose, C., Wang, Y., Mammarella, I., Katul, G., Vesala, T., Worsnop, D.
3529 R., Kulmala, M., Petäjä, T., Bianchi, F., and Ehn, M.: Vertical characterization of highly oxygenated
3530 molecules (HOMs) below and above a boreal forest canopy, *Atmos. Chem. Phys.*, 18, 17437–17450,
3531 doi:10.5194/acp-18-17437-2018, 2018.
- 3532 Zhang, J., Liu, C., and Chen, H.: The modulation of Tibetan Plateau heating on the multi-scale northernmost
3533 margin activity of East Asia summer monsoon in northern China, *Global Planet. Change*, 161, 149–161,
3534 2018.

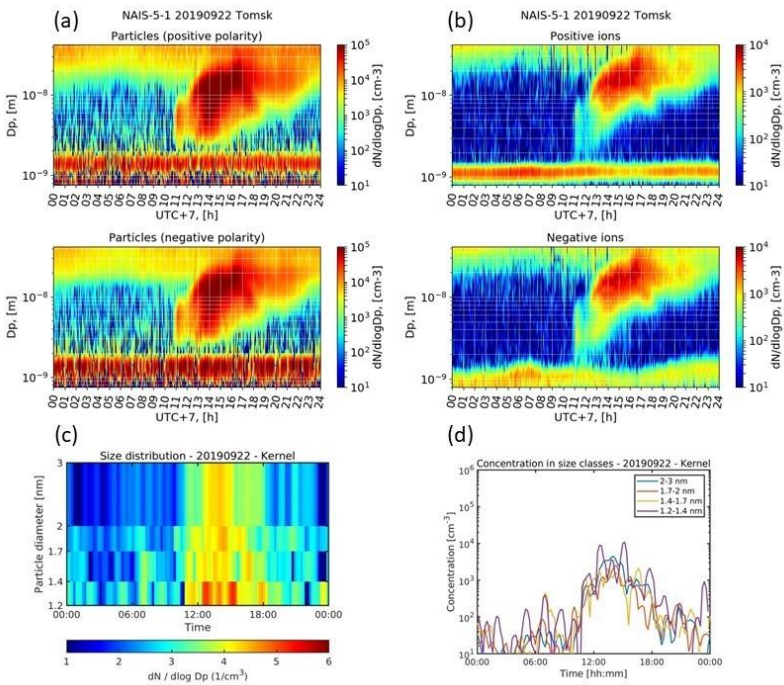
- 3535 Zhang, S., Zhang, J. H., Bai, Y., Koju, U. A., Igbawua, T., Chang, Q., Zhang, D., and Yao, F. M.: Evaluation
3536 and improvement of the daily boreal ecosystem productivity simulator in simulating gross primary
3537 productivity at 41 flux sites across Europe, *Ecol. Model.*, 368, 205-232,
3538 doi:10.1016/j.ecolmodel.2017.11.023, 2018.
- 3539 Zhang-Turpeinen, H., Kivimäenpää, M., Aaltonen, H., Berninger, F., Köster, E., Köster, K., Menyailo, O.,
3540 Prokushkin, A., and Pumpanen, J.: Wildfire effects on BVOC emissions from boreal forest floor on
3541 permafrost soil in Siberia, *Science of the Total Environment*, 134851, doi:10.1016/j.scitotenv.2019.134851,
3542 2020.
- 3543 Zhao, H., Li, X., Zhang, Q., Jiang, X., Lin, J., Peters, G. P., Li, M., Geng, G., Zheng, B., Huo, H., Zhang, L.,
3544 Wang, H., Davis, S. J., and He, K.: Effects of atmospheric transport and trade on air pollution mortality in
3545 China, *Atmos. Chem. Phys.*, 17, 10367–10381, doi:10.5194/acp-17-10367-2017, 2017.
- 3546 Zhdanova, E. Y., Chubarova, N. Y., and Lyapustin, A. I.: Assessment of urban aerosol pollution over the
3547 Moscow megacity by the MAIAC aerosol product, *Atmos. Meas. Tech.*, 13, 877–891, doi:10.5194/amt-13-
3548 877-2020, 2020.
- 3549 Zhou, Y., Dada, L., Liu, Y., Fu, Y., Kangasluoma, J., Chan, T., Yan, C., Chu, B., Daellenbach, K. R.,
3550 Bianchi, F., Kokkonen, T. V., Liu, Y., Kujansuu, J., Kerminen, V.-M., Petäjä, T., Wang, L., Jiang, J., and
3551 Kulmala, M.: Variation of size-segregated particle number concentrations in wintertime Beijing, *Atmos.*
3552 *Chem. Phys.*, 20, 1201–1216, doi:10.5194/acp-20-1201-2020, 2020.
- 3553 Zilitinkevich, S., Druzhinin, O., Glazunov, A., Kadantsev, E., Mortikov, E., Repina, I., and Troitskaya, Y.:
3554 Dissipation rate of turbulent kinetic energy in stably stratified sheared flows, *Atmos. Chem. Phys.*, 19, 2489–
3555 2496, doi:10.5194/acp-19-2489-2019, 2019.
- 3556 Öström, E., Putian, Z., Schurgers, G., Mishurov, M., Kivekäs, N., Lihavainen, H., Ehn, M., Rissanen, M. P.,
3557 Kurtén, T., Boy, M., Swietlicki, E., and Roldin, P.: Modeling the role of highly oxidized multifunctional
3558 organic molecules for the growth of new particles over the boreal forest region, *Atmos. Chem. Phys.*, 17,
3559 8887–8901, doi:10.5194/acp-17-8887-2017, 2017.
- 3560

Non-stressed conditions

Cold soil in spring

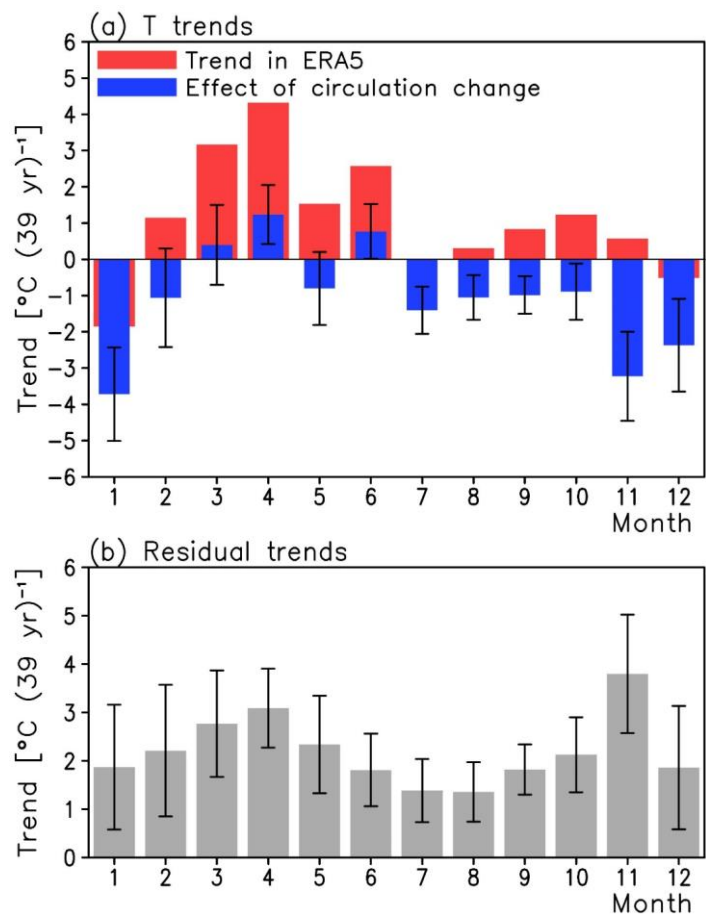


3561
3562 Figure 1.
3563

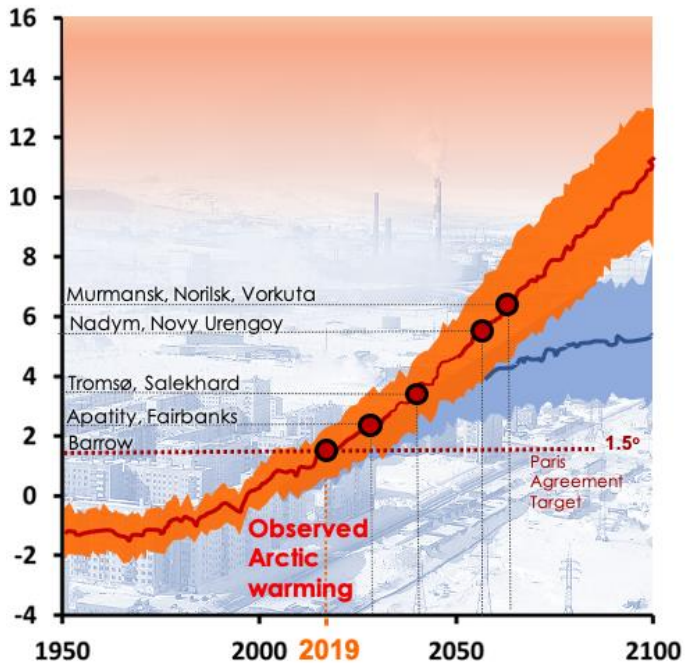


3564
101

3565 Figure 2.
3566

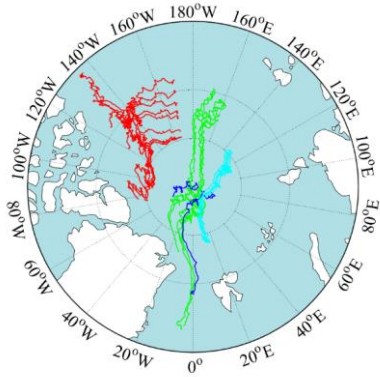


3567
3568 Figure 3.
3569



3570

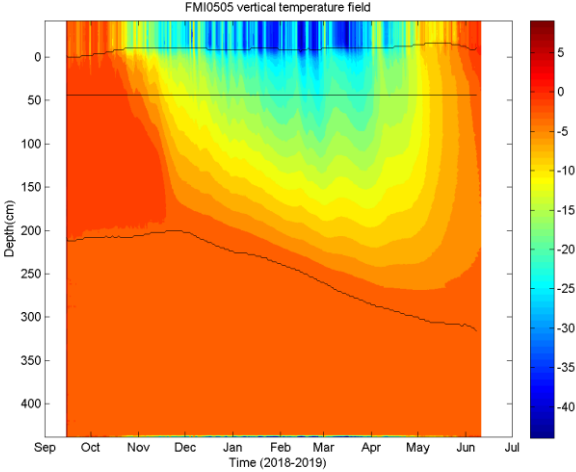
3571 Figure 4.



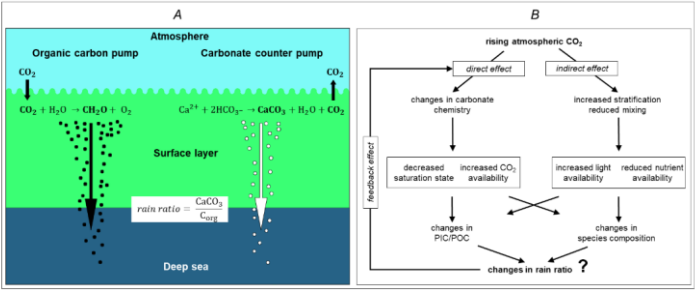
3572

3573 Figure 5.

3574



3575
3576 Figure 6.
3577



3578
3579 Figure 7.
3580

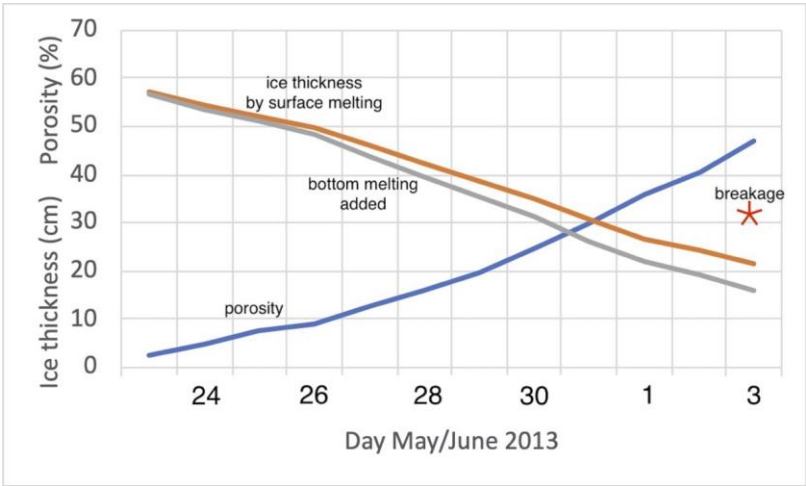


Figure 8.

A																	
	Fe	Al	Mn	Pb	Bi	Co	Be	V	Ni	Cr	Cd	Cu	Zn	As	B	U	Mo
Russian part of the catchment	65	69	56	46	77	59	71	65	48	29	49	41	25	22	11	5	2
Mongolian part of the catchment	98	96	100	95	87	89	71	57	56	55	71	70	86	10	19	4	2

B																	
	Fe	Al	Mn	Pb	Bi	Co	Be	V	Ni	Cr	Cd	Cu	Zn	As	B	U	Mo
Russian part of the catchment	60	70	52	45	75	57	41	56	40	47	19	42	26	39	18	6	4
Mongolian part of the catchment	78	83	59	72	76	59	49	43	35	49	13	62	23	12	10	1	1

Figure 9.

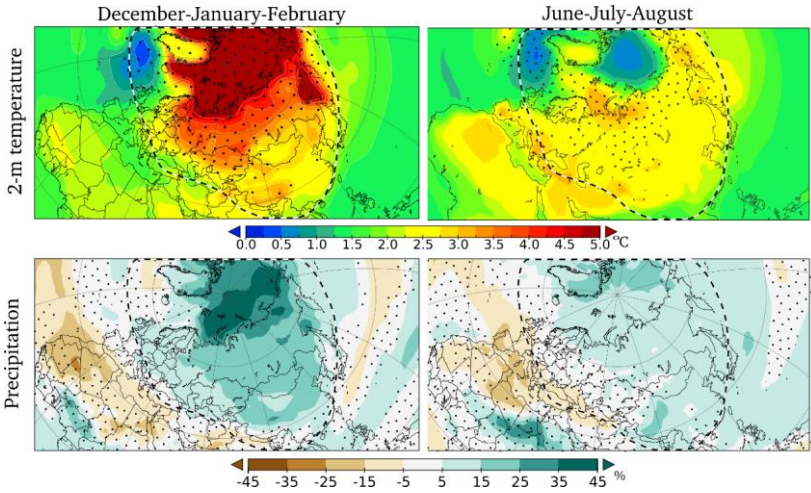


Figure 10.

Figure 1. A recent field and modelling study shows that cold soil decreases belowground hydraulic conductance (i.e. less root water uptake), and further canopy conductance in mature, boreal trees in spring (Lintunen et al. 2020). Cold temperature also decreases sink strength (i.e. less sugars are needed for metabolism and growth). Low sink strength increases sugar concentration in leaves, which decreases photosynthesis due to increased stomatal and non-stomatal limitations for photosynthesis (Hölttä et al., 2017; Salmon et al., 2020).

Figure 2. Example of results from the state-of-the-art aerosol instruments NAIS and PSM displaying NPF event at Fonovaya station, Siberia, on 22.09.2019. Particles of different polarity, NAIS (a), ions of different polarity, NAIS (b), particle number distribution at the smallest sizes, PSM (c), number concentration of the smallest particles in different size bins, PSM (d).

Figure 3. Linear trends of monthly mean temperature in Western Siberia (55°-65°N, 65°-90°E) in years 1979-2018. In (a), the red bars show the trend in the ERA5 reanalysis and the blue bars the circulation-related trend. In (b), the residual trends are shown. The error bars indicate the 5-95% uncertainty range in the circulation-related trend and the residual trend based on interannual variability. Redrawn from Räisänen (2021).

Figure 4. The northern urban heat islands are forerunners of the global warming. Winter season future temperatures for the Arctic (60–90°N) averaged over 36 CMIP5 global climate models and expressed as departures from the means for the 1981–2005 period. The red line is the ensemble mean for RCP8.5, the blue line is for RCP4.5. Shaded areas denote \pm one standard deviation from the ensemble mean (Overland et al., 2014; and Fig. 2.15 of AMAP, 2017). The observed surface UHIs are shown as red dots collocated with the expected future Arctic temperature anomalies, e.g., the observed wintertime urban temperature anomaly in Nadym corresponds to the regional warming as expected to be reached by 2060. Observe that the present Arctic climate is already 1.5°C warmer than the historical normals 1960-1990.

Figure 5. Trajectories of SIMBA buoys deployed in the Arctic in the period 2018-2019. Red: CHINARE (10 buoys), green: NABOS (5 buoys), dark blue: CAATEX (2 buoys), and light blue: MOSAiC (15 buoys). SIMBA is a thermistor string-based ice mass balance (IMB) buoy. It measures high-resolution (2 cm) vertical environment temperature (ET) profiles (4 times a day) through the air-snow-sea ice-ocean column. The heating temperature (HT) measured by the thermistor string once per day is based on the use of a small identical heater on each sensor. The ET and HT data are used to derive snow depth and ice thickness. SIMBA uses GPS module to track the buoy location. The Iridium satellite is used for data transmission. A total 15 SIMBA buoys have been deployed in the Arctic Ocean during the Chinese National Arctic Research Expedition (CHINARE) 2018 and the Nansen and Amundsen Basins Observational System (NABOS) 2018 field expeditions in late autumn. In 2019 17 SIMBA buoys were deployed during the CAATEX (2) and MOSAIC expeditions (15, leg 1).

Figure 6. SIMBA observations on the temporal evolution of the snow depth, ice thickness, and the temperature profile from the ocean through snow and sea ice to air. The results were obtained applying the algorithm by Liao et al. (2018). The black lines are snow surface (top), Initial freeboard (middle) and ice base (bottom). 0 level refers to snow/ice interface. The colors indicate the temperature in °C.

Figure 7. A: Biological pumps resulting in (i) atmospheric CO₂ sink and(ii) calcium carbonate transport from surface to deep ocean; **B:** anticipated forward and feedback alterations in ocean ecology driven by atmospheric CO₂ increase. PIC=particulate inorganic carbon; POC=particulate organic carbon (modified after Rost & Riebesell, 2004).

Figure 8. Field data for ice decay in Lake Kilpisjärvi in 2013 showing decrease of ice thickness by surface melting and bottom melting and increase of porosity until breakage of ice cover.

Figure 9. Hydrogeochemical signature of large river system –Selenga River case study. The figure represent metal(loid)s partitioning (Median values) in the Selenga river basin in the upper (Mongolian) and downstream (Russian) part between 20 July -10 August 2011 under dominant high water (A) and 07 June -10 July 2012 under dominant low water conditions. Dark orange fill corresponds to the share of suspended forms of elements > 75% (green), light orange – 75-50%, light blue – 50-25%, dark blue – < 25%. The

figure indicate that in the large river system some metals are mostly found in the dissolved form (84–96% of Mo, U, B, and Sb on an average), whereas many others predominantly existed in suspension (66–87% of Al, Fe, Mn, Pb, Co, and Bi). A consistently increasing share of metals in suspended particulate modes (about 2–6 times) is observed under high discharge conditions. For details and other hydrological seasons refer to (Kasimov et al., 2020b).

Figure 10. Changes in 2-meter temperature (°C, upper panels) and precipitation (% , lower panels) during the 21st century. Present-day climatology is averaged over years 1981-2010 and end-of-century climatology over 2070-2099. Winter (left) and summer (right) are shown separately. Dotted areas indicate high variability in model ensemble (for temperature: standard deviation of 21st century change exceeds 1°C; for precipitation: standard deviation of 21st century change exceeds 100% or present-day precipitation). The model results are from IPCC AR5, based on 42 individual models in CMIP5 experiments under the RCP4.5 scenario.

Table 1. Systems, key topical areas, research question introduced in the PEEEX Science Plan (SP) (Kulmala et al. 2015; 2016a, Lappalainen et al. 2018) connected to the addressed research themes over last 5 years by the PEEEX questionnaire (APPENDIX 1). The addressed research themes and the results are overviewed in section 3.

PEEX – SP System	PEEX - SP key topical area	PEEX - SP research question (Q-No)	Addressed research themes during the last 5 years
Land	Changing land ecosystem processes	How could the land regions and processes that are especially sensitive to climate change be identified, and what are the best methods to analyze their responses? (Q-1)	<ul style="list-style-type: none"> high-latitude photosynthetic productivity and vegetation changes (greening, browning) new methodologies determining Earth surface characteristics
Land	Risk areas of permafrost thawing	How fast will permafrost thaw proceed, and how will it affect ecosystem processes and ecosystem-atmosphere feedbacks, including hydrology and greenhouse gas fluxes ? (Q-2)	<ul style="list-style-type: none"> soil temperature evolution changing GHG fluxes, carbon sink-source dynamics due to permafrost thawing
Land	Ecosystem structural changes	What are the structural ecosystem changes and tipping points in the future evolution of the Pan-Eurasian ecosystem? (Q-3)	<ul style="list-style-type: none"> changes in soil microbial activity e.g. effect of forest fires changes of the Northern soils and functioning of the Arctic tundra in global carbon cycling context

Atmosphere	Atmospheric composition and chemistry	What are the critical atmospheric physical and chemical processes with large-scale climate implications in a northern context? (Q4)	<ul style="list-style-type: none"> carbon (C) balance in the boreal forests; methane (CH₄) balance at the Arctic; carbon monoxide (CO), ozone (O₃) at the Northern Eurasian region Sources and properties of atmospheric aerosols in boreal and Arctic environments black carbon and dust in the atmosphere and on snow at the Northern high latitudes methodological and model developments related to atmospheric chemistry and physics
Atmosphere	Urban air quality and megacities, ABL	What are the key feedbacks between air quality and climate at northern high latitudes and in China? (Q5)	<ul style="list-style-type: none"> recent observations on air quality in China Anthropogenic emissions and environmental pollution in Russia
Atmosphere	Weather and atmospheric circulation	How will atmospheric dynamics (synoptic scale weather, boundary layer) change in the Arctic-boreal regions? (Q6)	<ul style="list-style-type: none"> cold & warm episodes cyclone density dynamics circulation effect on temperature and moisture cloudiness in Arctic atmospheric boundary layer (ABL) dynamics
Water	The Arctic Ocean in the climate system	How will the extent and thickness of the Arctic sea ice and terrestrial snow cover change? (Q-7)	<ul style="list-style-type: none"> Sea ice dynamics and thermodynamics with atmospheric and ocean dynamics Snow depth/mass and sea ice thickness Sea ice research supporting navigation Ocean floor, sediments: composition and fluxes River runoff effecting the hydrological processes at coastal marine environments in Russia
Water	Arctic marine ecosystem	What is the joint effect of Arctic warming, ocean freshening, pollution load and acidification on the Arctic marine ecosystem, primary production and carbon cycle? (Q-8)	<ul style="list-style-type: none"> Living marine organisms weaken or even subdue CO₂ accumulation
Water	Lakes and large-scale river systems	What is the future role of Arctic-boreal lakes, wetlands and large river systems, including thermokarst lakes and running waters of all size, in biogeochemical cycles, and how will these changes affect societies? (Q-9)	<ul style="list-style-type: none"> organic carbon, carbon balance, ice cover at lakes in the Northern high latitudes specific characteristics of the Lake Baikal and Selenga River delta in Russia specific characteristics of Asian water lakes

Formatted: Font color: Auto

Society	Anthropogenic impact	How will human actions such as land-use changes, energy production, the use of natural resources, changes in energy efficiency and the use of renewable energy sources influence further environmental changes in the region? (Q-10)	<ul style="list-style-type: none"> • Mitigation e.g method for the natural risk assessment in Russia and new clean energy technologies
Society	Environmental impact	How do the changes in the physical, chemical and biological state of the different ecosystems, and the inland, water and coastal areas affect the economies and societies in the region, and vice versa? (Q-11)	<ul style="list-style-type: none"> • Reindeer grazing effects on the ground vegetation structure and biomass
Society	Natural hazards	In which ways are populated areas vulnerable to climate change? How can their vulnerability be reduced and their adaptive capacities improved? What responses can be identified to mitigate and adapt to climate change? (Q-12)	<ul style="list-style-type: none"> • Emerging zoonotic diseases • UV variation effects on health • Air pollution in different scales and environments (street-level urban air pollution, transported air pollution in urban environments, air pollution at the Arctic) and related health effects;
Feedbacks	Key topics: Atmospheric composition, biogeochemical cycles: water, C, N, P, S	How will the changing cryospheric conditions and the consequent changes in ecosystems feed back to the Arctic climate system and weather, including the risk of natural hazards? (Q-13)	<ul style="list-style-type: none"> • <i>Research needs:</i> quantification of the COntinental Biosphere-Aerosol-Cloud-Climate (COBACC) feedback loop at different Northern boreal environments • Gold & high region quantification of BVOC – aerosols feedback loop at the Tibetan /Himalayan Plateau:..
Feedbacks	Key topics: Atmospheric composition, biogeochemical cycles: water, C, N, P, S	What are the net effects of various feedback mechanisms on (i) land cover changes, (ii) photosynthetic activity, (iii) GHG exchange and BVOC emissions (iv) aerosol and cloud formation and radiative forcing ? How do these vary with climate change on regional and global scales? (Q-14)	<ul style="list-style-type: none"> • <i>Research needs:</i> The Arctic greening and browning calls for a multi-disciplinary scientific approach together, improved modelling tools and new data in order to solve scientific questions related to the net effects of various feedback mechanisms connecting the biosphere-atmosphere - human activities

Feedbacks	<p>Key topics: Atmospheric composition, biogeochemical cycles: water, C, N, P, S</p>	<p>How are intensive urbanization processes changing the local and regional climate and environment? (Q-15)</p>	<ul style="list-style-type: none">• <i>Research needs:</i> accelerating urbanization calls for studies on the effects of on air pollution, local climate and the effects these changes have on global climate. Integrated studies should lead to services for society, cities helping to mitigate hazards storms, flooding, heat waves, and air pollution episodes (see also 3.2.1)
-----------	--	--	---

3665

3666

3667

3668

3669

3670

Code/Data availability: This is an review paper and the data availability is introduced in the original articles.

Author contribution: Co-authors have provided text and/or relevant references. Some of them have been editors of the specific chapters of the manuscript.

Competing interests: no spesific competing interests

Formatted: Font color: Auto